DEVELOPMENT AND EXPERIMENTAL INVESTIGATION OF NEW SELF-CAN COOLING SYSTEMS

by

Jason Huang

A Thesis Submitted in Partial Fulfillment

of the Requirements for the Degree of

Master of Applied Science in Mechanical Engineering

Faculty of Engineering and Applied Science

University of Ontario Institute of Technology

April 2014

Abstract

In this thesis, two conceptual self-cooling beverage can designs are proposed. The methods of cooling are validated experimentally and certain parameters of interested are obtained for an analytical and numerical study of the conceptual designs. Optimization of the can geometry for heat transfer rate, volume of beverage, and total amount of cooling is performed.

Experiments are carried out using experimental test systems that evaluate the validity of two specific cooling methods. First method of cooling uses ammonia throttling followed by desiccant salt adsorption. The results show that there is satisfactory cooling for 300 ml of water in 3 minutes. The second method uses an endothermic reaction between ammonium thiocyanate and barium octahydrate as a cooling method. The results show that this method is also a valid cooling method.

The experimental work provides key parameters of interest for the analytical and numerical study of the proposed conceptual self-cooling can designs. The numerical study is conducted using computational fluid dynamics and heat transfer modeling. The goal of this study is to determine the best aspect ratio for the cooling vessel inside the beverage can, and to determine the effects of ambient temperature on the performance of the system. The results show that the best performing aspect ratio is aspect ratio 4. Aspect ratio 4 is the thinnest and longest cooling vessel and provides the best heat transfer performance. Ambient temperature does not significantly change the final temperature of the beverage at the end of 3 minutes.

A cooling effectiveness study is conducted to evaluate the performance of the self-cooling beverage can. The study only looks at the ammonia expansion design. The

best performance in terms of cooling effectiveness is achieved when using aspect ratio 4 at an ambient temperature of 35℃. The cooling effectiveness for this specific case is 0.834 for energy and 0.772 for exergy, respectively.

An optimization study of the self-cooling beverage can geometry is conducted. The objectives are to minimize cooling time, maximize volume of beverage, and maximize cooling effectiveness. The non-dominating optimal solutions are presented in Pareto front graphs. The results of this study provide a highly effective tool needed to make a decision on which dimensions to use in a final design of a self-cooling beverage can.

Acknowledgements

The research and hard work that went into this thesis would not have been possible if not for the many amazing and talented people in my life. I would first like to extend my deepest gratitude to Dr. Ibrahim Dincer for providing me with the opportunity to pursue a Masters of Applied Science degree. He has been one of the most challenging, yet understanding mentors that I have ever had in my academic career. He has pushed me to my limits, and I have learned many things from him. It was a pleasure to have him as my supervising professor.

I would like to thank Dr. Calin Zamfrescu for all of his support and teachings when it came to technical matters in and outside of the lab. His wealth of knowledge gave me great support for tackling the experimental and theoretical work.

I would like to thank Rami El-Emam for helping with the experimental work. His presence and experience was necessary to get the lab work done.

I would like to thank Steve and Gary from our sponsoring company Envirochill for providing financial support for the research, and for guiding us in the direction in order to arrive at positive solutions.

I would like to also thank George Yotis from the company Swagelok for providing us with unlimited support during the building the first experimental setup.

I would like to thank Janette Hogerwaard, Canan Acar, Hasan Ozcan, Abdullah Al Zahrani, and Nader Javani, my friends on the third floor. I very much appreciated their company and support during my time here at UOIT.

I would like to thank Ed Secnik at the Clean Energy Research Lab for providing us with administrative and safety guidance when it came to matters of the laboratories.

Finally I want to acknowledge my family for always being there for me. They have supported me through my every decision, and have encouraged me every step of the way.

Table of Contents

Abstract ..... **ii**

Acknowledgements ..... **iv**

Table of Contents ..... **vi**

List of Figures ..... **xii**

List of Tables ..... **xx**

Nomenclature ..... **xxi**

Chapter 1: Introduction **25**

1.1 Benefits of Self-Cooling Beverage Cans 25

1.2 Scope of Research and Objectives 29

1.3 Outline of Thesis 31

Chapter 2: Literature Review **32**

2.1 Literature Survey 32

2.2 Patent Survey 33

2.2.1 Direct Refrigerant Release Based 33

2.2.1.1 U.S Patent No. 3,597,937 34

2.2.1.2 U.S. Patent No. 4,656,838 35

2.2.1.3 U.S. Patent No. 5,447,039 35

2.2.1.4 U.S. Patent No. 5,555,741 A 36

2.2.1.5 U.S. Patent No. 5,765,385 37

2.2.2 Refrigerant Based with Capture 38

2.2.2.1 U.S Patent No. 5,325,680 38

2.2.2.2 U.S. Patent No. 6,167,718 B1 39

2.2.2.3 U.S. Patent No. 6,829,902 B1 40

2.2.3 Endothermic Reaction Based 41

2.2.3.1 U.S. Patent No. 20,120,144,845 A1 41

2.2.3.2 U.S. Patent No. 20,130,098,069 A1 42

2.2.3.3 U.S. Patent No. 20,130,174,581 A1 43

2.2.4 Patent Survey Summary 44

2.3 Market Survey 45

2.3.1 West Coast Chill 45

2.3.2 ICETEK 45

2.3.3 I.C Can 47

2.3.4 Market Survey Summary 47

Chapter 3: Background 49

3.1 Thermodynamics of Self-cooling Beverage Can 49

3.2 Conventional Can Cooling Systems 49

3.2.1 Refrigerator 49

3.2.2 Cooler 50

3.3 Types of Refrigerants 51

3.4 Adsorption Process 52

3.5 Endothermic Reactions 53

Chapter 4: Experimental Apparatus and Procedure 54

4.1 Experiment 1: Ammonia Expansion with Desiccant Salt Capture 56

4.1.1 Ammonia Vessel 58

4.1.2 Throttling Valve 59

4.1.3 Cooling Coil 59

4.1.4 Water Tray 60

4.1.5 Adsorption Bed 60

4.2 Experimental Procedure for System 1 62

4.2.1 Charging the Ammonia Vessel 62

4.2.2 Preparing the Adsorption Bed 63

4.2.3 Conducting the Experiment 64

4.3 Experiment 2: Endothermic Reaction 65

4.3.1 Beverage Can 66

4.3.2 Reaction Vessel 66

4.4 Experimental Procedure for System 2 67

4.4.1 Preparing the Beverage Can 67

4.4.2 Preparing the Reactants 67

4.4.3 Conducting the Experiment 68

4.5 Data Collection and Instruments Specifications 69

4.6 Proposed Conceptual Designs 69

4.6.1 Design 1 70

4.6.2 Design 2 71

Chapter 5: Analyses and Optimization 73

5.1 Analytical Study 73

5.2 Numerical Analysis 75

5.2.1 Numerical Modeling Software 75

5.2.2 Defining Geometry 75

5.2.3 Defining Materials 79

5.2.3.1 Aluminum 79

5.2.3.2 Water 79

5.2.3.3 Cola Compared to Water 80

5.2.4 Governing Equations 80

5.2.5 Defining Boundary Conditions 84

5.2.5.1 Thermally Insulated Boundaries 84

5.2.5.2 Temperature Boundaries 85

5.2.5.3 Convective Heating Boundary 86

5.2.6 Initial Conditions 87

5.2.7 Grid Independence Test 87

5.2.8 Time Step Tolerance 88

5.2.9 Defining Test Cases 89

5.3 Cooling Effectiveness Study 91

5.3.1 Balance Equations for the Self-Cooling Beverage Can 92

5.4 Can Design Optimization 94

5.4.1 Optimization Problem Definition 96

5.4.1.1 Physical Model 96

5.4.2 Mathematical Model 97

5.4.2.1 Objective Functions 99

5.4.3 Optimization Method 101

5.4.3.1 Multi-Objective Genetic Algorithm 101

5.4.3.2 Optimization Procedure 103

Chapter 6: Results and Discussion 106

6.1 Experimental Results 106

6.1.1 Experiment 1 106

6.1.1.1 Experimental Case 1 107

6.1.1.2 Experimental Case 2 109

6.1.1.3 Experimental Case 3 110

6.1.2 Experiment 2 111

6.1.2.1 Experimental Case 1 112

6.1.2.2 Experimental Case 2 113

6.1.2.3 Experimental Case 3 115

6.2 Analytical Results of Conceptual Can Designs 116

6.3 Numerical Results for Conceptual Designs 118

6.3.1 Grid Independence Test Results 118

6.3.2 Water and Cola Comparison 120

6.3.3 Aspect Ratio 124

6.3.4 Ambient Temperature 132

6.4 Cooling Effectiveness Results 141

6.5 Optimization Results 145

Chapter 7: Conclusions and Recommendations 151

7.1 Conclusions 151

7.2 Recommendations 153

References 154

List of Figures

Figure 1.1: Photograph a common cooler [1]. 26

Figure 2.1: Self-cooling can design by Parks [3]. 34

Figure 2.2: Self-cooling design by Shen [4]. 35

Figure 2.3: Self-cooling beverage can design by Allison [5]. 36

Figure 2.4: Self-cooling beverage can design by Envirochill International Limited. Oakley [6] 37

Figure 2.5: Self-cooling can design by Childs [7]. 38

Figure 2.6: Self-cooling can design by Baroso-Lujan and Galvan-Duque [8]. 39

Figure 2.7: Self-cooling beverage can design by Halimi and Gans [9]. 40

Figure 2.8: Self-cooling beverage can design by Claydon [10]. 41

Figure 2.9: Self-cooling beverage can design by Leavitt and Bergida [11]. 42

Figure 2.10: Self-cooling beverage can patent picture by Collins [12] 43

Figure 2.11:Self-cooling beverage can design by Rasmussen, et al. [13]. 43

Figure 2.12: West Coast Chill's self-chilling can [14]. 45

Figure 2.13: IceTek self-cooling can [16]. 46

Figure 2.14: Patented drawing of the Icetek's self-cooling beverage can [17]. 46

Figure 2.15: Self-cooling beverage can designed by Tempra Technology and Crown Holdings [18]. 47

Figure 3.1: Schematic diagram of a simple vapour compression refrigeration cycle. 50

Figure 4.1: An outline of the overall summary of the thesis research. 56

Figure 4.2: Ammonia and magnesium chloride test system for proof of concept. 57

Figure 4.3: Photograph of the experimental test system which is used for validating the ammonia and desiccant adsorption cooling method. 57
Figure 4.4: Ammonia vessel which contains saturated ammonia liquid-vapour under saturation pressure at the ambient temperature. The pressure vessel is fitted with glass level meter to visibly see the level of liquid ammonia in the vessel. 58
Figure 4.5: The throttling valve is a double pattern needle valve which can finely adjust the flow and expansion of the ammonia. 59
Figure 4.6: Cooling coil that is submerged in the volume of beverage to be cooled. 60
Figure 4.7: The water tray holds 1.25L of water to simulate the beverage to be cooled. 60
Figure 4.8: Photograph of the water tray and cooling coil in experimental setup 1. 61
Figure 4.9: The magnesium chloride bed stores the desiccant salt mixture used in the adsorption process. 61
Figure 4.10: Experimental test system for the endothermic reaction consisting of reaction vessel inside of a beverage can. 65
Figure 4.11: Schematic diagram of the beverage can with energy flow from experimental setup 2. 66
Figure 4.12: Reaction vessel for the two-salt endothermic reaction configuration. 67
Figure 4.13: Self-cooling beverage can with ammonia expansion and desiccant adsorption. Viewed in the upside-down orientation. 71
Figure 4.14: Proposed conceptual self-cooling beverage can design using endothermic reaction as cooling method. 72

Figure 5.1: a) Cross sectional view of the self-cooling beverage can from the side. b) Cross sectional view of the self-cooling beverage can with axis of symmetry drawn vertically down the middle of the can. c) Final geometry used in the modeling of the can. 76
Figure 5.2: Geometry of the can labeled with parameters of interest. 77
Figure 5.3: An enlarged image of part of the aluminum wall which surrounds the beverage. 78
Figure 5.4: Schematic diagram of a simple two concentric cylinder model used in the introduced dimensionless parameters of the model. 83
Figure 5.5: Thermally insulated boundary layers. 85
Figure 5.6: Cooling vessel wall boundary highlighted. 86
Figure 5.7: Convective heating boundary along the wall of the outer surface of the can. 86
Figure 5.8: COMSOL automatically generated meshes (a) finer, (b) normal, (c) coarse, (d) coarser, and (e) extremely coarse. 88
Figure 5.9: All 5 aspect ratio geometries displayed from A1 through A5. 90
Figure 5.10: Energy flow of the self-cooling beverage can during the cooling process. 92
Figure 5.11: schematic drawing of the cooling system that is implemented inside the 355 ml soft drink can. d is the diameter of the vessel, h is the height of the vessel, Q is heat energy leaving the beverage and transferring into the cooling vessel. 95
Figure 5.12: Multi-objective genetic algorithm pseudo code taken from [24]. 102
Figure 5.13: Multi-Objective Genetic Algorithm structure taken from [24]. 103

Figure 5.14: MATLAB optimization toolbox graphical interface. 104
Figure 6.1: Ammonia expansion experiment run at 3 turns of the throttling valve and only magnesium chloride in the adsorption bed..... 107
Figure 6.2: Ammonia expansion experiment run at 3 turns of the throttling valve and magnesium chloride (50%wt) and aluminum oxide (50%wt) in the adsorption bed. 109
Figure 6.3: Ammonia expansion experiment run at 3 turns and vented directly into the fume hood after evaporation for zero back pressure. 111
Figure 6.4: Endothermic reaction experiment with 300 ml of cola as beverage with initial temperature of 20. 8℃..... 113
Figure 6.5: Endothermic reaction experiment with 300 ml of water as beverage with initial temperature of 20.4℃. 114
Figure 6.6: Ice formation on the reaction vessel due to high rate of cooling from endothermic reaction. 115
Figure 6.7: Endothermic reaction experiment with 300 ml water as beverage with initial temperature of 26.5℃. 116
Figure 6.8: Temperature profile across the radial direction of the cylinder for the analytical analysis with inner temperature of -20℃. 117
Figure 6.9: Temperature profile across the radial direction of the cylinder for the analytical analysis with inner temperature of -30℃. 117
Figure 6.10: Temperature distributions after 6 seconds for different mesh densities. (a) finer, (b) normal, (c) coarse, (d) coarser, (e) extremely coarse. 119

Figure 6.11: Results of average volume temperature of water over time with varying mesh densities. 120
Figure 6.12: Average velocity of water and cola over 180 seconds for the same test case. 121
Figure 6.13: Average temperature of water and cola over 180 seconds for the same test case. 122
Figure 6.14: Average total heat flux of water and cola over 180 seconds for the same test case. 122
Figure 6.15: Heat capacity at constant pressure of water and cola over 180 seconds for the same test case. 123
Figure 6.16: Outer can surface temperature of water and cola over 180 seconds for the same test case. 124
Figure 6.17: Average velocity of the 355 ml of water for different aspect ratios over 180s, with a cooling vessel temperature of -30℃. 125
Figure 6.18: Average velocity of the 355 ml of water for different aspect ratios over 180s, with a cooling vessel temperature of -20℃. 126
Figure 6.19: Average total heat flux of the system at different aspect ratios over 180s, with a cooling vessel temperature of -30℃. 127
Figure 6.20: Average total heat flux of the system at different aspect ratios over 180s, with a cooling vessel temperature of -20℃. 128
Figure 6.21: Heat capacities for water inside the can at constant pressure for different aspect ratios over 180s, with a cooling vessel temperature of -30℃. 129

Figure 6.22: Heat capacities for water inside the can at constant pressure for different aspect ratios over 180s, with a cooling vessel temperature of -20℃. 130
Figure 6.23: Average temperature of the 355 ml of water for different aspect ratios over 180s, with a cooling vessel temperature of -30℃. 130
Figure 6.24: Average temperature of the 355 ml of water for different aspect ratios over 180s, with a cooling vessel temperature of -20℃. 131
Figure 6.25: Average out can surface temperature for different aspect ratios over 180s, with a cooling vessel temperature of -30℃. 133
Figure 6.26: Average out can surface temperature for different aspect ratios over 180s, with a cooling vessel temperature of -20℃. 133
Figure 6.27: Average velocity of the 355 ml of water for different ambient temperatures over 180s, with a cooling vessel temperature of -30℃ for the same test case. 134
Figure 6.28: Average velocity of the 355 ml of water for different ambient temperatures over 180s, with a cooling vessel temperature of -20℃ for the same test case. 135
Figure 6.29: Average total heat flux of the can system for different ambient temperatures over 180s, with a cooling vessel temperature of -30℃ for the same test case. 136
Figure 6.30: Average total heat flux of the can system for different ambient temperatures over 180s, with a cooling vessel temperature of -20 for the same test case. 136

Figure 6.31: Heat capacities at constant pressure of the water inside the can for different ambient temperatures over 180s, with a cooling vessel temperature of -30℃ for the same test case. 137
Figure 6.32: Heat capacities at constant pressure of the water inside the can for different ambient temperatures over 180s, with a cooling vessel temperature of -20℃ for the same 138
Figure 6.33: Average temperature of the 355 ml of water for different ambient temperatures over 180s, with a cooling vessel temperature of -30℃ for the same test case. 138
Figure 6.34: Average temperature of the 355 ml of water for different ambient temperatures over 180s, with a cooling vessel temperature of -20℃ for the same test case. 139
Figure 6.35: Average outer can surface temperature for different ambient temperatures over 180s, with a cooling vessel temperature of -30℃ for the same test case. 140
Figure 6.36: Average outer can surface temperature for different ambient temperatures over 180s, with a cooling vessel temperature of -20℃ for the same test case. 140
Figure 6.37: Cooling effectiveness with vary aspect ratios at ambient temperature of 25℃ and 100 ml of ammonia. 142
Figure 6.38: Cooling effectiveness with vary aspect ratios at ambient temperature of 25℃ and 120 ml of ammonia. 143

Figure 6.39: Cooling effectiveness with vary ambient temperatures using aspect ratio 4 and 100 ml of ammonia. 144
Figure 6.40: Cooling effectiveness with vary ambient temperatures using aspect ratio 4 and 120 ml of ammonia. 144
Figure 6.41: Pareto front for objective functions 1 and 2. 146
Figure 6.42: Pareto front for objective functions 2 and 3. 147
Figure 6.43: Pareto front for objective functions 1 and 3. 147
Figure 6.44: Pareto front for objective functions 1, 2 and 3. 148
Figure 6.45: Optimization study variable space shows the optimal diameter and height for each optimal solution..... 149

List of Tables

Table 2.1: Comparison of the patent survey with advantages and disadvantages. 44

Table 2.2: Comparison of the market survey with advantages and disadvantages. 48

Table 4.1: Sensor data for experimental setups. 69

Table 5.1: Properties of Aluminum used in the COMSOL simulation. 79

Table 5.2: Properties of water used in the COMSOL simulations. 80

Table 5.3: Properties of cola used in the COMSOL simulations. 80

Table 5.4: Studied cases for the numerical model for proposed conceptual designs. 89

Table 5.5: Dimensions of length of vessel, radius of vessel for each aspect ratio and surface area of heat transfer. 90

Table 6.1: Ammonia expansion with desiccant experimental cases. 106

Table 6.2: Endothermic reaction experimental cases with experimental parameters. 112

Table 6.3: Computation time and maximum and minimum mesh sizes for the different mesh densities. All tests are done using the same aspect ratio, T_c and T_{amb}. 118

Table 6.4: Table of some non-dominated solutions of interest. 150

Nomenclature

A	Area (m^2)
Bi	Biot number
c_p	Specific heat capacity (kJ/kg· ℃)
d	Diameter (m)
cv	Valve constant
Ex	Exergy (kJ)
ex	Specific exergy (kJ/kg)
F_0	Fourier number
Gr	Grashof number
g	Gravity constant (m/s^2)
H	Specific enthalpy (kJ/kg)
h	Heat transfer coefficient ($W/m^2 \cdot K$)
h	Height (m)
J_0	Bessel function of the first order
k	Thermal conductivity (W/m·K)
l	Length (m)
m	Mass (kg)
$\dot{m}$	Mass flow rate (kg/s)
Nu	Nusselt Number
P	Pressure (kPa, psi)
P	Dimensionless pressure
Pr	Prandtl number

Pr	Prandtl number
Q	Heat transferred (kJ)
$\dot{Q}$	Heat transfer rate (kW)
R	Dimensionless axial coordinate
Ra	Rayleigh number
r	Radius (m)
S	Source term
s	Specific entropy (kJ/kg·K)
$\dot{S}_{gen}$	Entropy generation rate (kW/K)
SG	Specific gravity
T	Temperature (K, °F, ℃,)
t	Time (s)
U	Dimensionless velocity in x direction
u	Velocity in x direction (m/s)
X	Dimensionless axial coordinate
V	Dimensionless velocity in z direction
v	Velocity in z direction (m/s)
v	Kinetic viscosity
W	Work (kJ)
$\dot{W}$	Work rate (kW)

Greek Symbols

α	Thermal diffusivity (m^2/s)

β	Volumetric coefficient
η	Energy cooling effectiveness
θ	Dimensionless temperature
ρ	Density (kg/m^3)
Φ	Dependent variable
ϕ	Exergy cooling effectiveness
Γ	Diffusion coefficient
λ	Heat conductance coefficient (W/m·K)

Subscripts and Superscripts

a	Ammonia
act	Actual
amb	Ambient
c	Can
cond	Conduction
conv	Convection
cv	Cooling vessel
dest	Destruction
en	Energy
ex	Exergy
in	In
overall	Overall
ph	Physical

ref	Refrigerant
rxn	Reaction
theoretical	Theoretical
tot	Total
v	Vessel
w	Water

Acronyms

EES	Engineering Equation Solver
CERL	Clean Energy Research Lab
CPU	Central Processing Unit
GWP	Global Warming Potential
HC	Hydrocarbons
HCFC	Hydrochlorofluorocarbons
HEU	Heat exchanging unit
HFC	Hydrofluorocarbons
MOGA	Multi-Objective Optimization Genetic Algorithm
MOP	Multi-Objective Optimization Problem
ODP	Ozone Depletion Potential
UOIT	University of Ontario Institute of Technology

Chapter 1: Introduction

1.1 Benefits of Self-Cooling Beverage Cans

Temperature control is very important to a modern society. Everyday processes require some form of temperature control, whether it is for comfort, prevention of overheating, keeping food fresh for longer, or having a cold beverage. Buildings are kept at a desirable temperature for comfortable operating conditions. Manufacturing processes may require very hot or very cold environments, such as in drying processes or cold storage. Electronic devices may require temperature control so that devices do not overheat and cause damage. When it comes to food, it is important to keep meat, vegetables, fruits, and dairy products at cool temperatures so that they do not decompose as quickly as compared to being left outside at room temperatures. Certain beverages such as soda pop, alcoholic beverages, and even water are refrigerated so that they are more refreshing to drink. All these examples utilize temperature control devices which provides cooling or heating to the products. This thesis is concerned with the cooling of beverages in scenarios where it is inconvenient or not possible to have conventional refrigeration.

Conventionally, beverages are cooled in refrigerators. A refrigeration system takes thermal energy away from one medium and transfers it to a heat sink. A heat sink is a medium in which heat energy is transferred into, outwards from the refrigeration system. When beverages are placed into a refrigerator, thermal energy is transferred out of the beverage into the surrounding colder air. The thermal energy that is received by the cold air inside the refrigerator is then transferred to a refrigerant circulating around the interior and exterior of the refrigerator. The refrigerant expels the thermal energy into the surrounding air. This all happens because of the refrigeration cycle. This cycle uses a

refrigerant which undergoes compression and throttling to provide a means to take thermal energy from inside the refrigerator and then reject it to the surroundings.

In certain scenarios, cooling of beverage products are required where the conventional refrigerator is not available. For example, during an outdoor picnic, barbeque, or camping trip it is desirable to have a cold drink. The common method used today is the use of a cooler. Coolers are boxes which are designed to have high insulation walls. They are filled with ice along with the beverages as shown in Figure 1.1. The beverages cooled by thermal contact with the ice. However, this method only works for a finite period of time. The cooler, and all of the contents inside, eventually reaches thermal equilibrium with its surroundings. Thus, there is a time limitation on how long the drinks can remain cool. It is also an inconvenience to carry additional equipment to provide the necessary cooling.

Figure 1.1: Photograph a common cooler [1].

A potential solution to having a cold beverage at any time one desires, which does not have the limitation of a cooler box, is the utilization of self-cooling devices. An

example of such device is the common ice pack which can be found in most medical and first aid kits. This invention takes advantage of an endothermic chemical reaction to provide readily available cooling for swelling from an unfortunate injury. There are multiple reactions known in the literature which are more powerful than what is used in the ice pack. This simple concept of an endothermic reaction may be applied to a beverage can to create a self-cooling beverage can.

A self-cooling beverage can is a device which can cool the beverage it contains on demand. There are a few necessary parts for a can to be a self-cooling can. First component is the can itself which is the main container of the beverage. It has an addition of an internal device which provides the cooling. The device must have a triggering mechanism to initiate the cooling process. It must have a boundary for heat exchange where the cooling process may be applied to beverage. Inside the devices houses the cooling medium from which the temperature potential is generated. Finally, it may or may not have another compartment to store expended refrigerant or chemicals.

There are several advantages that the self-cooling beverage can has over the traditional portable beverage cooling solutions. They do not require any prior or continuous cooling such as cooler boxes. Beverages are able to cool from the ambient temperature, down to a desired temperature as if the beverage came out of a refrigerator. Self-cooling beverage cans would reduce the energy spent on refrigerators in supermarkets and convenience stores which are normally stocked with soda pop, water, energy drinks etc. There would not be a need to keep certain beverages refrigerated since a self-cooling beverage can would cool a beverage in a matter of minutes. This technology would only apply to beverages which do not spoil in relatively short periods

of time without refrigeration. Some of the beverages which are well suited for this technology are water, juice, soda pop, energy drinks, sports drinks and alcoholic beverages.

There are many scenarios for when a self-cooling beverage can would be appropriate. As mentioned before, outdoor picnics, barbeques and picnics would be an ideal scenario where self-cooling beverage cans may be used to enjoy a refreshing cold drink. It eliminates the need to have additional equipment for cooling ones' beverages. Other applicable scenarios this product would be highly useful in are outdoor concerts, military rations, outdoor parties and festivals, outdoor sports stadiums, a self-packed lunch, or whenever one desires to have a cold beverage. The technology is not limited to individual sized beverages. Self-cooling beverage can technology can be applied to larger applications such as large metal kegs. For example beer kegs for an outdoor party or festival may benefit from the implementation of this technology, making it a self-cooling keg.

Self-cooling beverage cans have a definitive advantage when it comes to the convenience of having a cold beverage during outdoor activities. However, there is also an increase in materials spent on the production of the can itself. There is the matter of additional metal, and also materials for additional components and additional fluids or chemicals that provides the cooling potential for the beverage. Consumers would have to pay a premium for the convenience factor that this technology would bring to the table. That being said, some consumers are willing to pay a little extra for this convenience.

The idea of a self-cooling beverage can is not new. It has been around for several decades. There are multiple patents worldwide pertaining to self-cooling can devices.

There are a few products which are out there on the market, but have not met widespread popularity. There is still more research and development that needs to be done. This technology needs to be optimized so that it is environmentally friendly and cost effective. The main focus of this research is on the development of a self-cooling beverage can which can provide adequate cooling which is environmentally friendly. It is important to develop a system which provides the necessary cooling, yet during its use, it does not expel any refrigerants or chemicals into the environment. There is ongoing competition in the beverage canning industry to design a product which can be mass manufactured at a low cost. During the research, multiple methods of cooling are considered to obtain solutions which are effective and environmentally benign.

1.2 Scope of Research and Objectives

The focus of the research is on the investigation and development of a self-cooling beverage cans which are completely safe for human use and safe for the environment. What this entails is research of the multiple cooling methods, current products available in the market, and patented designs of self-cooling beverage cans. There is also the need to develop a physical and analytical model for predicting the performance of the proposed designs. This allows for a complete understanding of where the self-cooling beverage can technology is in terms of its maturity, and also creates a tool which can be used to analyse any self-cooling beverage can device.

The motivation for the research is from an entrepreneurial standpoint. The Company Envirochill International Limited is striving to be the first company to provide a popular self-cooling beverage can solution for the beverage industry in North America.

Their goals are to develop a product which has minimal impact on the current manufacturing line, to have a method of cooling which is effective in cooling a beverage, and it must be environmentally friendly and safe for human use.

To accomplish these goals, there are several key objectives that this research follows. When meeting with the company representatives, they express that the self-cooling beverage can should be completely environmentally friendly and safe for human usage, must provide adequate cooling for 300 to 355 ml of beverage, and must be able to decrease the temperature by approximately 15℃ to 20℃ in less than 3 minutes. The following list outlines the key objectives of the research.

- To build two experimental systems that test the feasibility of cooling a beverage via ammonia expansion with desiccant salt capturing, and endothermic reaction
- To determine key parameters to be used in the analytical and numerical modeling of the self-cooling beverage can based on experimental data.
- To conceptually develop two self-cooling beverage can designs which use the cooling methods validated experimentally.
- To perform an analytical and numerical analysis of the two proposed cooling methods.
- To study the cooling effectiveness of a self-cooling beverage can using the ammonia expansion method in terms of energy and exergy.
- To conduct an optimization study of the geometry affecting cooling time, beverage volume, and cooling effectiveness of the self-cooling beverage can.

1.3 Outline of Thesis

The thesis is organized into 7 chapters which form a logical sequence of presenting the research. Chapter 1 introduces the concept of a self-cooling and the motivation behind the development of this technology. Chapter 2 presents a comprehensive survey of the existing patents and methods used for self-cooling cans, along with a market survey of current products on the market. Chapter 3 provides the scientific knowledge to understand how a self-cooling beverage can works. Chapter 4 presents the experimental test systems that are used to determine the validity of two proposed cooling methods. It also describes the procedures that are used during the experiments. Two proposed conceptual designs are conceived from confirming the feasibility of the cooling methods. Chapter 5 explains how the analytical and numerical analysis is performed. This chapter also explains the optimization study of a self-cooling beverage can, using multi-objective genetic algorithm. Chapter 6 presents all the results of the research work and the analysis of the results are given. Finally Chapter 7 presents all of the major findings in the research, with recommendations for future work related to self-cooling beverage cans.

Chapter 2: Literature Review

The concept of the self-cooling beverage can is not new. There is still much work to be done to develop a product that is popular and widely used. The self-cooling can has been around for several decades. Many companies, entrepreneurs and inventors have patents for self-cooling can devices. There are also other related works that it is important to mention about other miniature cooling systems. In this section, a brief literature review is presented, followed by a comprehensive patent survey of self-cooling beverage cans.

2.1 Literature Survey

Currently in the literature there are no openly published studies on specifically a self-cooling beverage can. However there are scientific studies on other technologies and/or devices that are of the self-cooling nature. In this section a study of a self-cooled solid desiccant cooling system based on desiccant coated heat exchanger is presented as a potential technology which can be applied to self-cooling beverage cans.

Ge, et al. [2] have investigated a solid desiccant cooling technology that has become of interest in the application of cooling of water. This technology works by integrating a desiccant coated heat exchanger and regenerative evaporative cooler. Water is chilled when it passes over the regenerative evaporative cooler. The chilled water then passes through to the desiccant coated heat exchanger where dehumidification occurs. The regenerative cooling technology may play a part in helping further the development of self-cooling beverage can devices. However the systems are too large to implement into a smaller mechanical design. It is possible in the future to investigate this technology further so that it may be scaled down for its application for self-cooling beverage cans.

The lack of published scientific self-cooling beverage can studies is most likely due to intellectual property issues. The fact that many self-cooling can designs are already patented does not indicate whether or not they are thoroughly investigated. The companies holding these patents have a high interest in keeping such information as secretive as possible. In the next section a patent survey is presented to show the current development of the self-cooling beverage cans.

2.2 Patent Survey

In this section a patent survey is conducted to explore the current and past patents pertaining to self-cooling beverage cans. There are multiple methods for cooling a beverage in a self-cooling can. The 3 main categories of self-cooling beverage can designs are direct refrigerant release based, refrigerant based with capture, and endothermic reaction based. Multiple patents are presented in each category to present a comprehensive understanding of 3 main types of self-cooling beverage cans.

2.2.1 Direct Refrigerant Release Based

Direct refrigerant release based self-cooling beverage can designs utilize a compressed refrigerant which undergoes throttling. After the evaporation of the refrigerant, the refrigerant gas is expelled into the surrounding atmosphere. This design is only viable if an environmentally friendly refrigerant is used. Even though a safe refrigerant is used in the operation of these types of devices, it is still somewhat problematic because it introduces additional gases into the environment. The effects of releasing collectively large amounts of *safe* refrigerant into the atmosphere may pose an environmental hazard

in the long run. There are many designs that are direct refrigerant release designs; five of them are presented here in this subsection.

2.2.1.1 U.S Patent No. 3,597,937

U.S patent number 3,597,937 is invented by Eugene H. Parks, and has been published in august 1971. The patent is for a self-cooling device for beverage containers. The device uses the expansion of a refrigerant to cool the beverage. The can contains a chamber that holds compressed saturated liquid refrigerant. There is a heat exchanger which could be a single or a set of multiple tubes. The tubes are orientated with multiple bends allowing for more length of the tube resulting in higher surface area of heat transfer. The refrigerant throttles into a heat exchanger unit which is then evaporated and then expelled through a hole at the top of the can to the surroundings [3]. An image of the design is presented in Figure 2.1.

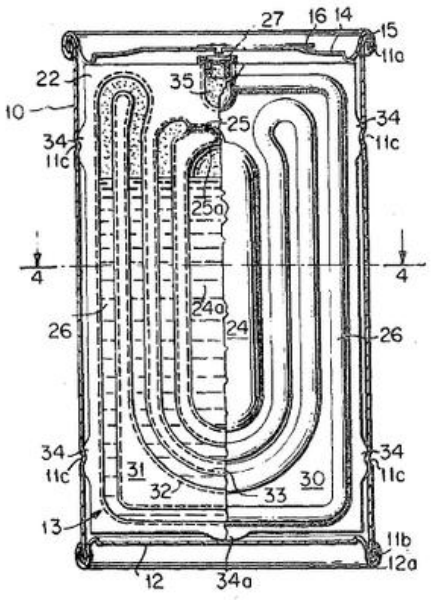

Figure 2.1: Self-cooling can design by Parks [3].

2.2.1.2 U.S. Patent No. 4,656,838

U.S patent number 4,656,838 is invented by Hwang K. Shen and Suan Fu Chun, Ming Hsiun Hsiang, and Chia Yi Hsien in 1987. The patent is for cooling device for a can containing a beverage which operates using a cylindrical vessel filled with liquid refrigerant, which is integrated with the bottom of the can. An orifice is created at the bottom of the can which leads into the refrigerant reservoir and allows for the refrigerant to expand into the atmosphere. The release of the refrigerant causes it to expand and cool thus cooling the beverage [4]. This is a poor design because most of the expanded refrigerant would not come in contact with the can to provide effective cooling.

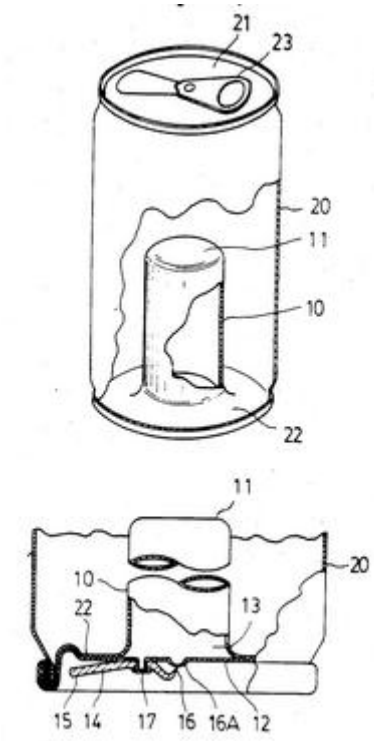

Figure 2.2: Self-cooling design by Shen [4].

2.2.1.3 U.S. Patent No. 5,447,039

U.S. patent number 5,447,030 is invented by Robert S. Allison. The patent describes a self-cooling can that uses expanding refrigerant to achieve cooling. The refrigerant

expands and cools in the tube to provide the cooling. The heat exchanger unit is a vertically oriented serpentine tube. The serpentine tube spirals radially outwards from the refrigerant storage unit to cover more regions of the can to cool the beverage faster. The refrigerant exits through the top of the can into the atmosphere at the end of the tube [5]. This design is effective because it has a high surface area of heat transfer for the refrigerant and is relatively easy to manufacture.

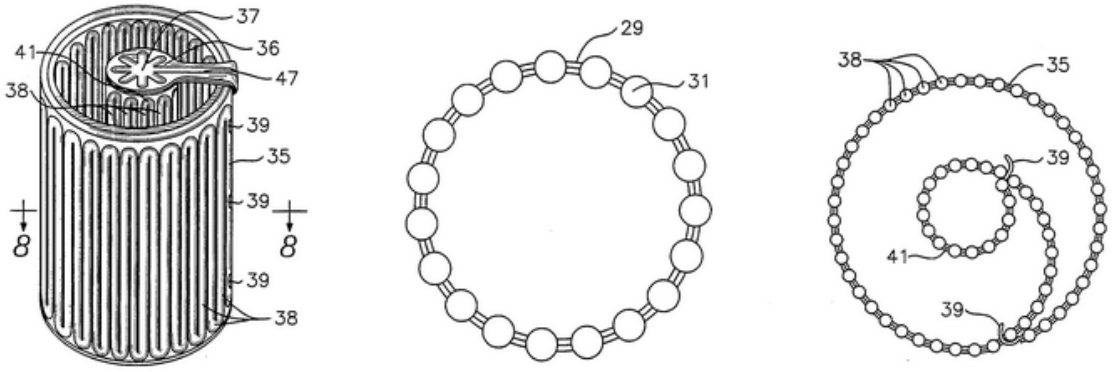

Figure 2.3: Self-cooling beverage can design by Allison [5].

2.2.1.4 U.S. Patent No. 5,555,741 A

U.S Patent No. 5555741 A is the current patent that our sponsoring company Envirochill International Limited holds. This design for a self-cooling beverage can device has its refrigerant stored in a vessel which is created by making a redraw of the metal of the original can. This cavity stores liquid refrigerant at high pressure until it is pierced. The cavity is a vessel which is an integral part of the original can. This is integration of the cooling vessel is what makes the design unique. The refrigerant then releases into an expansion chamber which hugs the bottom part of the original can. The cooling happens on the outer surface of the can near the bottom, and also the redraw portion of the can [6].

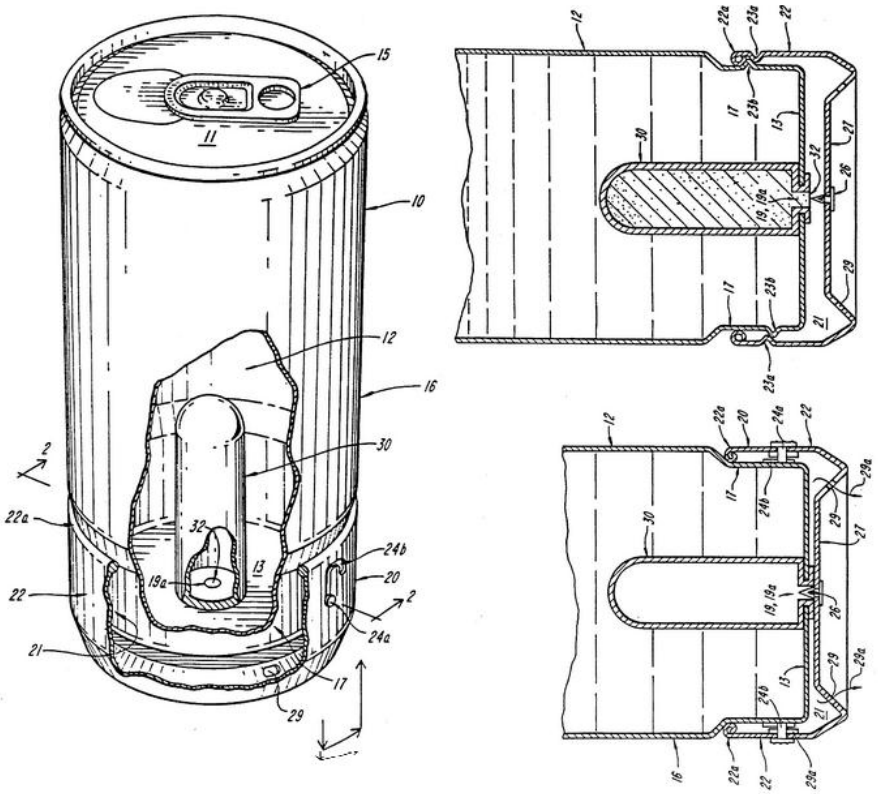

Figure 2.4: Self-cooling beverage can design by Envirochill International Limited. Oakley [6]

2.2.1.5 U.S. Patent No. 5,765,385

U.S patent number 5,765,385 is invented by Michael A. Childs. The patent is for a self-cooling beverage container which couples to an external refrigerant storage device. The refrigerant is separately stored as a saturated liquid in an external vessel which can be attached securely to the can. The can has an internal single or double helix tube which runs the vertical length of the can. One end of the tube connects to the refrigerant vessel when attached, and the other end is open to the atmosphere when the consumer opens the beverage cap. Refrigerant is expanded into the helical tubes to provide the cooling of the beverage inside the can [7].

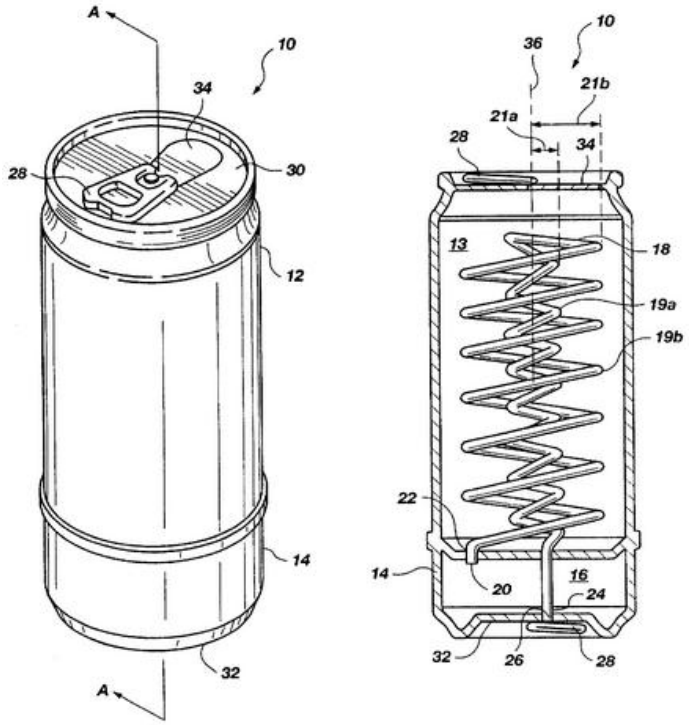

Figure 2.5: Self-cooling can design by Childs [7].

2.2.2 Refrigerant Based with Capture

Refrigerant based designs with capture work similar to direct refrigerant release designs because the cooling is provided in much the same way. However, the refrigerant gases produced after evaporation is captured as to not release any refrigerant gases into the environment. Either the refrigerant gases are absorbed into the beverage, like in U.S. Patent No. 6,167,718 B1, or it is completely absorbed by a desiccant like in U.S. Patent No. 6,829,902 B1.

2.2.2.1 U.S Patent No. 5,325,680

U.S patent number 5,3225,68 is invented by Francisco J. Baroso-Lujan and Ernesto M. Galvan-Duque. The patent is for a self-cooling beverage container with evacuated refrigerant receiving chamber. The design consists of a can which has an integral cooling

system which does not release any refrigerant. The cooling system contains two compartments. One compartment holds the compressed liquid refrigerant such as R22, or a refrigerant of similar or thermal properties. The other compartment is used to hold the expanded refrigerant and prevent it from escaping to the environment [8]. This design is not effective because there is not sufficient volume for the refrigerant to expand into for the refrigerant to throttle effectively.

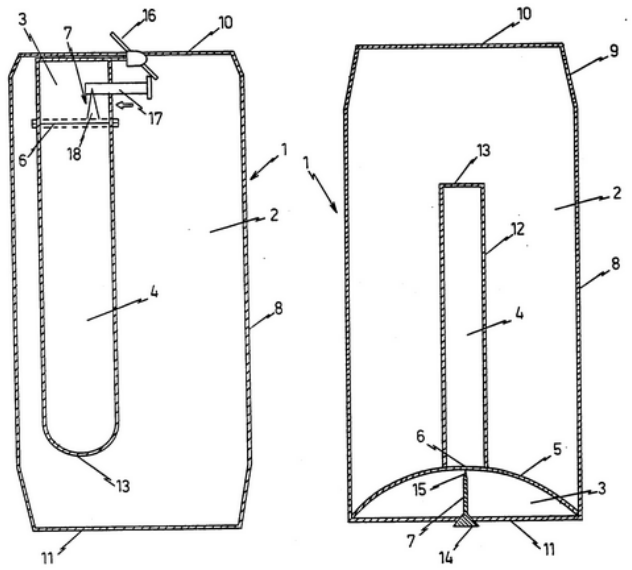

Figure 2.6: Self-cooling can design by Baroso-Lujan and Galvan-Duque [8].

2.2.2.2 U.S. Patent No. 6,167,718 B1

U.S patent number 6,167,718 B1 is invented by Edward M. Halimi and W. Carl Gans. The system that is proposed in this patent is a self-carbonating, self-cooling beverage container. The idea is to store compressed liquid carbon dioxide in an internal vessel which is used to carbonate and cool the intended beverage. The vessel is situated internally in the middle of the can. A puncturing system releases the liquid carbon dioxide from the storage container which allows for rapid expansion of the carbon dioxide. The throttled carbon dioxide has direct heat transfer the beverage and provides

carbonation [9]. This design is also not effective because the amount volume the carbon dioxide has to expand into is not sufficient for effective throttling. Also, carbon dioxide has a low heat of evaporation, thus it requires large quantities of carbon dioxide to provide the necessary cooling.

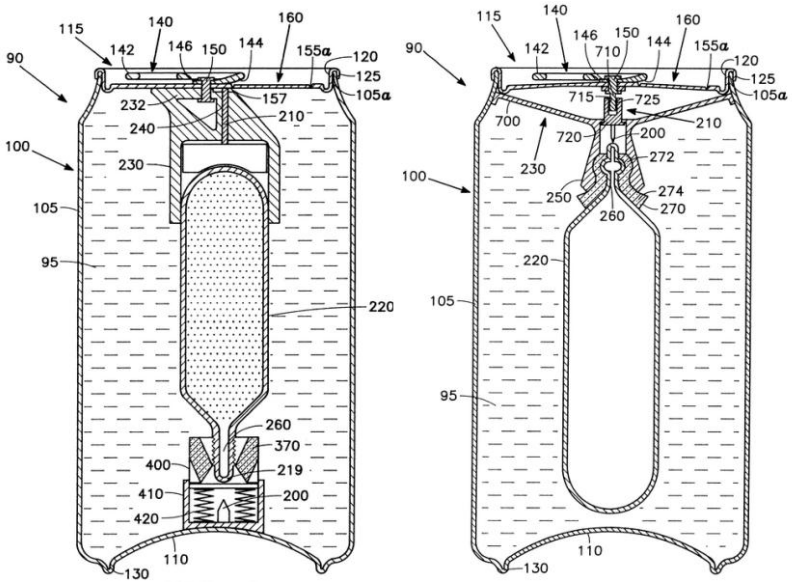

Figure 2.7: Self-cooling beverage can design by Halimi and Gans [9].

2.2.2.3 U.S. Patent No. 6,829,902 B1

U.S patent number 6,829,902 is invented by Paul Charles Claydon. The design can cool a 300 ml beverage by 30°F in within 3 minutes. The can contains an integral heat evaporator and an absorber unit which is fixed to the bottom of the can. Cooling is initiated by connecting the external adsorption unit to the evaporator. Heat is removed from the evaporator by evaporating a refrigerant. The adsorption unit adsorbs all the vapour from the evaporated refrigerant and then becomes hot. The heat is then released into the environment [10].

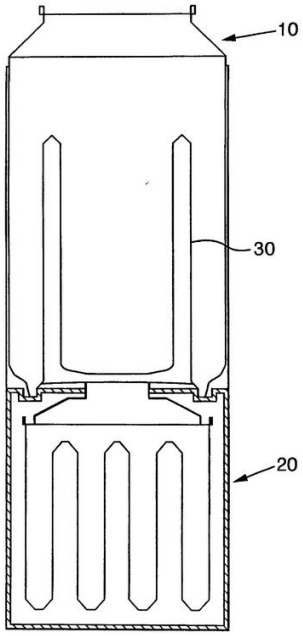

Figure 2.8: Self-cooling beverage can design by Claydon [10].

2.2.3 Endothermic Reaction Based

Endothermic reaction based designs differ from the previous two methods. It does not use refrigerant expansion to provide the necessary cooling to the beverage. Instead, it uses strong endothermic reactions to provide the cooling load. Some designs use endothermic dissolution reactions, and some designs use endothermic reactions where there are chemical changes to the reactants. In this subsection, three patents are presented which use some form of endothermic reaction cooling method.

2.2.3.1 U.S. Patent No. 20,120,144,845 A1

U.S. patent number 20,120,144,845 A1 is invented by Daved D. Leavitt, John R. Bergida. This is a self-cooling beverage can which utilizes an endothermic reaction to cool the beverage inside the can. The reaction is with ammonia nitrate and water dissolution to provide the cooling. The endothermic reaction is activated by puncturing a film dividing

the two reactants. The patent proposes that the liquid solution containing the ammonia nitrate may be used later during recycling as fertilizer for plant life [11].

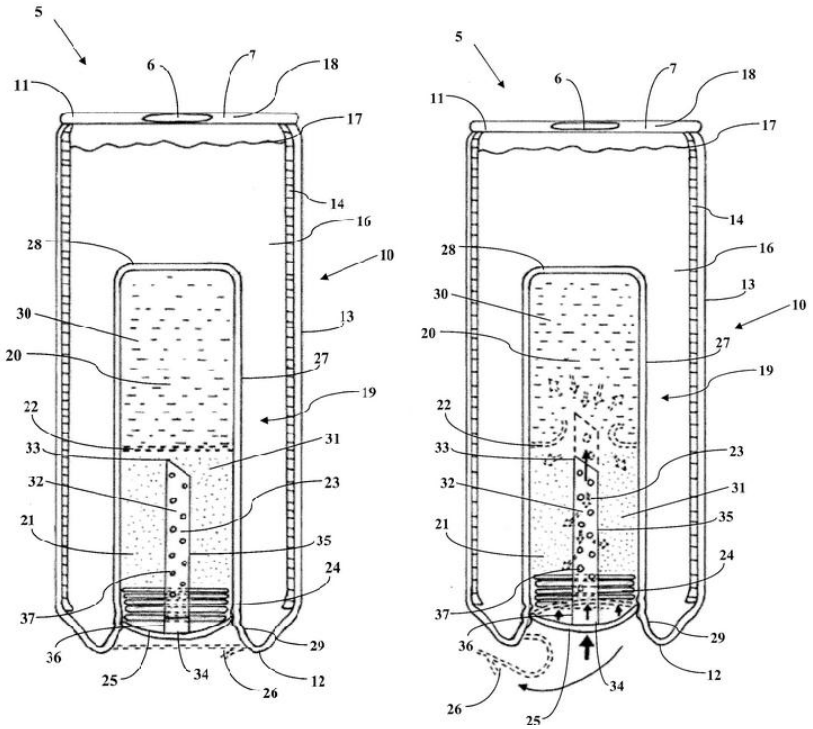

Figure 2.9: Self-cooling beverage can design by Leavitt and Bergida [11].

2.2.3.2 U.S. Patent No. 20,130,098,069 A1

U.S. patent number 20,130,098,069 A1 is invented by Patrick Collins. In his proposed self-cooling beverage can design there is an outer wall surround an inner can which contains the beverage. In between the wall is a liquid which is mixed with a chemical, thus producing an endothermic reaction which cools the beverage on the exterior wall of the beverage container. The chemicals are stored in the base of the can, and are released by a rupturing device which allows for the mixing of the two reactants. This design is unique, but it has a major challenge of accessing the drink once it is cooled [12].

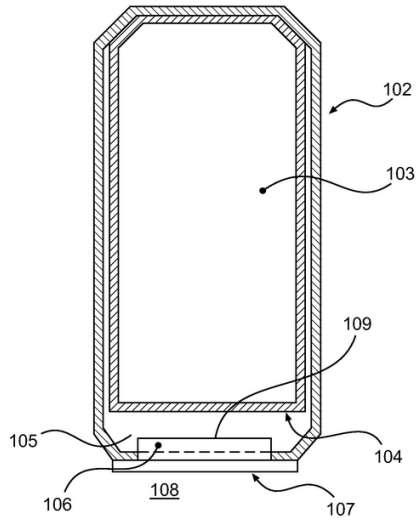

Figure 2.10: Self-cooling beverage can patent picture by Collins [12]

2.2.3.3 U.S. Patent No. 20,130,174,581 A1

U.S. patent number 20,130,174,581 A1 is invented by Jan Norager Rasmussen, Steen Vesborg, and Martin Gerth Andersen. Their design for a self-cooling beverage can involves having a separate free container situated inside of the beverage can to provide cooling by means of endothermic reaction between two salts. Their proposed reaction is non-toxic, producing non-toxic products. The reaction is triggered via mechanical means. There is a great challenge to mechanically actuate the cooling method since the reaction vessel does not seem to have a connection with the exterior of the can [13].

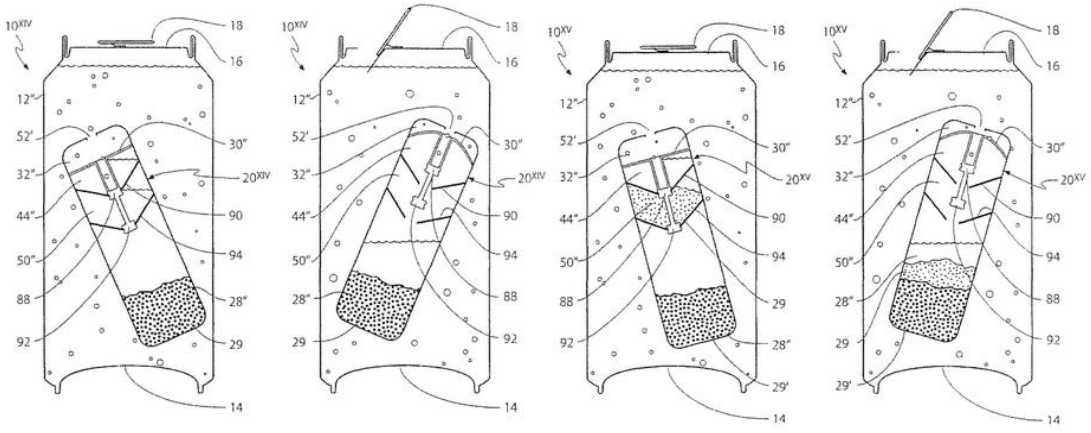
Figure 2.11:Self-cooling beverage can design by Rasmussen, et al. [13].

2.2.4 Patent Survey Summary

In this section a comparison of all the patents that are discussed in the previous section are presented in Table 2.1. This table summary of the patents is useful in helping the reader understand the advantages and disadvantage of each of the patents.

Table 2.1: Comparison of the patent survey with advantages and disadvantages.

Type	U.S. Patent Number	Advantages	Disadvantages
Direct Refrigerant Release	3,597,937	- High surface area of heat transfer -Throttling in coil provides better cooling	- Lower beverage volume - Complicated design
	4,656,838	- Simple design	- Throttled refrigerant is not effectively used
	5,447,039	- Very high surface area of heat transfer	- Complicated design leading to more material costs
	5,555,741A	- Manufacturing process is solved	- Low heat transfer surface area
	5,765,385	- Effective use of cooling coil for heat transfer surface area	- Double coil design may have complications in manufacturing
Refrigerant Based with Capture	5,325,680	- Simple refrigerant capture design	- Ineffective due to low expansion volume
	6,167,718 B1	- Carbonation and cooling in one process	-Cooling is not effective with carbon dioxide
	6,829,902 B1	- High surface area of heat transfer - Desiccant capture method	- Heat generated from desiccant may cause heating to the beverage - Additional materials
Endothermic Reaction Based	20,120,144,845 A1	- High reaction rate with fluid and solid	- Dissolution reaction may not provide a high enough heat of reaction
	20,130,098,069 A1	- Entire exterior of beverage container is the heat transfer surface area	- Additional outer can required - Cooling may be affected greatly by ambient condition
	20,130,174,581 A1	- Uses environmentally safe chemical salts	-Activation of reaction is uncertain

2.3 Market Survey

2.3.1 West Coast Chill

A small, but expanding United States company by the name Joseph Company International has developed a self-cooling beverage can which is commercially available. They have developed a self-cooling energy drink product which self-cools within several minutes. The product's name is West Coast Chill. However the technology behind the cooling is not from refrigerant expansion or endothermic reactions. Their can works using a built in Heat Exchanger Unit (HEU) which uses a C-CO2 adsorbent-desorption system to cool the beverage in the can. Their design uses a physical cooling process. Figure 2.12 shows a picture of the product. Note the activation tab is at the bottom which starts the cooling process [14]. The West Coast Chill self-chilling can is patented under U.S. Patent No. 20130213080 A1 [15].

Figure 2.12: West Coast Chill's self-chilling can [14].

2.3.2 ICETEK

The company Icetek has produced a commercially available product which uses direct refrigerant release shown in Figure 2.13. The company claims that the refrigerant being

used in the cooling of the beverage is safe for humans and the environment. The specific refrigerant, or refrigerant blend, is proprietary information. The design is based on the patent US 6,619,068 B2 as seen in Figure 2.14. The inventor of the Icetek can is Won Gil Suh. This product originated in South Korea, but may be ordered online through their website [16].

Figure 2.13: IceTek self-cooling can [16].

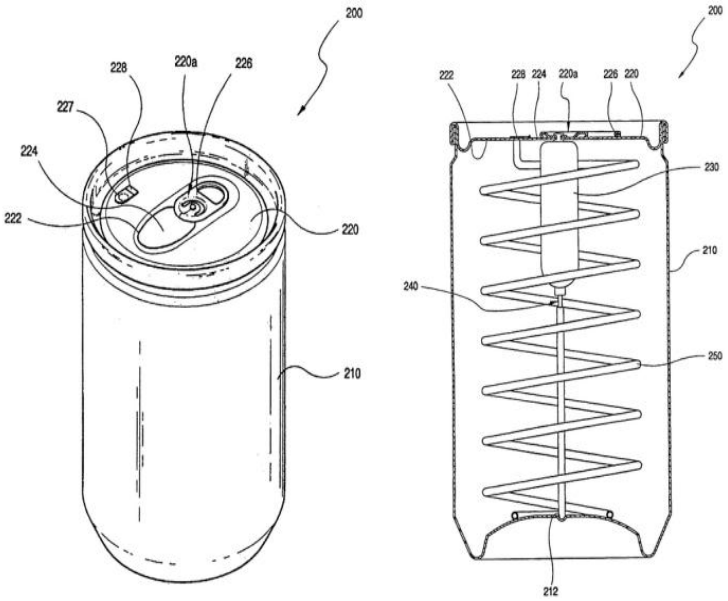

Figure 2.14: Patented drawing of the Icetek's self-cooling beverage can [17].

2.3.3 I.C Can

The company Tempra Technology and Crown Holdings has a self-cooling beverage can which is commercially available. They claim that it is 100% environmentally safe. It uses water evaporation as a means of providing the cooling. This design is based off of their patent, U.S. Patent No. 6,829,902 B1. On their website, they claim to be able to provide a temperature drop of 16.7℃ in just 3 minutes. This cooling is possible because of the "latest breakthrough in thermal, insulating and vacuum heat pump technology." However, more information about the specifics of the process is not released. The total volume of the can is approximately 500 ml [18].

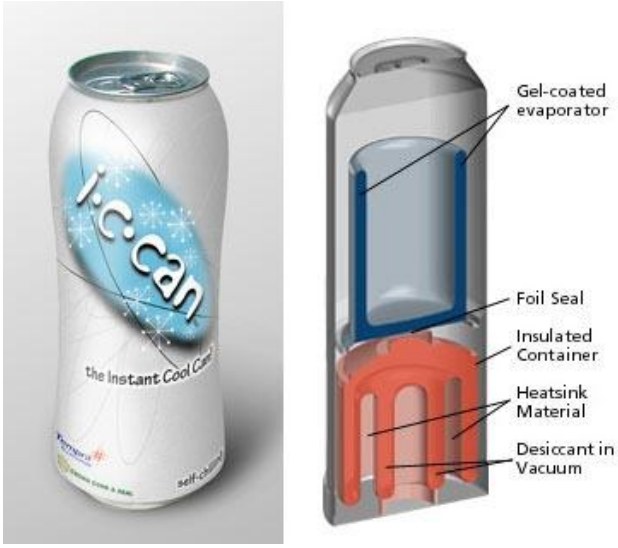

Figure 2.15: Self-cooling beverage can designed by Tempra Technology and Crown Holdings [18].

2.3.4 Market Survey Summary

In this section a comparison of the current products on the market are summarized in a table to show their advantages and disadvantages. The market survey is summarized in Table 2.2. This is table allows the reader to quickly assess the key differences between the products.

Table 2.2: Comparison of the market survey with advantages and disadvantages.

Product	Advantages	Disadvantages
West Coast Chill	- Uses desorption process for cooling - Takes in carbon dioxide during operation	- Small volume of beverage - Heavy can design, a lot of additional material
IceTek	- Effective cooling with coil design - Uses safe refrigerant	- Release of refrigerant may have long term environmental issues
I. C. Can	- High surface area of heat transfer	- Heat generated from desiccant can cause heating to the beverage - Additional materials

Chapter 3: Background

3.1 Thermodynamics of Self-cooling Beverage Can

The first law of thermodynamics states that energy cannot be created nor destroyed, energy can only transform from one form to another. This law is important to understand because the process of cooling is a thermodynamic process. In the case of a self-cooling beverage can, potential energy is stored in a separate compartment from the beverage to provide a temperature difference. This temperature difference is what is required for cooling of the beverage.

3.2 Conventional Can Cooling Systems

3.2.1 Refrigerator

Conventional refrigeration systems operate on the refrigeration cycle. Refrigeration is a major application of thermodynamics. Refrigeration deals with the transfer of heat from one region to another to cool an objective medium. The most frequently used refrigeration cycle is the vapour-compression refrigeration cycle in which the refrigerant is vaporized and condensed to achieve heat rejection out of the system and provides the cooling effect for the objective fluid. Figure 3.1 shows a diagram of the vapour compression refrigeration cycle.

Refrigerant is compressed in the compressor which increases its temperature and pressure. Leaving the compressor, the refrigerant is a superheated gas. The hot refrigerant gas is sent to the condenser. The temperature of the refrigerant at this point is higher than the temperature of the surrounding ambient condition. This allows for the heat to be rejected out of the system. The refrigerant is condensed because of the loss of heat to the

surroundings. From there the refrigerant is expanded in a throttling valve. The rapid expansion of the refrigerant drops the refrigerant pressure from high pressure to a very low pressure. This causes the refrigerant to cool down dramatically due to the Joule–Thomson effect. Usually the temperature drops well below 0℃ when considering R134a. The refrigerant is now very cold, and it is colder than the medium surrounding the evaporator. This allows for the refrigeration system to cool the medium surrounding the evaporator thus providing the refrigeration. This is the basic operating principle all refrigerators used to keep food items cold.

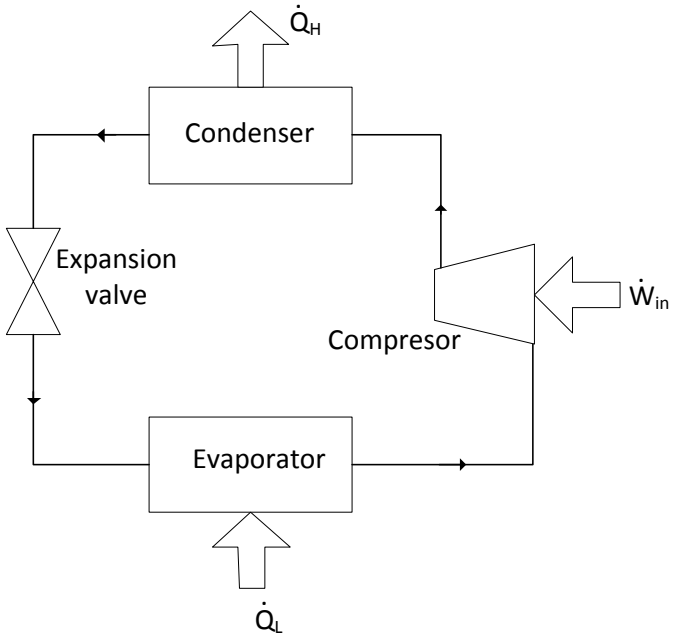

Figure 3.1: Schematic diagram of a simple vapour compression refrigeration cycle.

3.2.2 Cooler

Coolers work by using a phase changing material to provide cooling. A cooler is basically a well-insulated box where beverages or other food items are cooled by ice. The ice provides cooling over a long period of time by extracting thermal energy from the beverages it is in contact with; by melting into its liquid form, hence the phase changing

material. The heat of fusion of water is 334 kJ/kg at 0℃. For every kilogram of ice that is melted, 334 kilojoules of energy is ideally removed from the beverages inside of the cooler. That equates to about 10 cans of 355 ml beverages, cooled down by 20℃.

3.3 Types of Refrigerants

There are several types of refrigerants that exist. Some of the common refrigerants are hydrochlorofluorocarbons (HCFC) hydrofluorocarbons (HFC) hydrocarbons (HC), and natural refrigerants.

HCFCs are organic and synthetic chemical refrigerants. HCFCs have a potential to deplete the ozone layer, therefore has and ozone depletion potential (ODP). Because of their ODP, this type of refrigerant is not acceptable for self-cooling cans that use direct refrigerant release methods. Also it is toxic to human inhalation [19].

HFCs are refrigerants that only contain fluorine, carbon and hydrogen. They are also synthetically produced. HFCs are used in applications such as refrigeration, and fire-extinguishers. HFCs do not have an ODP, however, they can contribute to global warming. HFCs are still not an option for utilizing in self-cooling beverage cans since they are also toxic to human inhalation [19].

HCs are refrigerants that are composed of hydrocarbon chains such as isobutane, propylene, propane etc. These refrigerants are considered to have low environmental impact. They do not have and ODP, but they still may have adverse effects on the environment. HCs are not toxic to humans in small volumes, which makes this type of refrigerant a possible candidate for release and capture methods [19].

Natural refrigerants are naturally occurring substances that exist in nature. Some naturally occurring refrigerants are HCs (i.e. propane, isobutane) , carbon dioxide, ammonia, water and air. Some of these substances are used in refrigerators and air conditioners. Natural refrigerants do not harm the ozone layer and have little to no global warming impact. It is ideal to use a natural refrigerant as the refrigerant of choice for refrigeration throttling based self-cooling beverage cans [19].

In this study ammonia is the refrigerant of choice for the proposed conceptual self-cooling beverage can design. This refrigerant is easily adsorbed by a desiccant salt mixture of magnesium chloride and aluminum oxide. Desiccant salt mixtures are explained in the next section.

3.4 Adsorption Process

Adsorption is the process of an adsorbate attaching to an adsorbent. Adsorbate is the material being adsorbed in the adsorption process. The adsorbate can either be solid, liquid or gas. The molecules of adsorbate physically bond to the surface of the adsorbent, but it does not undergo a chemical reaction where chemical compositions of the adsorbate and adsorbent change. This process is important to the research, because strong adsorbents can provide an attractive solution for refrigerant expansion with capture based self-cooling beverage can designs. Using a strong chemical desiccant, it is possible to adsorb the all of the evaporated refrigerant which is released during the cooling process.

Some examples of desiccants are phosphorus pent-oxide, calcium chloride, calcium bromide, zinc bromide, zinc chloride, aluminum oxide, sodium hydroxide, potassium hydroxide and magnesium perchlorate [20]. Sharonov and Aristov have tested

mixtures of desiccants showing a higher yield for adsorption capacity. Their most successful experiment is the adsorption of ammonia into a descant mixture of aluminum oxide and magnesium chloride. The adsorption that is achieved in their experiment involving the adsorption of ammonia in nitrogen stream with magnesium chloride is 58.6mg of ammonia to 1 gram of desiccant mixture [21].

3.5 Endothermic Reactions

An endothermic reaction is a chemical reaction or chemical change that requires heat energy input for it to occur. This means when a reaction occurs between two substances, the reaction takes in thermal energy from its surrounding to provide the energy for the reaction. The endothermic reaction that is considered in this study is the reaction between ammonium thiocyanate and barium hydroxide octahydrate. This reaction is tested in an experimental setup to confirm its validity to provide cooling to 300 ml of beverage. The chemical reaction is discussed further in a later section of the thesis.

Chapter 4: Experimental Apparatus and Procedure

In this chapter, two experimental systems are presented that are used to test the validity of the two previously mentioned cooling methods. From the experiments, key parameters are determined for the analytical and numerical modeling of two proposed designs which are presented later in this chapter. Each component of the experimental systems are described and an explanation of their purposes are given. The experimental procedures for both experiments are presented. Finally a description of the conceptual self-cooling beverage cans designs which incorporate the tested methods are presented.

The objective of creating a self-cooling beverage can that is environmentally friendly limits the choices for cooling methods. Direct release of refrigerant is definitely not an option. The methods of cooling that are left are refrigerant throttling with capture and endothermic reaction based. In this research the just mentioned methods of cooling are tested experimentally.

The first cooling method is the refrigerant throttling with capture. The refrigerant that is chosen for providing the cooling is ammonia. Ammonia is a good choice of refrigerant for this application because the system is limited by the volume of stored refrigerant. Since ammonia has a high heat of evaporation, only a small volume of throttled ammonia is required to cool a beverage to satisfactory temperatures. The evaporated ammonia gases are adsorbed by a desiccant salt mixture which Sharonov and Aristov have tested [20]. A mixture of aluminum oxide and magnesium chloride are used in the experiments. Magnesium chloride has a high adsorption capacity, whereas aluminum oxide has a lower adsorption capacity, but it is highly porous when compared

to magnesium chloride. The combination of the two-salts provides a high capacity porous desiccant mixture which can adsorb ammonia gas in large amounts at a fast rate.

The second method that is tested is the endothermic reaction based cooling method. The endothermic reaction that is considered is the reaction between ammonium thiocyanate and barium hydroxide octahydrate. The stoichiometric reaction is presented as follows:

$$Q_{rxn} + Ba(OH)_2 \cdot 8H_2O(s) + 2NH_4SCN(s) \rightarrow Ba(SCN)_2(s) + 10H_2O(l) + 2NH_3(g) \quad (4.1)$$

This reaction is one of the strongest and most well-known endothermic reactions. As such it is used to test the effectiveness of endothermic based self-cooling beverage cans. The ammonia gas released in the experiments is vented into a fume hood, but in the proposed can design, it is adsorbed by the desiccant salt mixture as previously mentioned.

Following the experimental work there are two proposed conceptual designs that are presented. The conceptual designs incorporate the cooling methods that are tested experimentally into compact cooling systems to make a self-cooling beverage can. These conceptual designs are studied analytically and numerically using the aid of a software programs. Engineering Equation Solver (EES) is used for the analytical analysis, and COMSOL is used for the numerical analysis.

A flowchart of the work that is done for this thesis study is presented in Figure 4.1. This flowchart shows the overall progression of the thesis work in a chronological order.

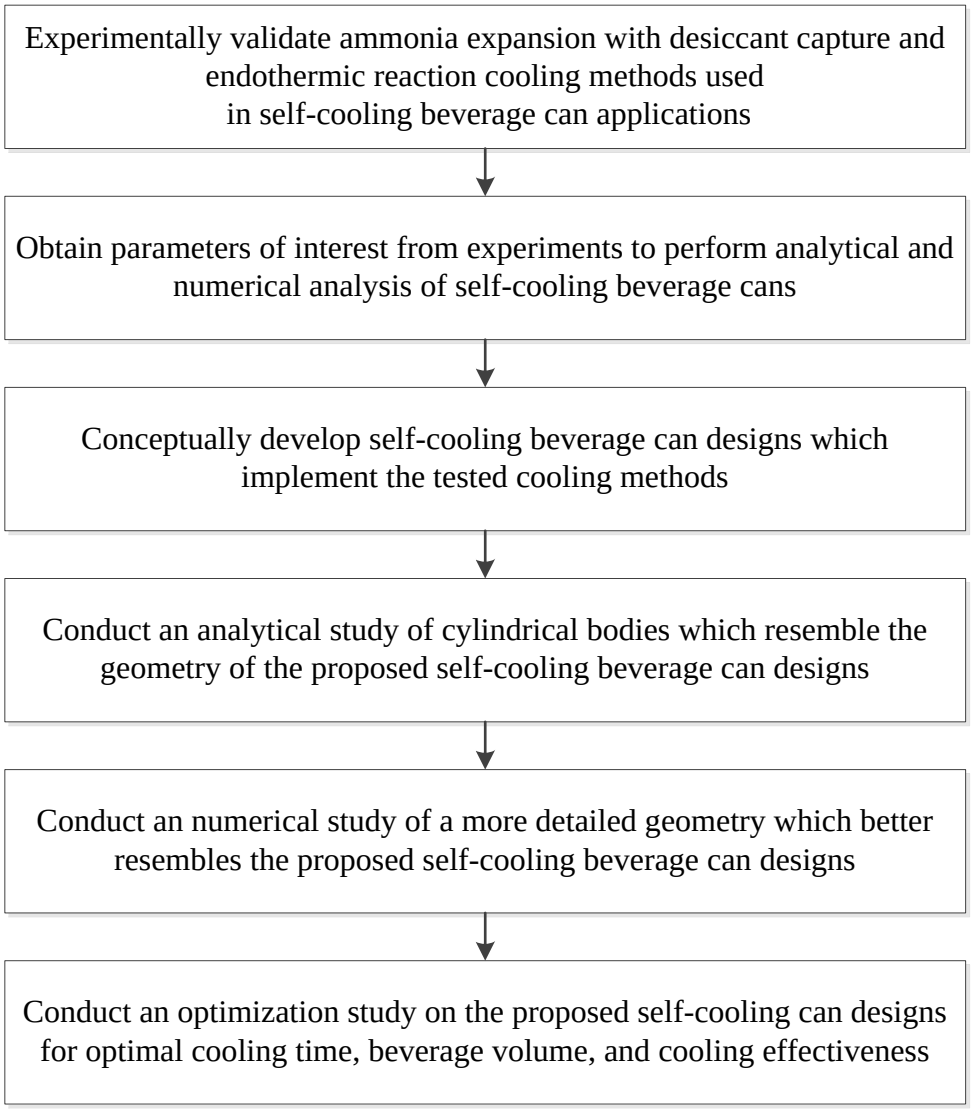

Figure 4.1: An outline of the overall summary of the thesis research.

4.1 Experiment 1: Ammonia Expansion with Desiccant Salt Capture

Experiment 1 tests the validity of cooling a volume of beverage using expansion of liquid ammonia. It also tests the capturing of the ammonia gas using magnesium chloride and aluminium oxide as a desiccant salt mixture, such that ammonia does not escape into the surrounding atmosphere. A schematic diagram of the system is presented in Figure 4.2, followed by a photograph of the system shown in Figure 4.3.

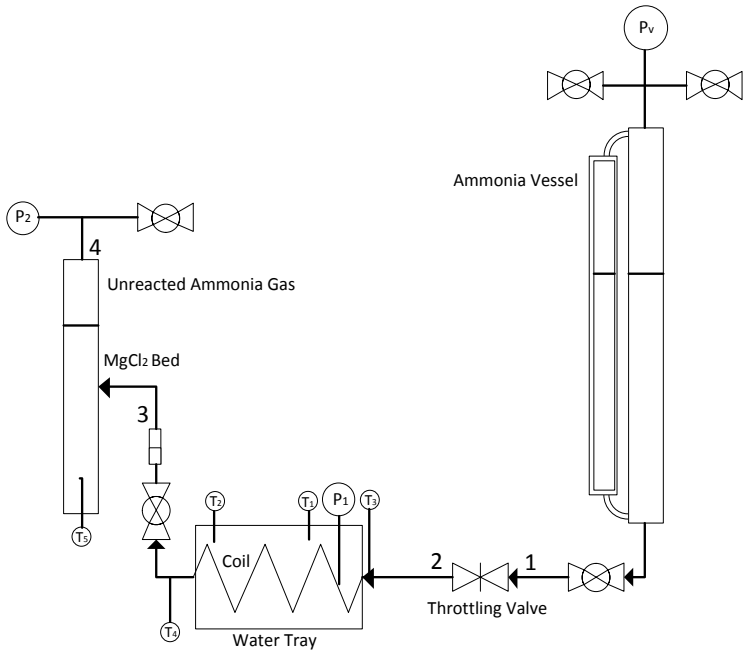

Figure 4.2: Ammonia and magnesium chloride test system for proof of concept.

Figure 4.3: Photograph of the experimental test system which is used for validating the ammonia and desiccant adsorption cooling method.

4.1.1 Ammonia Vessel

The purpose of the ammonia vessel (Figure 4.4) is to store liquid ammonia at the ambient temperature at the corresponding saturation pressure. The ammonia is released through the bottom of the vessel so that only liquid ammonia is released for throttling. During the experiment, liquid ammonia is released from the ammonia vessel to be expanded through the throttling valve opening ball valve. There is a pressure gauge that reads the saturation pressure P_v and a metering glass which shows the level of liquid ammonia inside the system.

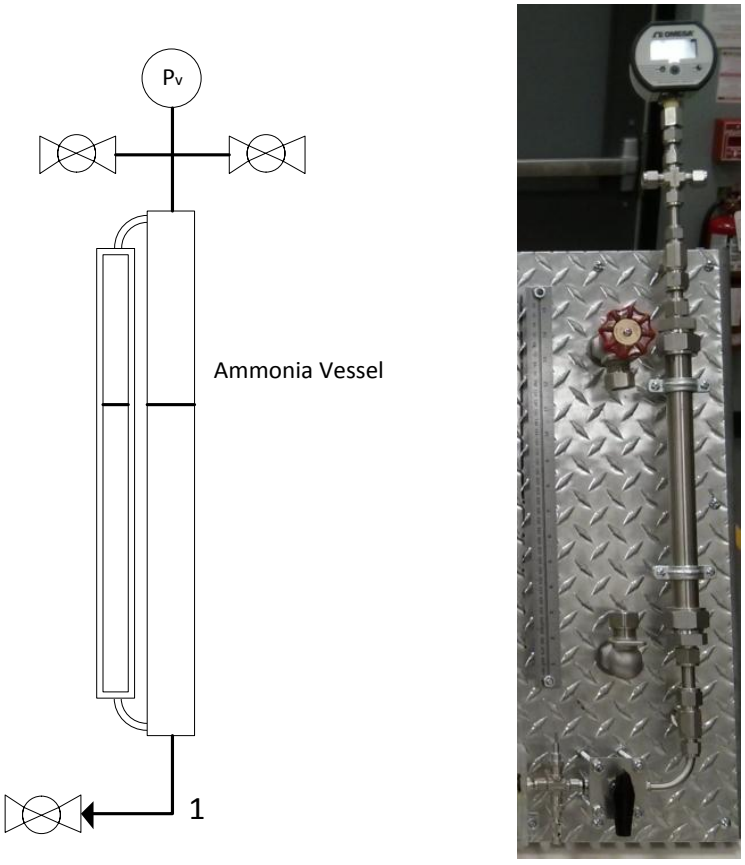

Figure 4.4: Ammonia vessel which contains saturated ammonia liquid-vapour under saturation pressure at the ambient temperature. The pressure vessel is fitted with glass level meter to visibly see the level of liquid ammonia in the vessel.

4.1.2 Throttling Valve

The purpose of the throttling valve (Figure 4.5) is to expand the ammonia from a saturated liquid to a significantly cooler saturated liquid vapour mixture. The flow of the ammonia can be very finely adjusted to provide the optimal flow of ammonia to be throttled. The valve in use is a Swagelok SS-SS2-D Valve, which is a twin needle valve having a cv between 0 to 0.004.

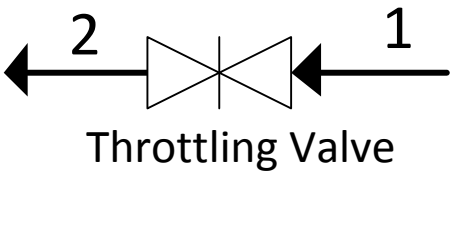

Figure 4.5: The throttling valve is a double pattern needle valve which can finely adjust the flow and expansion of the ammonia.

4.1.3 Cooling Coil

The purpose of the cooling coil (Figure 4.6 and Figure 4.8) is to provide the means of thermal contact to cool the beverage with ammonia. During the experiment the thermal energy of the beverage is drawn into the coil due to the much cooler ammonia, thus cooling the beverage. Saturated liquid-vapour ammonia is evaporating inside the coil due to the heat obtained by the beverage. The cooling coil is the heat exchanger for beverage and ammonia. Ammonia leaves the coil as a vapour. There is a temperature and pressure sensor at the beginning of the coil and there is a second temperature sensor at the end of the coil.

4.1.4 Water Tray

The purpose of the water tray (Figure 4.8 and Figure 4.7) is to hold water that is to simulate the volume of beverage to be cooled. The cooling coil is submerged in the water to provide the cooling. There are two temperature sensors which read the water temperature.

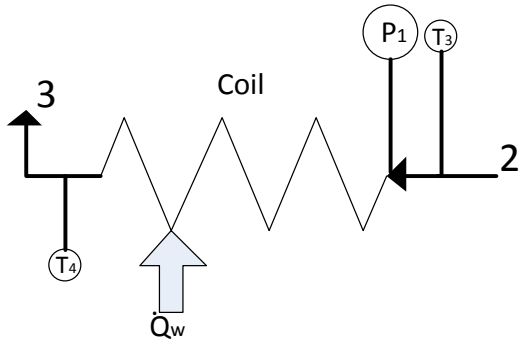

Figure 4.6: Cooling coil that is submerged in the volume of beverage to be cooled.

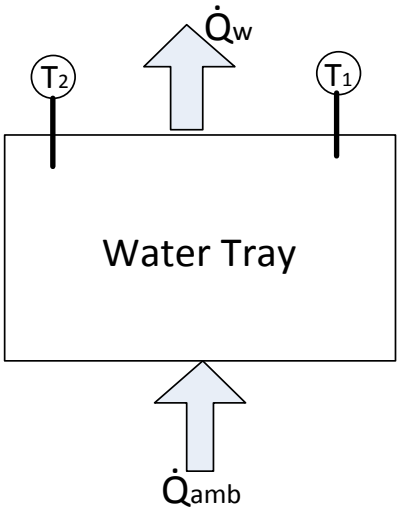

Figure 4.7: The water tray holds 1.25L of water to simulate the beverage to be cooled.

4.1.5 Adsorption Bed

The purpose of the magnesium chloride bed (Figure 4.9) is to provide a reactor for the ammonia and magnesium chloride absorption. NH_3 vapour enters the $MgCl_2$ Bed and is

absorbed into the powder $MgCl_2$. The adsorption process also releases some heat. Some ammonia may not be absorbed instantly and may remain in the area above the desiccant salts due to poor surface area of adsorption. There is a temperature sensor which is in direct contact with the magnesium chloride bed which reads the temperature during the absorption process. The adsorption bed is connected to the coiling coil by a quick release valve which makes removal of the adsorption bed easier. Removal and cleaning of the adsorption bed is done in-between experiments for cleaning and preparation.

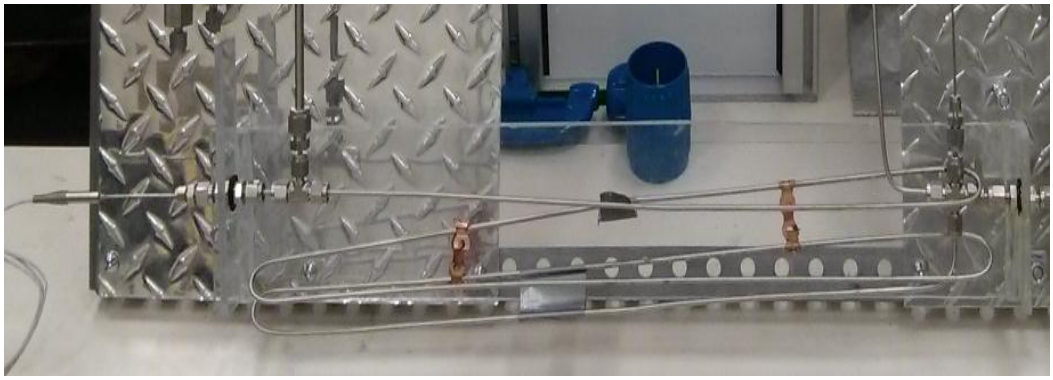

Figure 4.8: Photograph of the water tray and cooling coil in experimental setup 1.

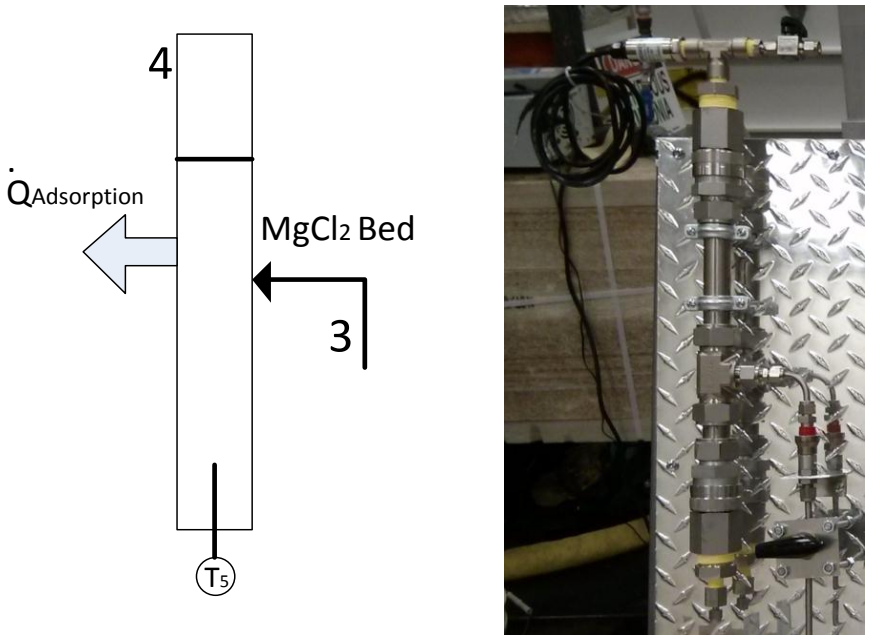

Figure 4.9: The magnesium chloride bed stores the desiccant salt mixture used in the adsorption process.

4.2 Experimental Procedure for System 1

4.2.1 Charging the Ammonia Vessel

To charge the ammonia the following procedure is taken to ensure that liquid ammonia enters into the system. Valve 1 is the ball valve located to the left side of the T-fitting, valve is the ball valve to the right of the T-fitting, and Valve 3 is the ball valve near the bottom of the ammonia vessel.

1) Ensure all valves leading to and from the ammonia vessel are in the off position.
2) Connect the nitrogen gas line to valve 1 and then open valve 1 and 3. Turn on the nitrogen gas to purge the ammonia vessel of all other gases.
3) Close valve 3, then valve 1, and turn off the nitrogen gas before disconnecting the nitrogen gas line.
4) Secure the cylinder containing the ammonia upside down on the cylinder stand situated above the ammonia vessel. Connect the ammonia cylinder to valve 2 using the pressure hose.
5) Connect a vacuum pump to valve 1, and turn on the pressure gauge and vacuum pump.
6) Open valve 1 and 2 to let the vacuum pump draw out the nitrogen gas to create a vacuum in the vessel and the pressure hose. Close valve 1 when the pressure gauge has stabilized in vacuum pressures. Turn off vacuum pump.
7) Open the ammonia cylinder valve to allow the flow of ammonia into the ammonia vessel. Observe the level glass to see how much liquid is in the ammonia vessel.
8) Close ammonia cylinder valve when liquid ammonia has reached half the vertical height of the glass tube. Let the remaining ammonia in the hose flow into the ammonia vessel and then turn close valve 2.

9) Disconnect the ammonia hose from valve 2.

4.2.2 Preparing the Adsorption Bed

The following procedure is used to fill the adsorption bed with the magnesium and aluminum oxide salt mixture. Since desiccants are highly sensitive to moisture in the atmosphere, all preparations are done inside a semi-vacuum glove box with a dry nitrogen environment.

1) Open the glove box and place electronic mass measuring scale, funnel, scapula, plastic trays, magnesium chloride container, aluminum oxide container, and adsorption bed vessel before sealing the glove box shut.
2) Connect the vacuum pump and the nitrogen gas line to the glove box in their appropriate places and turn on the vacuum pump until a partial vacuum is formed (If the pressure inside the glove box gets too low, it may cause structural failure to the glove box.)
3) Fill glove box with nitrogen until the pressure inside the glove box is back to ambient pressure. Repeat steps 2 and 3 one more time to reduce the moisture level even further.
4) Turn the electronic mass scale on, and place a tray on top of the scale. Zero the scale by pressing the tare button. Using a separate scapula for each salt, fill each tray with 50 g of each salt.
5) Mix the two-salts together in a separate tray so that they are evenly mixed. Open the adsorption bed by removing the top end of the vessel and pour the salt mixture into the adsorption bed with the help of the funnel.
6) Seal the reaction bed by replacing the top end of the vessel.

7) Replace the lids for the salt containers before opening the glove box.
8) Take the sealed adsorption bed out of the glove box and connect it to the vacuum pump. Vacuum the remaining gases inside the adsorption bed to remove as much nitrogen as possible. Hold the adsorption bed in its vertical position as to not let the salts get vacuumed out.
9) Reattach the adsorption bed back into the experimental setup via quick release valve.

4.2.3 Conducting the Experiment

Once the ammonia vessel and adsorption bed are prepared, the experiment can be conducted under a fume hood. The following procedures are used to run the experiment:

1) Place experimental setup into the fume hood and setup data acquisition devices and laptop next to the fume hood. Ensure all sensors are connected and are in the correct location. Turn on the ammonia vessel pressure gauge.
2) Set the throttling valve to the correct amount of turns for the current experiment.
3) Open the cooling coil valve to allow the flow of ammonia to reach the adsorption bed.
4) Launch data acquisition software and begin reading the data from the sensors.
5) After 30 seconds of continuous data recording open the valve 3 to start the experiment.
6) Observe and record the ammonia pressure gauge readings and level of ammonia left in the system every 30 seconds.
7) Allow for experiment to run until pressure in the adsorption bed reaches 100 psi.

8) Shut off ammonia vessel valve and cooling coil valve. Save all the data and notes for further analysis.

4.3 Experiment 2: Endothermic Reaction

Experiment 2 tests the two-salt endothermic reaction cooling method. It works by reacting ammonium thiocyanate and barium hydroxide octahydrate to provide cooling to beverage. The chemical equation which provides the cooling is as stated,

$$Ba(OH)_2 \cdot 8H_2O\ (s) + 2\ NH_4SCN\ (s) \rightarrow Ba(SCN)_2\ (s) + 10H_2O\ (l) + 2NH_3\ (g) + \text{Cooling}$$

This reaction occurs in the reaction vessel of the can system as depicted in Figure 4.10. The thermal energy of the beverage is drawn in towards to the reaction vessel due to the endothermic reaction, thus cooling the beverage.

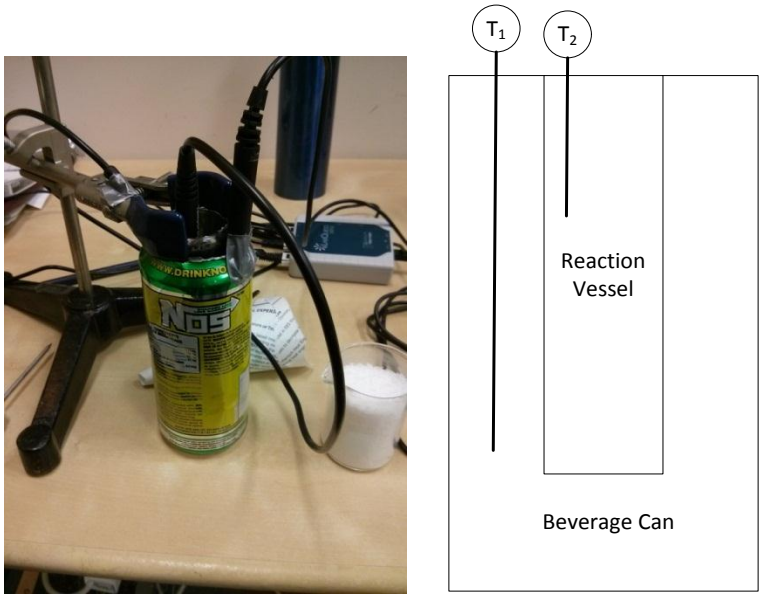

Figure 4.10: Experimental test system for the endothermic reaction consisting of reaction vessel inside of a beverage can.

4.3.1 Beverage Can

The purpose of the beverage can is to provide a container for the beverage. The beverage can is subjected to two sources of heat transfer. Heat leaving the beverage into the reaction is $\dot{Q}_{rxn}$. Heat entering the beverage from natural convection with the air is defined as $\dot{Q}_{in}$. The volume of beverage the can holds during the experiment is 300 ml with the reaction vessel submerged in the beverage inside. A thermocouple is used to measure the temperature of the beverage and its temperature is measured as T_1.

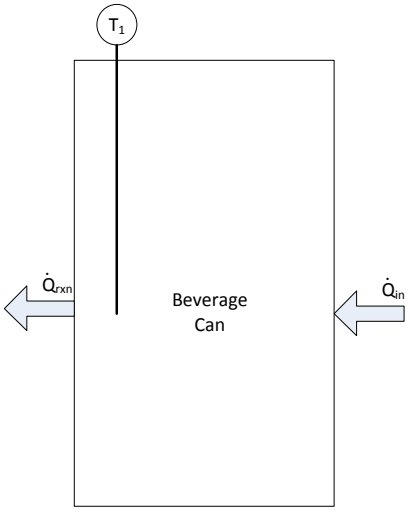

Figure 4.11: Schematic diagram of the beverage can with energy flow from experimental setup 2.

4.3.2 Reaction Vessel

The purpose of the reaction vessel is to provide a reactor for the endothermic reaction to occur. The two-salt endothermic reaction requires heat as described earlier. This heat is defined as $\dot{Q}_{rxn}$, and it is the main heat transfer load which provides the cooling. A thermocouple is used to measure the temperature of the contents inside the reaction. Temperature inside the reaction vessel is measured as T_2. The reaction vessel has a volume of 140 ml.

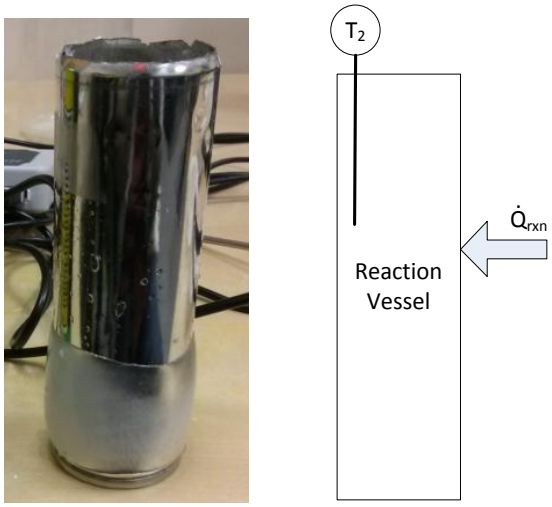

Figure 4.12: Reaction vessel for the two-salt endothermic reaction configuration.

4.4 Experimental Procedure for System 2

4.4.1 Preparing the Beverage Can

The following procedure is used to prepare the beverage can for experimentation.

1) Empty the contents of a 475 ml can of its contents.
2) Using a saw, cut off the top of the can, thus exposing the inside of the can.
3) Fill the can with 300 ml of beverage or water, depending on the experiment.

4.4.2 Preparing the Reactants

The following procedure is used to prepare the ammonium thiocyanate and barium hydroxide octahydrate for the experiment. The apparatus required for preparing the two chemicals are the chemicals themselves, two scapulae, two trays and an electronic mass scale.

1) Place a tray on the electronic mass scale and tare the scale.
2) Using the scapula place 50 g of barium hydroxide octahydrate on the first tray.
3) Repeat steps 1 and 2 for 100 g of ammonium thiocyanate.

4.4.3 Conducting the Experiment

The following procedure is used to conduct the two-salt endothermic reaction cooling method. At this point of the experiment, the reaction vessel is empty and the beverage can is filled with 300 ml of beverage. The experiment requires a retort stand, retort stand clamp, data acquisition, funnel and stirring rod.

1) Move all apparatus under the fume hood.
2) Attach the retort stand clamp to the report stand. Secure the reaction vessel in the retort stand clamp.
3) Place the beverage and beverage can on the surface of the fume hood directly beneath the reaction vessel.
4) Submerge the reaction vessel into the beverage by lowering the clamp and then securing it in place.
5) Secure the two thermocouples in place, one in the main body of the beverage, and one inside the reaction vessel.
6) Place the funnel inside the reaction vessel and start the data acquisition recording.
7) After 30 seconds of continuous data acquisition readings, pour both salts simultaneously into the funnel at a rate at which they can fall freely into the reaction vessel. This is to prevent clumping of the salts in the funnel.
8) Remove the funnel and note the time and begin to stir the reactants.
9) Stir the reactants until the constituents become a slushy mass.
10) Continue recording data until the temperature inside the reaction vessel has a 5 degrees different from the beverage temperature.

4.5 Data Collection and Instruments Specifications

For both the experiments, the same sets of sensors are used in their respective configurations. Their specifications and tolerances are presented in Table 4.1.

Table 4.1: Sensor data for experimental setups.

Device Function	Device Name/Model	Absolute Error	Relative Error
Temperature Sensor	Omega RT PT-100	0.15K	-
Temperature Sensor	Vernier Stainless Steel Temperature Probe	0.2K	-
Pressure Sensor	Omega PX309-100GI	-	0.25%

4.6 Proposed Conceptual Designs

The proposed designs presented in this section are designed to mimic the processes presented in the two experimental setups. Both designs are operated untouched during the cooling phase while placed on a flat horizontal surface in the upside-down orientation. The analytical and numerical analyses are conducted based on these operating conditions.

The cost of this can is higher than the conventional beverage can. This is due to additional materials and manufacturing processes. The additional materials also add a bit of extra weight to can, but nothing that would compare to the weight of a cooler box with ice. The consumer is paying for the convenience factors of using a self-cooling beverage can during outdoor activities. The additional materials from the self-cooling beverage can may be recycled to cut down cost of production. To encourage recycling, a recycling deposit is charged to the product at the time of purchase. Recycling facilities may be designed in a way, such that they are able to separate the ammonia from the desiccant salts. For the endothermic reaction based cans, special processes can be implemented to

convert the products back to the original reactants; however this may not be cost effective to do so.

The desiccant salt and ammonia can be separated by exposing them to high temperatures exceeding 300℃. This causes the ammonia to release from the magnesium chloride and aluminum oxide salts. Separated ammonia and salts can then be used to fill new self-cooling beverage cans. The endothermic reaction is a strong product favoured reaction. To restore the product chemicals in the reaction vessel to the original reactants, the products must undergo multiple other reactions.

4.6.1 Design 1

Figure 4.13 shows the conceptual design of the ammonia expansion and desiccant capture system. When triggered, ammonia reservoir is moved 1 mm down in a piercing device. Cold ammonia flows through the orifice and throttled liquid ammonia accumulates at the bottom part of the extruded cavity. Felt, a porous medium is glued around the wall to help spread the ammonia along the walls of the cooling vessel, thus enhancing the evaporation of the throttled ammonia. Eventually ammonia vapor is absorbed in the MgCl2 + AlO_2 bed located at the top.

The design has an ammonia vessel just like in experimental setup 1. The orifice in this design is related to the throttling valve. The cooling vessel space in the design is for the ammonia to evaporate; just like the cooling coil. Finally the design also has an adsorption bed just like in the experiment

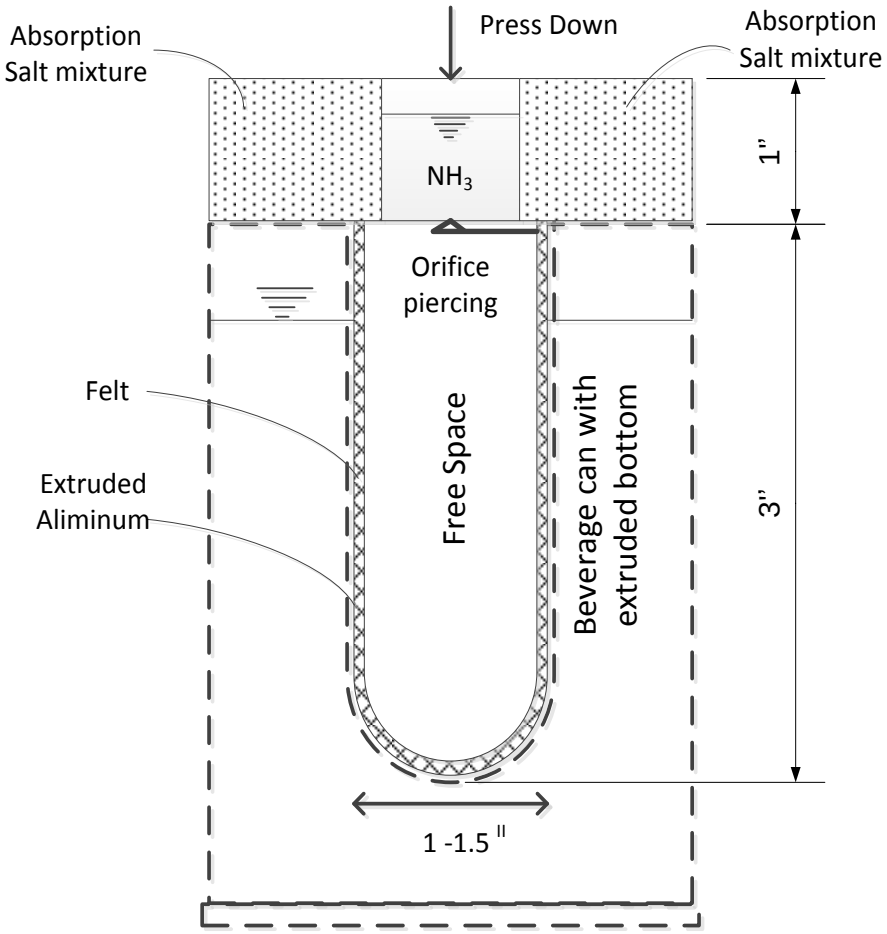

Figure 4.13: Self-cooling beverage can with ammonia expansion and desiccant adsorption. Viewed in the upside-down orientation.

4.6.2 Design 2

In this design, the two-salts are initially physically separated and do not react until they come in contact with each other. This reaction is product favoured, which means that the almost all of the salts are consumed and provide a high amount of cooling. The emanated ammonia remains mostly dissolved in water. However, some gas is also produced. Thence, a magnesium chloride absorption bed is included to absorb the ammonia gas.

The preferred conceptual design for the endothermic mixing process with ammonia absorption is shown in Figure 4.14. The salts are kept in separate containers. When the consumer turns the key, an arm rotates to peel-off the containers with

ammonium thiocyanate and barium hydroxide octahydrate. Salts flow down to the bottom of the reaction vessel and are mixed by the turning brush. Endothermic reaction occurs at the periphery of the extruded cavity. The emanated ammonia does not release outside, but rather it is adsorbed in an $MgCl_2$ bed of small volume. The cooling is very effective; however, the mixing action is required.

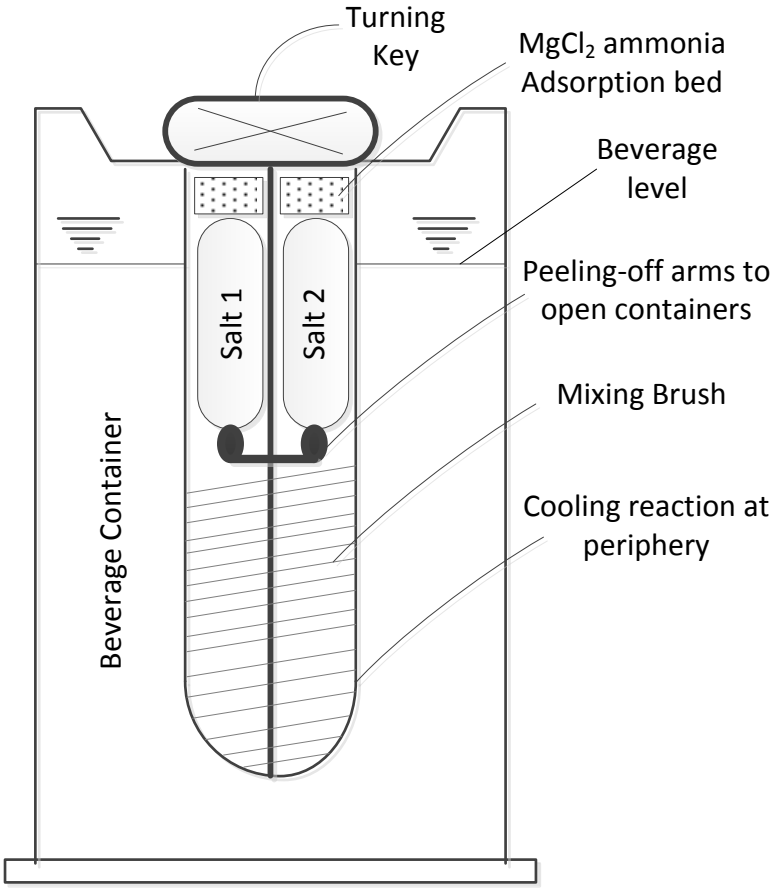

Figure 4.14: Proposed conceptual self-cooling beverage can design using endothermic reaction as cooling method.

Chapter 5: Analyses and Optimization

In this chapter the analytical and numerical analysis and optimization study of the conceptual designs are presented. A detailed explanation is given for how the analysis is conducted. The conceptual designs are analyzed analytically using dimensionless transient heat transfer, the numerical modeling is performed using COMSOL software, the cooling effectiveness study assessed using EES, and the optimization study is conducted using MATLAB. In the analysis of any of the models or studies, it is assumed that the self-cooling beverage can designs are operated in the upside-down orientation. During the cooling phase the can is left untouched while it is sitting on a horizontal surface, as described in Chapter 4. The heat transfer of the beverage occurs from the heat sink generated by the cooling process and the ambient air which surrounds can.

5.1 Analytical Study

The transient heat transfer model is used to analyse and study the heat transfer process through the can. The general heat transfer equation in the cylindrical coordinates can be obtained from elemental energy balance as follows:

$$\rho c_p \frac{\partial T}{\partial t} - \left[\frac{1}{r}\frac{\partial}{\partial r}\left(kr\frac{\partial T}{\partial r}\right) + \frac{1}{r^2}\frac{\partial}{\partial \phi}\left(k\frac{\partial T}{\partial \phi}\right) + V\frac{\partial}{\partial z}\left(\frac{\partial T}{\partial z}\right)\right] = 0 \qquad (5.1)$$

In this equation, there is no heat generation considered. The equation is also reduced to one dimensional form considering that the heat transfer predominantly is in the radial direction. The following boundary conditions are considered for the analysis:

Boundary at the centre: $\frac{\partial T(0,t)}{\partial r} = 0$ (5.2)

Boundary at any radius: $-k\frac{\partial T(r,t)}{\partial r} = h(T(r,t) - T_{amb})$ (5.3)

The initial condition is considered for the temperature at the centre of the cylinder is equal to -20℃ or -30℃ for either the endothermic reaction method or ammonia expansion method respectively.

The analytical solution can be provided to this differential equation. It gives a better understanding and valuable insight to the heat transfer mechanism and the physics of the process. The one-term approximation is used to find the solution of the equation and it can be given as:

$$\theta = Ae^{-\lambda^2\tau}J_o\left(\frac{\lambda r}{r_o}\right) \qquad \tau > 0.2 \tag{5.4}$$

where A and λ are functions, Biot number. The function J_o is the zeroth-order Bessel function of the first kind, and its value depends on λ.

The solution is given as function of the dimensionless time parameter, Fourier number, F_o, and the dimensionless temperature, θ. They are given as follows:

$$\tau = \frac{\alpha t}{r^2} \tag{5.5}$$

$$\theta = \frac{T(r,t) - T_{amb}}{T_i - T_{amb}} \tag{5.6}$$

where $\alpha = k/\rho c_p$ and this solution is valid for Fourier number greater than 0.2. The values of $A, \lambda \; and \; J_o$ are available at different heat transfer references [22]

5.2 Numerical Analysis

5.2.1 Numerical Modeling Software

COMSOL is a very powerful engineering simulation tool. It has the capability of providing multiple physics analysis in a single simulation. The reason COMSOL is chosen to perform the numerical analysis on the self-cooling beverage can design is because there is fluid dynamics and heat transfer that is considered. COMSOL has the ability to study the fluid dynamics and heat transfer of the self-cooling can model simultaneously. This is important because there are convective currents that are produced in the beverage during the cooling phase. It is important to study their effects for the overall heat transfer of the beverage.

5.2.2 Defining Geometry

The two conceptual self-cooling beverage cans have the very similar geometries when it comes to the main body of the can. The main body contains the beverage and the integral cooling vessel. The cooling vessel acts as the evaporator for the throttled ammonia, or acts as the reaction vessel. Envirochill has determined a manufacturing process which creates a cavity in the main body of the can (creating the cooling vessel) that is quick and easy to implement into the existing canning line. The cooling vessel contains the materials needed to provide the cooling. For the ammonia expansion method, the vessel

provides a surface for evaporating. In the two-salt endothermic reaction method, the vessel contains the reactants, and serves as a reactor for the reaction.

The self-cooling beverage can is a cylindrical object by nature. As such, it is possible to study the system in 2 dimensions with an axis of symmetry which runs vertically in the centre of the can. The geometry that this model uses is half of the cross sectional view one would see if they are looking at the can from the side view. Figure 5.1 shows how the final geometry is defined. Figure 5.1 a) depicts a cross section of the can showing the domain where the beverage and cooling vessel are with respects to each other. Figure 5.1 b) depicts where the line of symmetry is, thus only half of the geometry is required to model the system. Figure 5.1 c) depicts the final geometry with which the self-cooling beverage can is modeled by.

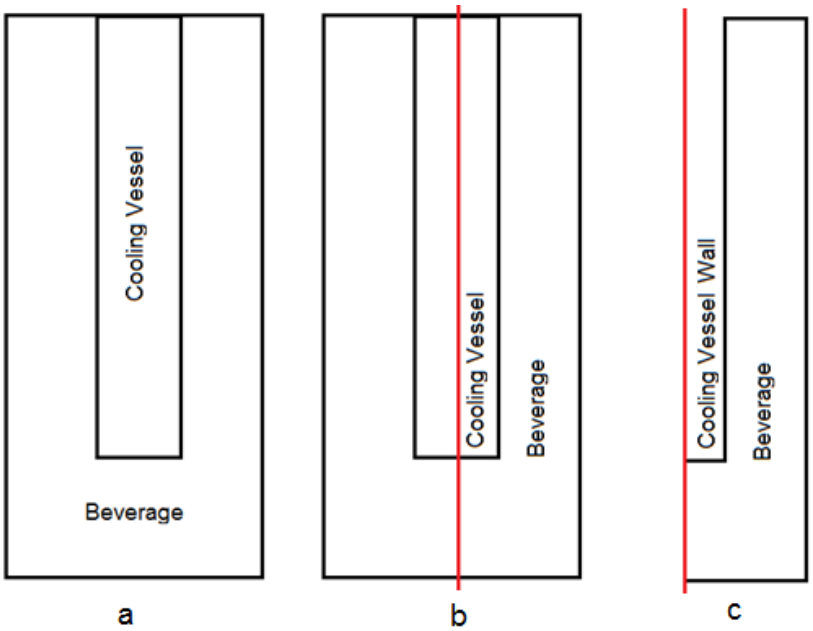

Figure 5.1: a) Cross sectional view of the self-cooling beverage can from the side. b) Cross sectional view of the self-cooling beverage can with axis of symmetry drawn vertically down the middle of the can. c) Final geometry used in the modeling of the can.

The parameters of interest are the length and radius of the can, which are defined as r_c and l_c, and the length and radius of the cooling vessel, which are defined as r_v and l_v. These parameters are labeled in Figure 5.2. The length and radius of the can stays constant for the model. The empty can volume is 500 ml, but with the vessel occupying a space inside the can, the maximum beverage volume is 355 ml; which is the volume of beverage most commonly served in a can in North America. Therefore the cooling vessel volume displaces 145 ml of volume inside the can. The size of the cooling vessel is sufficient for both cooling process. The volume of saturated liquid ammonia at 25℃ required to cooling 355 ml of water from 25℃ to 5℃ is approximately 50 ml. The combined volume of the two-salts used in the endothermic reaction is approximately 150 ml to provide the same amount of cooling. The remaining volume is used for additional materials such as mixing mechanisms, ammonia vessel container, etc.

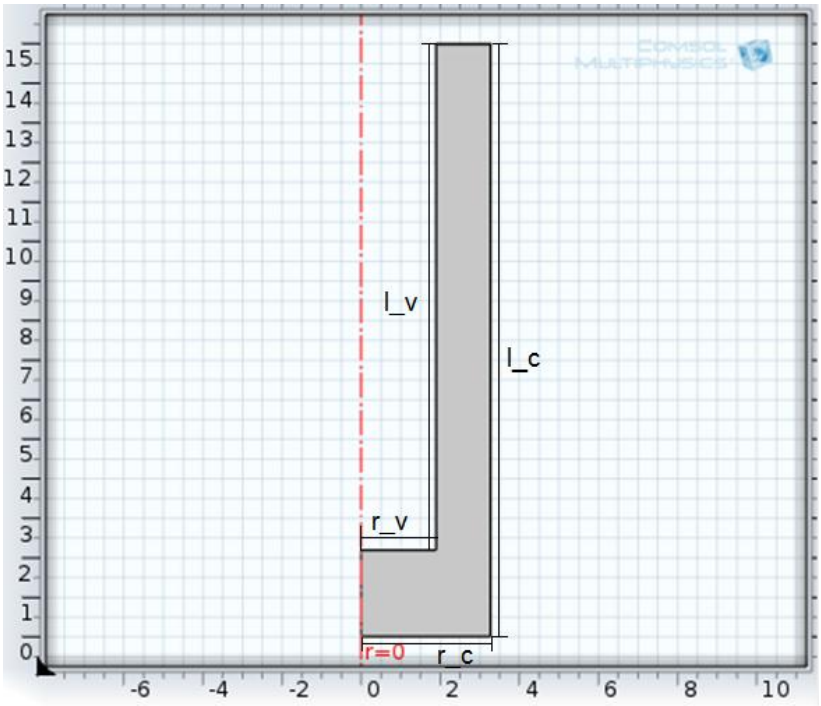

Figure 5.2: Geometry of the can labeled with parameters of interest.

The beverage is contained in an aluminum can. In the model there is an aluminum wall which surrounds the beverage. The thickness of the aluminum wall is 0.11938 mm. In Figure 5.3 an enlarged image of the aluminum wall is shown. The thickness of this wall is defined as l_h. This wall surrounds the entire beverage domain except the side where the geometry of the system meets the line of symmetry.

In this study the aspect ratio between the radius of the vessel and the length of the vessel is studied. The aspect ratio is defined as follows:

$$AR = \frac{l_v}{r_v} \tag{5.7}$$

The volume of the vessel does not change but the aspect ratio changes. This parameter is interesting to study since it greatly affects the heat transfer rate.

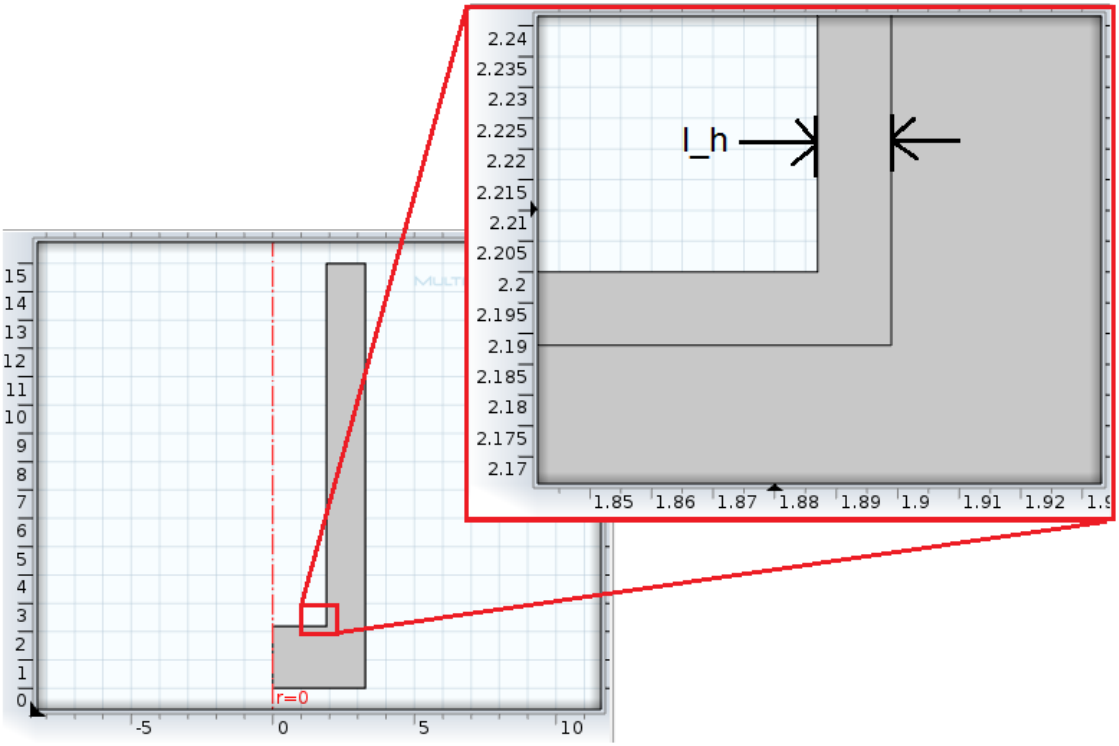

Figure 5.3: An enlarged image of part of the aluminum wall which surrounds the beverage.

5.2.3 Defining Materials

The materials used in the model are aluminum, water and cola. Aluminum is used for the then wall surrounding the beverage, just like in an actual can. Water is used to simulate for the beverage. Cola is used as a test case for commercial beverages. The properties for cola are from Dincer and Kanoglu [19]. Specific heat (cp), thermal conductivity (k) and specific gravity (SG) of cola are 3831.0060 $\mathrm{J/kg \cdot K}$, 0.5155 $\mathrm{W/m \cdot K}$, and 1.11 respectively.

5.2.3.1 Aluminum

The properties that are used in the simulation for aluminum are listed in Table 5.1.

Table 5.1: Properties of Aluminum used in the COMSOL simulation.

Name	**Value**	**Unit**
Specific Heat Capacity	900	J/kg·K
Thermal conductivity	160	W/m·K
Density	2700	$\mathrm{kg/m^3}$

5.2.3.2 Water

The properties that are used in the simulation for water are listed in Table 5.2. The properties are changing with temperature so the values of the parameters are presented as their function used in COMSOL.

Table 5.2: Properties of water used in the COMSOL simulations.

Name	**Value**	**Unit**
Dynamic viscosity	eta(T[1/K])	Pa·s
Ratio of specific heats	1.0	1
Specific Heat Capacity	Cp(T[1/K])	J/kg·K
Density	rho(T[1/K])	kg/m^3
Thermal conductivity	k(T[1/K])	W/m·K

5.2.3.3 Cola Compared to Water

Using the heat transfer properties of cola as listed before, a factor is multiplied into the water properties of COMSOL. It is assumed that since cola has 89.4% mass by water, the heat transfer properties for cola changes similarly to water as the temperature changes [19].

Table 5.3: Properties of cola used in the COMSOL simulations.

Name	**Value**	**Unit**
Dynamic viscosity	eta(T[1/K])	Pa·s
Ratio of specific heats	1.0	1
Specific Heat Capacity	((3831.0060/4180)*Cp(T[1/K]))	J/kg·K
Density	((1.11)*rho(T[1/K]))	kg/m^3
Thermal conductivity	((0.5155/0.58)*k(T[1/K]))	W/m·K

5.2.4 Governing Equations

The governing equation of the prescribed problem can be described in the general form of conservation laws of continuity, momentum and energy are as follows:

$$\frac{\partial \rho \phi}{\partial t} + \nabla \rho \boldsymbol{u} \phi = \nabla \Gamma_{\phi} \nabla \phi + S_{\phi} \quad (5.8)$$

where $\boldsymbol{u}$ is the velocity vector, ρ is the fluid density, φ is representing the dependent variable, Γ_{φ} is the diffusion coefficient and S_{φ} is the source term. The density of the working fluid can be considered as constant with the change in temperature. The following dimensionless parameters are considered in the description of the governing equations, with respect to Figure 5.4 shown below.

Dimensionless axial coordinates:

$$X = x/r_o \quad (5.9)$$

$$R = r/r_o \quad (5.10)$$

Dimensionless velocity components:

$$U = u\, r_o/\nu \quad (5.11)$$

$$U = v\, r_o/\nu \quad (5.12)$$

Dimensionless time:

$$\tau = \nu\, t/{r_o}^2 \quad (5.13)$$

Dimensionless pressure:

$$P = p{r_o}^2/\rho\nu^2 \quad (5.14)$$

Dimensionless temperature:

$$\theta = \frac{T - T_{amb}}{T_i - T_{amb}} \tag{5.15}$$

Grashof Number:

$$Gr = \frac{g\beta(T - T_{amb}){r_o}^3}{\nu^2} \tag{5.16}$$

where u and v are the velocity components as shown in the diagram in the x and r directions respectively. X and R are the dimensionless axial coordinates. β in Grashof Number is the volumetric coefficient of thermal expansion. θ is the dimensionless temperature and τ is the dimensionless time. ν is the kinematic viscosity.

COMSOL uses finite element to solve the governing equations of flow and heat transfer. In the prescribed problem, incompressible fluid is considered. However, the continuity, momentum and energy equations, based on the general form given earlier, can be written for general flow case as follows, by substituting the dependant variable and the diffusion coefficient with the corresponding parameters, for the continuity equation:

$$\frac{\partial U}{\partial X} + \frac{1}{R}\frac{\partial (RV)}{\partial R} = 0 \tag{5.17}$$

For the momentum equations:

$$\frac{\partial U}{\partial \tau} + U\frac{\partial U}{\partial X} + V\frac{\partial U}{\partial R} = -\frac{\partial P}{\partial X} + \left(\frac{\partial^2 U}{\partial X^2} + \frac{\partial^2 U}{\partial R^2} + \frac{1}{R}\frac{\partial U}{\partial R}\right) - \theta Gr \tag{5.18}$$

$$\frac{\partial V}{\partial \tau} + U\frac{\partial V}{\partial X} + V\frac{\partial V}{\partial R} = -\frac{\partial P}{\partial R} + \left(\frac{\partial^2 V}{\partial X^2} + \frac{\partial^2 V}{\partial R^2} + \frac{1}{R}\frac{\partial V}{\partial R}\right) - \frac{V}{R^2} \tag{5.19}$$

For the energy equation:

$$\frac{\partial \theta}{\partial \tau} + \frac{\partial \theta}{\partial X} + V\frac{\partial \theta}{\partial R} = \left(\frac{\partial^2 \theta}{\partial X^2} + \frac{\partial^2 \theta}{\partial R^2} + \frac{1}{R}\frac{\partial \theta}{\partial R}\right)/Pr \tag{5.20}$$

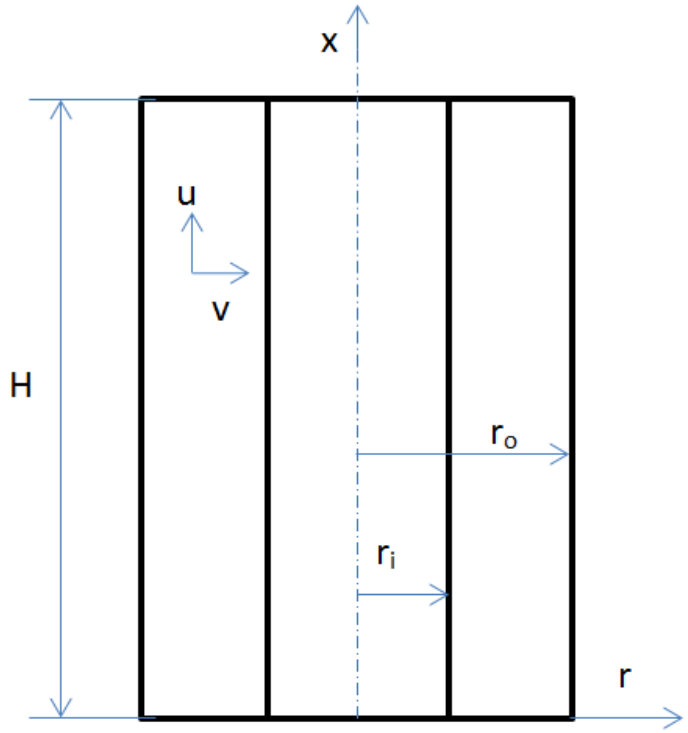

Figure 5.4: Schematic diagram of a simple two concentric cylinder model used in the introduced dimensionless parameters of the model.

With regard to the heat transfer in the proposed analysis, Nusselt number is proposed as function of Rayleigh number and the ratio of H/r_o as described by Hadjadj et al. [23], where it is given as:

$$Nu = 0.133\ Ra^{0.33}(H/r_o)^{-0.32} \tag{5.21}$$

This formula is found by using the least squares method to calculate an average value of Nusselt number for concentric vertical cylinder under natural convection heat transfer for incompressible flow

5.2.5 Defining Boundary Conditions

The boundary conditions in a simulation are very important and should be defined very carefully. They should resemble what the actual conditions of the system are in operating conditions. The boundary conditions for the model are explained in this section along with assumptions that are used to arrive at these boundary conditions.

5.2.5.1 Thermally Insulated Boundaries

There are two boundaries which are considered as having negligible heat transfer. The boundaries are at the top and bottom of the can are highlighted in Figure 5.5. For the first conceptual design this boundary is insulated with a material so that the heat from the adsorption process is reduced significantly and there is negligible heat entering from the top. For the second conceptual design, the area which is exposed to the atmosphere is so small that the heat transfer rate is assumed negligible. The bottom of the can is considered thermally insulated because when the can is placed on the surface there is about 1.5 mm to 2 mm of air gap with the surface. The can is supported by the rim of the top part of the can. The heat transfer from the bottom is assumed negligible due to the high insulating properties of still air.

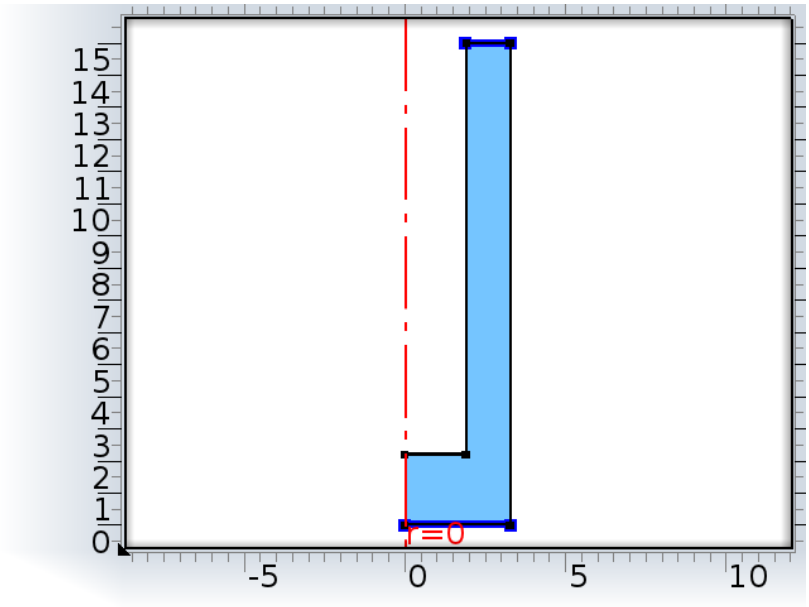

Figure 5.5: Thermally insulated boundary layers.

5.2.5.2 Temperature Boundaries

A temperature boundary is defined for the vessel wall which is highlighted in Figure 5.6. The temperature of this boundary remains constant throughout out the simulation. It is assumed that during the operation of the ammonia expansion process the temperature is maintained at -30℃. The assumption is that the flow rate of the ammonia and adsorption rate of the ammonia into the adsorption bed allows for continuous throttling and boiling of the ammonia such at the throttled ammonia maintains -30℃. For the two -salt endothermic reaction method, it is assumed that the vessel wall temperature maintains a temperature of -20℃. The assumption made is that the reactants are continuously stirred and the reaction rate maintains the products inside the cooling vessel at a constant temperature. These assumptions are proven reasonable based on the experimental results.

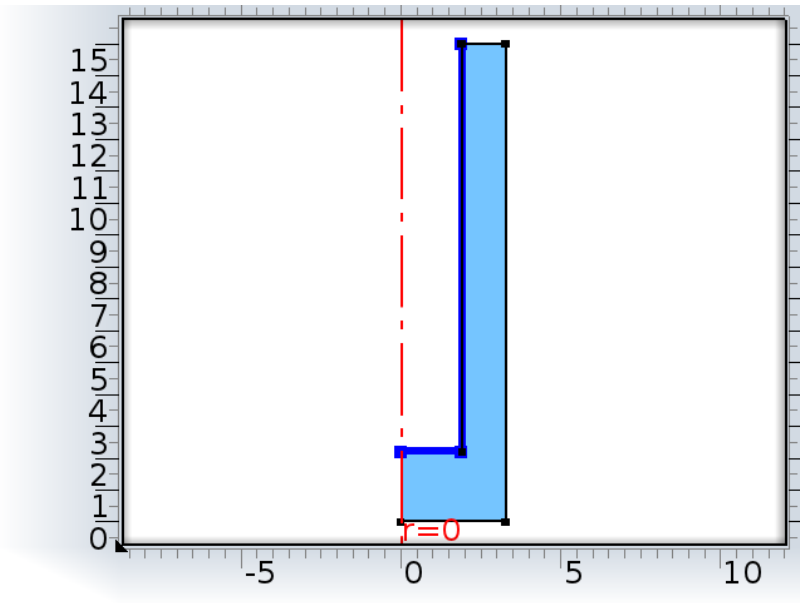

Figure 5.6: Cooling vessel wall boundary highlighted.

5.2.5.3 Convective Heating Boundary

The outer wall of the beverage can is exposed to the ambient air surrounding the can. Figure 5.7 shows the highlighted outer wall which is subjected to convective heating by the surrounding air. The air surrounding the can is at ambient temperature. The ambient temperature is described in the next boundary condition.

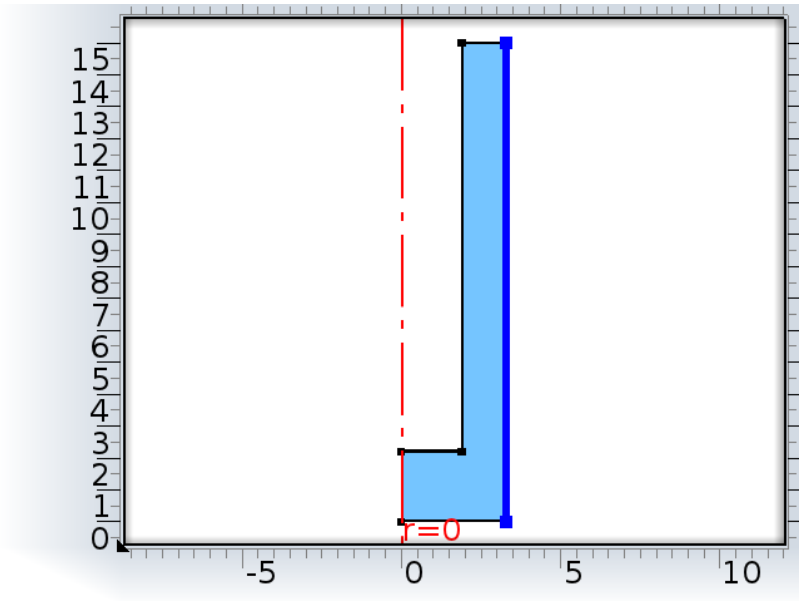

Figure 5.7: Convective heating boundary along the wall of the outer surface of the can.

5.2.6 Initial Conditions

Initially the water and the aluminum are at ambient temperature. Ambient temperature is set as T_{amb} in the parameters of the COMSOL simulation. This parameter is varied from 25℃, 30℃, to 35℃. The assumption is that the self-cooling beverage can is initially at thermal equilibrium with its surroundings. Also, there is zero momentum in system initially and all of the motion of the fluid is generated by the convective currents produced by the heat transfer between the beverage and cooling vessel wall.

5.2.7 Grid Independence Test

A grid independence test is performed to study the effects of the different mesh sizes. COMSOL has an automated meshing function, which automatically creates an optimized meshed based the geometry of the can. The mesh that COMSOL generates is a hybrid mesh consisting of triangular and rectangular elements for a 2D geometry. The finer mesh would give the most accurate results, but it requires the most CPU power and computation time. An extremely coarse mesh generates less accurate results, but requires less CPU power and computation time. In this study, a balance of power and accuracy is achieved by using a normal mesh generated by COMSOL. The meshes that are used in the grid independence test are presented in Figure 5.8. From highest density of elements to lowest, the mesh densities that are considered are finer, normal, coarse, coarser, and extremely coarse. Results of the grid independence are presented in the results chapter of the thesis.

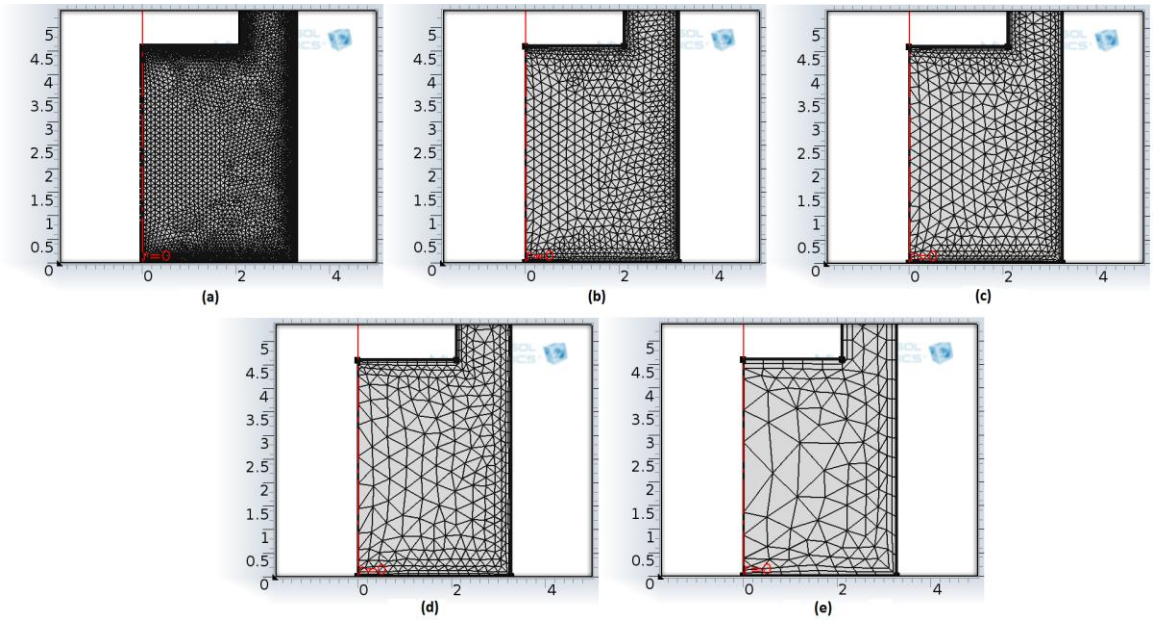

Figure 5.8: COMSOL automatically generated meshes (a) finer, (b) normal, (c) coarse, (d) coarser, and (e) extremely coarse.

5.2.8 Time Step Tolerance

Time step tolerance is important for achieving accurate results. Since there are secondary flow effects in during the simulation a tight tolerance is needed. The time dependent solver is set for 3 minutes with a time step of 3 seconds. The relevance tolerance is set to 1e-3 seconds. The absolute tolerance is set to 2.5e-5 seconds. These tolerances allow for more accuracy in the model's solution. 3 minutes is chosen because of it is the maximum desired time of cooling for a self-cooling beverage can. However, 0.1 seconds time step is used to in the best case scenario to produce a video simulation of the cooling process. The shorter time step increases the computation time, thus a 3 second time step is used for all other runs. A 3 second time step is sufficient for an accurate solution, when compared with a time step of 0.1 seconds. The differences in the results are negligible between using a time step of 3 seconds versus 0.1 seconds.

5.2.9 Defining Test Cases

There are 30 cases that have been simulated using this numerical model. In Table 5.4 it shows all the test cases that are studied. Each box marked with an "x" indicates that the specific test case is considered in the study. There are 3 parameters that are changing to test the diverse scenarios that the self-cooling beverage can may encounter. A parametric study for the ambient temperature is done to study the effects of using the self-cooling can in different climates.

Table 5.4: Studied cases for the numerical model for proposed conceptual designs.

Vessel Wall Temperature	**Ammonia Expansion -30℃**			**Endothermic Reaction -20℃**		
Ambient Temperature (℃)	**25**	**30**	**35**	**25**	**30**	**35**
Aspect Ratio 1	x	x	x	x	x	x
Aspect Ratio 2	x	x	x	x	x	x
Aspect Ratio 3	x	x	x	x	x	x
Aspect Ratio 4	x	x	x	x	x	x
Aspect Ratio 5	x	x	x	x	x	x

A parametric study is done on the aspect ratio of the cooling vessel walls to determine the configuration which would provide the best heat transfer rate, with a constraint of 355 ml beverage volume, and 145 ml for cooling vessel. The aspect ratio is varied from 1.307 to 8.609, as presented in Table 5.5. The aspect ratios are depicted in Figure 5.9. A1 and A5 are the extreme cases for the aspect ratios. A1 has the largest vessel radius and shortest vessel length. A5 has the longest vessel length and smallest vessel radius. In fact, in the extreme cases, certain sides of the vessel walls do not exist in

their respective cases. Finally a parametric study of the cooling vessel wall temperature (T_c) is changed between -30℃ and -20℃ to simulate for the ammonia expansion method and the two-salt endothermic reaction method, respectively.

Table 5.5: Dimensions of length of vessel, radius of vessel for each aspect ratio and surface area of heat transfer.

Aspect Ratio	**Aspect Ratio [l_v/r_v]**	**Length of Vessel [cm]**	**Radius of Vessel [cm]**	**Surface Area [cm^2]**
A1	1.307	4.274	3.271	33.85
A2	3.1325	7.653	2.443	78.05
A3	4.958	10.39	2.095	82.82
A4	6.7835	12.8	1.887	87.76
A5	8.609	15	1.742	82.73

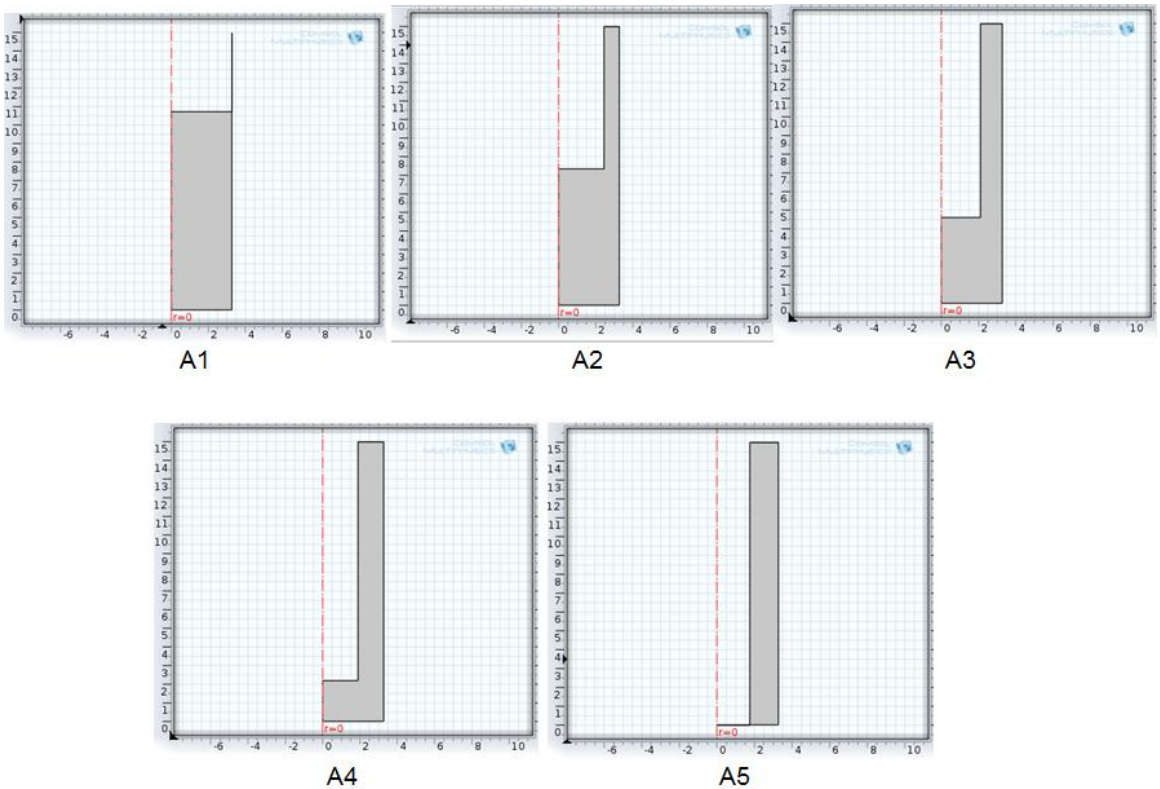

Figure 5.9: All 5 aspect ratio geometries displayed from A1 through A5.

5.3 Cooling Effectiveness Study

The cooling effectiveness of the self-cooling beverage can is a quantity of interest. This value is a comparison of the total theoretical cooling capacity compared with the actual cooling achieved. The cooling effectiveness can be studied in terms of the energy or exergy cooling effectiveness. These values are defined as follows:

$$\eta_C = \frac{Q_{act}}{Q_{theoretical}} \tag{5.22}$$

$$\phi_C = \frac{Ex^{Q_{act}}}{Ex^{Q_{theorectical}}} \tag{5.23}$$

where η_C is the energy cooling effectiveness, ϕ_C is the exergetic cooling effectiveness, Q_{act} is the energy that is extracted from the beverage, $Q_{theoretical}$ is the theoretical maximum cooling that the cooling method could provide, and Ex^Q is the exergetic heat.

For the ammonia expansion method, $Q_{theoretical}$ is determined by the volume of stored saturated liquid ammonia. In the endothermic reaction based method, it is determined by the amount of reactions stored in the reaction vessel. Q_{act} is determined by the volume of the beverage and its temperature change during the cooling process. These values are calculated using the balance equations presented in the next section.

A cooling effectiveness study is performed for the ammonia expansion case only. Modeling of the chemical reaction kinetics of the endothermic reaction method is considered to be beyond the scope of this master's thesis. The initial volumes of saturated liquid ammonia are 100 ml and 120 ml. These values are based on design parameters of the cooling vessel in the numerical model, which has 145 ml. The volume of stored

ammonia needs to be less than size of the cooling vessel to accommodate for the ammonia vessel and for pressure fluctuations due to inevitable temperature changes.

5.3.1 Balance Equations for the Self-Cooling Beverage Can

For the beverage inside the can, the balance equations are presented as follows. There is the mass, energy, entropy, and exergy balance equations that are considered for the cooling process. These equations are formulated on the scenario that the beverage can is left to cool on its own during the cooling process as described before in Chapter 4. In Figure 5.10 a schematic diagram of the self-cooling can system is presented to aid in defining the balance equations.

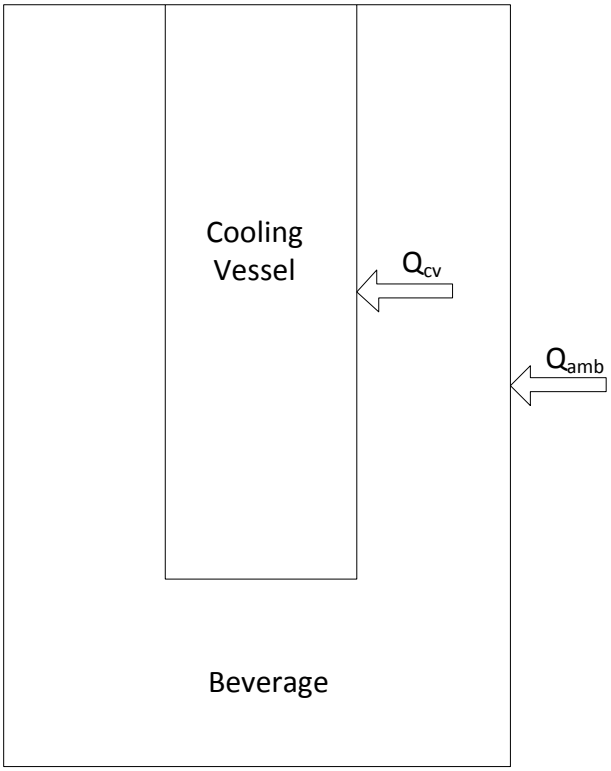

Figure 5.10: Energy flow of the self-cooling beverage can during the cooling process.

During the cooling process, the mass of the water does not change. Therefore the mass balance equation shows a change of mass over time of zero.

MBE: $\frac{\mathrm{d}m_w}{\mathrm{d}t} = 0$ (5.24)

where $\mathrm{d}m_w$ is the change in mass of the water and $\mathrm{d}t$ is the change in time.

The energy balance equation considers the energy that is entering the beverage can from the outer surface, and the energy that is transferred from the beverage into the cooling vessel.

EBE: $Q_{amb} = m_w c_p \frac{\mathrm{d}T_w}{\mathrm{d}t} + Q_{cv}$ (5.25)

where Q_{amb} is the heat the enters into the beverage from the surrounding warmer air, and Q_{cv} is the heat that is taken away from the beverage by the cooling vessel. The term $m_w c_p \frac{\mathrm{d}T_w}{\mathrm{d}t}$ is the change in energy of water based on the initial and final temperatures acquired from the numerical modeling.

EnBE: $m_w \cdot s_1 + S_{gen} = m_w \cdot s_2$ (5.26)

The entropy balance equation considers the entropy flow in the system, where s_1 and s_2 are the entropies before and after the cooling process, and S_{gen} is the entropy generation of the cooling process.

$$\text{ExBE:} m_w \cdot ex_1 + Ex^{Q_{amb}} = m_w \cdot ex_2 + Ex^{Q_{cv}} + Ex^D \quad (5.27)$$

The exergy balance equation takes into consideration the exergy of the system. ex_1 and ex_2 are the exergies before and after the cooling process and Ex^D is the exergy destruction.

These balance equations are used to help determine the quantities used for determining the energy and exergy cooling effectiveness of self-cooling beverage can system. The cooling effectiveness has a range of values between 0 and 1, where 1 is the highest cooling effectiveness, meaning that the system is thermodynamically ideal.

5.4 Can Design Optimization

The design goals for the self-cooling soft drink cans are very simple. It must be able to quickly cool the beverage inside the can, the cooling vessel must not take too much space, and the cooling effectiveness of the can design should be as high as possible. A contradiction occurs when increasing for the heat transfer rate to decrease the cooling time. This is because as the heat transfer rate increases, so does the cooling vessel size; which should be minimized if the volume of the beverage is to be maximized. There are multiple design goals for this technology so therefore the optimization problem is multi-

objective in nature. In this section a multi-objective genetic algorithm is used to solve the multi-objective problem for a generic 355 ml can with an addition of a cooling vessel.

The 355 ml soft drink can widely available in North America is shown in Figure 5.11. It is 12.19 cm tall and has a diameter of 6.35 cm. The self-cooling soft drink can has an addition of a cylindrical vessel. This cooling vessel is located internally at the bottom centre of the can. Inside the vessel contains a highly pressurized refrigerant, or in the case of for endothermic reaction based cooling method, chemicals are stored in the cooling vessel. The cooling vessel takes in the thermal energy from the beverage, thus cooling it. The optimization study is performed for the ammonia expansion case only, because the cooling effectiveness study is only performed on the ammonia expansion case.

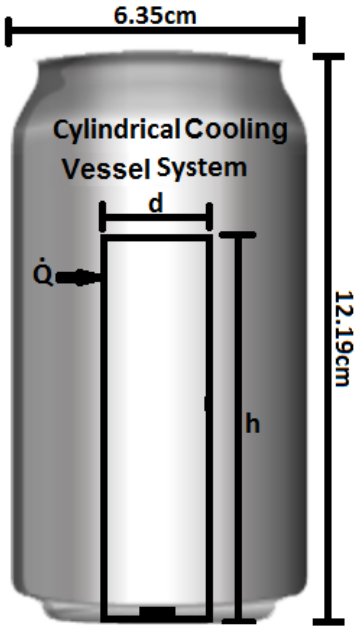

Figure 5.11: schematic drawing of the cooling system that is implemented inside the 355 ml soft drink can. d is the diameter of the vessel, h is the height of the vessel, Q is heat energy leaving the beverage and transferring into the cooling vessel.

Heat transfer between the cooling vessel and beverage is present inside the can during the refrigerant expansion process. To better understand what physically is happening inside, some heat transfer knowledge must be introduced. There are three

forms of heat transfer, conduction, convection and radiation. Inside the can there is convection and conduction. Convection occurs when heat is transferred in a moving medium, conduction occurs when heat is transferred in a still medium. There is convection and conduction which occurs in the beverage with the cooling vessel wall.

5.4.1 Optimization Problem Definition

The design goals defined previously are used to define the objectives of this thesis. The challenges for the designing of a self-cooling can are to minimize the cooling time, maximize the volume of beverage, and to maximize cooling effectiveness. In this section a physical and mathematical model is presented to determine the objective functions that are used in the multi-objective genetic algorithm in MATLAB.

5.4.1.1 Physical Model

In this section some more parameters are defined to further develop the physical model. Referring back to Figure 5.11 there are two variables that define the geometry of the cylindrical cooling vessel. The parameter d defines the diameter and h defines the height of the cooling vessel inside the 355 ml can. The unit of these two parameters are in centimeters. The surface area of the cylindrical cooling system is defined as follows:

$$A_{vessel} = \frac{\pi d^2}{4} + \pi dh \tag{5.28}$$

Volume of the beverage that is available in the can after the implementation of the cylindrical cooling vessel is calculated by the following:

$$V_{beverage} = 355ml - \frac{h\pi d^2}{4} \tag{5.29}$$

Finally the volume of the cooling vessel is defined as follows:

$$V_{vessel} = \frac{h\pi d^2}{4} \tag{5.30}$$

These equations define the major geometric influences on the design goals of the self-cooling beverage can. In the next section these geometric equations are used to define the objective functions for optimization problem.

5.4.2 Mathematical Model

The mathematical model defines the equations that govern the design goals. Firstly it is discussed that one of the design goals is to maximize the heat transfer rate. The two main types of heat transfer that is occurring inside the self-cooling beverage can are convection and conduction. Convective heat transfer is governed by Eq. 5.31, and the conduction heat transfer is governed by Eq. 5.32.

$$\dot{Q}_{conv} = hA \cdot \mathrm{dT} \tag{5.31}$$

where $\dot{Q}_{conv}$ is the heat transfer rate, h is the convective heat transfer coefficient, A is the surface area of the heat transfer surface, and dT is the change in temperature from the cooling vessel surface to the beverage temperature.

$$\dot{Q}_{cond} = -kA\left(\frac{dT}{dx}\right) \tag{5.32}$$

where $\dot{Q}_{cond}$ is the heat transfer rate, k is thermal conductivity, A is the surface area of the heat transfer surface, dT is the change in temperature from the one end to the other, and dx is the width of the material. It is possible the convection and conduction equations be combined into one equation which defines the overall heat transfer that occurs between the beverage and the cooling vessel wall. The overall heat transfer rate is defined as follows:

$$\dot{Q}_{overall} = UA \cdot dT \tag{5.33}$$

where $\dot{Q}_{overall}$ is the overall heat transfer rate which includes convective and conductive forms, U is the universal heat transfer coefficient of self-cooling beverage can, and A is the surface area of the vessel, and dT is the change in temperature between the beverage and the cooling vessel.

The amount of heat that can be transferred to the ammonia is directly affected by the volume of the vessel. The amount of heat that is transferred into the cooling vessel for the ammonia expansion design can be defined in the following:

$$Q_t = m_a(\mathrm{H}_2 - \mathrm{H}_1) \tag{5.34}$$

where H_1 and H_2 are the enthalpies of the ammonia before and after the cooling process and m_a is the mass of the refrigerant which is defined as follows:

$$m_a = V_{capsule} \cdot \rho_a \tag{5.35}$$

where ρ_a is the density of saturated liquid ammonia at ambient temperature.

The amount of energy cooled from the beverage is defined in as follows:

$$Q_w = m_w \cdot c_p \cdot \Delta T \tag{5.36}$$

where Q_w is the heat energy extracted from the beverage, m_w is the mass of the beverage (water), and ΔT is the change in temperature of the water after the cooling process.

5.4.2.1 Objective Functions

The three design objectives of the self-cooling soft drink can are to maximize heat transfer rate, maximize amount of beverage inside the can, and to maximize the cooling effectiveness. The parameters that are being varied to find an optimal design are the cooling vessel's diameter and height. Therefore each objective function has a dimensionality of two.

The first objective function considers the heat transfer rate. The function evaluates the time it takes to cool the volume of beverage inside the can by a difference of 20℃. Objective function 1 is presented in Eq. 5.38, the units are in seconds. This function should be minimized because it is desired to have the shortest cooling time.

$$f_1(d, h) = \frac{Q_w}{\dot{Q}_{overall}} \tag{5.37}$$

$$f_1(d,h) = \frac{U\left(\frac{\pi d^2}{4}+\pi dh\right)dT}{\left(355ml-\frac{h\pi d^2}{4}\right)\rho_w \cdot cp\Delta T} \tag{5.38}$$

where dT is 20℃, ΔT is an assumed average temperature difference between the cooling vessel wall and beverage temperature of 30℃ (for ammonia expansion cooling method), and ρ_w is the density of water.

The second objective function considers the beverage volume and the units are in millimetres. Objective function 2 is presented in Eq. 5.39. This function should be maximized as to have more beverages for the consumer to consume.

$$f_2(d,h) = 355ml - \frac{h\pi d^2}{4} \tag{5.39}$$

The third objective function considers the cooling effectiveness of the design. The cooling effectiveness is defined in Section 5.3. Objective function 3 is defined in Eq. 5.41. This function should be maximized as to have the best cooling effectiveness, thus having less wasted space and materials.

$$f_3(d,h) = \eta_C = \frac{Q_w}{Q_a} \tag{5.40}$$

$$f_3(d,h) = \frac{\left(355ml-\frac{h\pi d^2}{4}\right)\rho_w \cdot c_p\Delta T}{\rho_a\left(\frac{h\pi d^2}{4}\right)(\mathrm{H_2}-\mathrm{H_1})} \tag{5.41}$$

where H_1 is 317.6 kJ/kg·K and H_2 is 1418.3 kJ/kg·K. These enthalpy values correspond to saturated liquid ammonia at an ambient temperature of 25℃ and saturated gaseous ammonia at ambient pressure of 101.325 kPa, respectively.

The constraint for the self-cooling beverage can is that the cooling vessel size cannot exceed the size of the can, and must have dimensions so that it can exists. That means $6 < h < 12$ and $3 < d < 6$. These are hard constraints and must be adhered to or else the vessel would simple not exist inside the can, or would not function properly.

5.4.3 Optimization Method

The design of the self-cooling beverage can is a multi-objective problem (MOP) and should be solved using a multi-objective algorithm [24]. For the purpose of this study a multi-objective genetic algorithm (MOGA) is used to solve the MOP. The choice for using MOGA is because Multi-Objective Evolutionary algorithms are well known for their robustness and ability to solve a large variety of complex problems.

5.4.3.1 Multi-Objective Genetic Algorithm

Genetic algorithms are inspired by the evolutionist theory which explains the origins of a species. They try to imitate the natural world of survival of the fittest. A random population is generated to represent a species. Each member in the population is a chromosome or parent that can be subjected to mutation, recombination, and selection to create the new generation. Every generation is meant to be stronger than the last or else they tend to fail. The better solution is allowed to continue to the next generation.

MOGA is a population based multi-objective based meta heuristic. It is able to search different regions of a solution space which makes it possible to find a diverse set

of solutions for difficult problems with non-convex, discontinuous, and multi-modal solution spaces. MOGA is one of the most popular algorithms chosen to solve most MOP, this is because it does not require users to prioritize, scale or weigh the objectives. The results from the MOGA are a set of non-dominating solutions called the Pareto set. The algorithm pseudo code is seen in Figure 5.12 and the algorithm structure can be seen in Figure 5.13.

In MOGA the individual solutions are assigned a rank of 1, while dominated solutions are penalized according to the population density of the corresponding region of the trade-off surface [24].

```
Initialize Population
Evaluate Objective Values
Assign Rank Based on Pareto Dominance
Compute Niche Count
Assign Linearly Scaled Fitness
Assign Shared Fitness
   For i = 1 to number of Generations
         Selection via Stochastic Universal Sampling
         Single Point Crossover
         Mutation
         Evaluate Objective Values
         Assign Rank Based on Pareto Dominance
         Compute Niche Count
         Assign Linearly Scaled Fitness
         Assign Shared Fitness
    End Loop
```

Figure 5.12: Multi-objective genetic algorithm pseudo code taken from [24].

Multi-Objective Genetic Algorithm

1. **Procedure** MOGA $\left(N', g, f_k(x)\right) \triangleright N'$ members evolved g generations to solve for $f_k(x)$
2. Initialize Population $\mathbb{P}'$
3. Evaluate Objective Values
4. Assign Rank based on Pareto Dominance
5. Compute Niche Count
6. Assign Linearly Scaled Fitness
7. Shared Fitness
8. **for** $i = 1$ to g **do**
9. Selection via Stochastic Universal Sampling
10. Single Point Crossover
11. Mutation
12. Evaluate Objective Values
13. Assign Rank Based on Pareto Dominance
14. Compute Niche Count
15. Assign Linearly Scaled Fitness
16. Assign Shared Fitness
17. **end for**
18. **end procedure**

Figure 5.13: Multi-Objective Genetic Algorithm structure taken from [24].

5.4.3.2 Optimization Procedure

MATLAB is used to solve the multi-objective. MATLAB is capable of algorithm development, data analysis, visualization, and numerical computation. It can be used to solve a wide range of technical problems. The software is loaded with many useful features such as the optimization toolbox. In the optimization toolbox are a variety of optimization algorithms such as simulated annealing, quadratic programming, genetic algorithm, and multi-objective genetic algorithm, etc.

The objective functions are defined in the function file @objfnc. The number of variables is 2, because the dimensionality of the problem is 2. The bounds are the constraints set to the 2 variables, which is $6 < h < 12$ and $1 < d < 6$.

The procedure that is used to obtain the optimization results is now discussed. The objective functions are defined in a MATLAB function that holds all three at once. Figure

5.14 is a picture of the MATLAB toolbox interface setup for solving the objective functions. The algorithm parameters that are used for the runs are presented as follows:

- Population size: 100
- Selection function: Tournament
- Tournament size: 2
- Crossover fraction: 1
- Mutation function: Constraint dependent
- Crossover ratio: 1
- Max Number of generations: 400
- Lower bound: [3,6]
- Upper bound: [6,12]
- Distance measure function: @distancecrowding
- Pareto front population fraction: 0.35

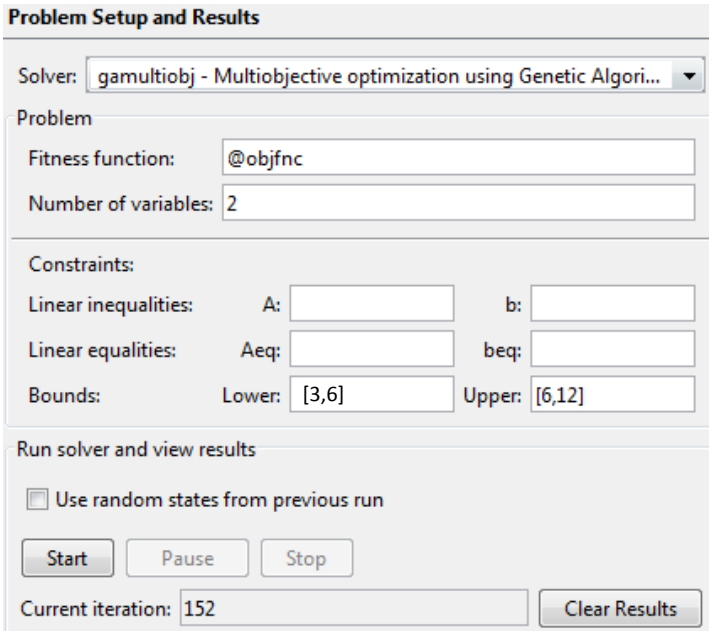

Figure 5.14: MATLAB optimization toolbox graphical interface.

Then the optimization tool is run 30 times to see if the results are consistent. The results show consistency after 30 runs. The MOGA in MATLAB demonstrated a high level of repeatability. Only one run is chosen for analysis for this study. The results are graphed to make the Pareto front charts. The population size of 100 is chosen for achieving a good spread of the optimal results. There are 4 Pareto Frontier charts created to compare each objective function against each other. The Pareto graphs are generated for the manufacturer to choose the best design for the market. The results are presented in the results and discussing.

Chapter 6: Results and Discussion

The results for all of the experimental and theoretical work are presented in this chapter. The experimental results from the ammonia expansion and two-salt endothermic reaction experiments are presented and discussed. Next, the numerical modeling results from the COMSOL simulations are presented. The cooling effectiveness results are presented after the COMSOL results. Lastly, the optimization results are discussed.

6.1 Experimental Results

6.1.1 Experiment 1

The experiments that are considered for the ammonia expansion with desiccant adsorption are presented in Table 6.1. Adsorption of the ammonia with 100% by weight of magnesium chloride is tested, and then a salt mixture of 50% by weight of magnesium chloride mixed with 50% by weight of aluminum oxide. Finally, a direct release of ammonia expansion into atmospheric pressure under the fume hood is tested for the zero ideal zero back pressure case. Each experiment is conducted with having throttling valve opened to 3 turns.

Table 6.1: Ammonia expansion with desiccant experimental cases.

Experimental Case	**Wt. $MgCl_2$ (%)**	**Wt. AlO_2 (%)**	**Number of Turns of Throttling Valve**
1	100	0	3
2	50	50	3
3	N/A	N/A	3

6.1.1.1 Experimental Case 1

For the first experimental case, cooling of 7.2℃ is achieved over 782 seconds as shown in Figure 6.1. This rate of cooling did not meet the goal of what is outlined in the objective of the research which is 180 seconds. Ammonia is throttled into the cooling coil continuously for approximately 200 seconds. At this time the pressure in the coil has reached 500 kPa. With such a high pressure in the coil, any further ammonia that is released into the coil does not throttle effectively to provide cooling. In fact, the addition of more ammonia into the coil at this pressure can feed liquid ammonia at 4℃ into the coil, which does not provide effective cooling. This also poses a safety concern as the pressure build up may reach critical point and can cause mechanical failure of the can. This is dangerous and may cause the can to explode. However this issue is addressed in the next experimental case where to adsorption rate is improved to mitigate this problem.

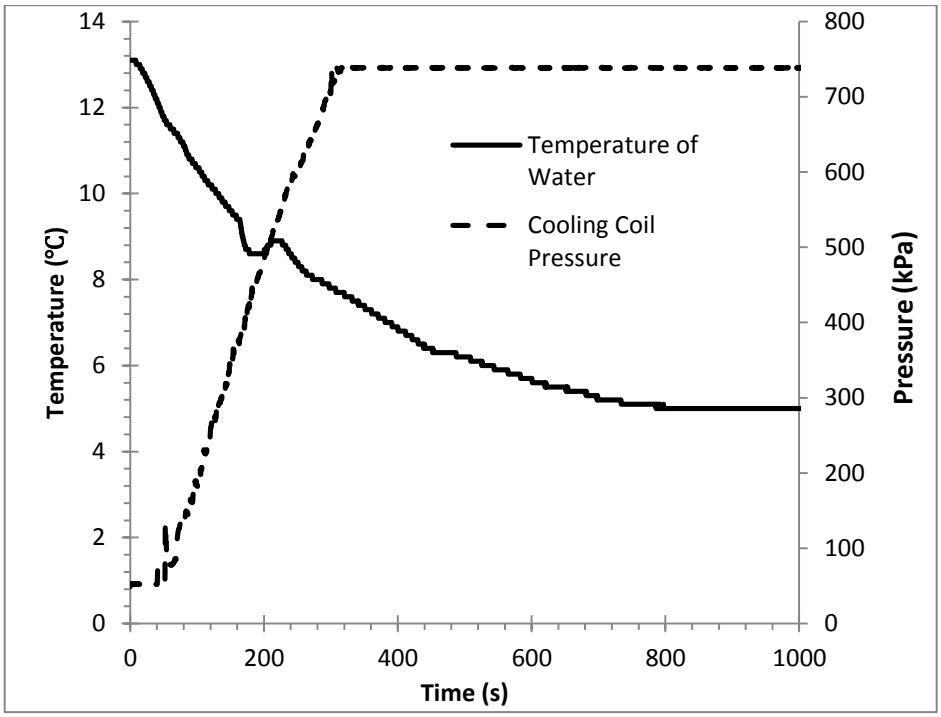

Figure 6.1: Ammonia expansion experiment run at 3 turns of the throttling valve and only magnesium chloride in the adsorption bed.

At 300 seconds, the pressure inside coil has reached the maximum limit of the pressure reading of the pressure sensor (689.47 kPa). This means that there is a buildup of ammonia gas in the cooling coil. Between 738 seconds to 1000 seconds, the pressure remains constant at the maximum pressure. Therefore the adsorption process is no longer occurring.

Later, when the adsorption bed is opened for cleaning, it is discovered that the problem is caused by a blockage inside adsorption bed. The ammonia which is adsorbed in magnesium chloride salt, prior to 200 seconds, caused the salt to solidify and block the entrance into the adsorption bed. Further expelling of ammonia into cooling coil after 200 seconds is not effective. The ammonia accumulates in the coil and builds up pressure from being heated by the water. This is potentially a dangerous scenario that may cause structural failure of the coil. The pressure in the coil must be controlled better for safe and effect operating conditions.

The ammonia expansion experiment with adsorption has two main issues. The first issue is to maintain the cooling coil at low enough pressures for continuous and effective throttling of ammonia. For this to happen, the adsorption rate from desiccant salt(s) must be fast enough to capture the rate of ammonia gas being formed in the cooling coil, thus keeping a low back pressure. Second issue is the fine tuning of the throttling valve to allow for the optimum flow rate of ammonia. Ideally the flow ammonia should match the rate of adsorption. In the next experimental case the adsorption rate is improved by mixing aluminum oxide with the magnesium oxide to increase the adsorption rate.

6.1.1.2 Experimental Case 2

Experimental case 2 uses the desiccant salt mixture with 50% wt $MgCl_2$ and 50% wt AlO_2. The desiccant salt mixture increases the diffusivity of the ammonia into the desiccant thus increasing the rate of adsorption and minimizing the pressure in the cooling coil. In Figure 6.2 the rate of cooling that is obtained is 8.8℃ of cooling in 80 seconds. The rate of cooling achieved in this experiment proves that ammonia expansion with desiccant salt capture is a feasible cooling method. This method of cooling is capable of cooling 300 ml of water by 10℃ in less than 3 minutes.

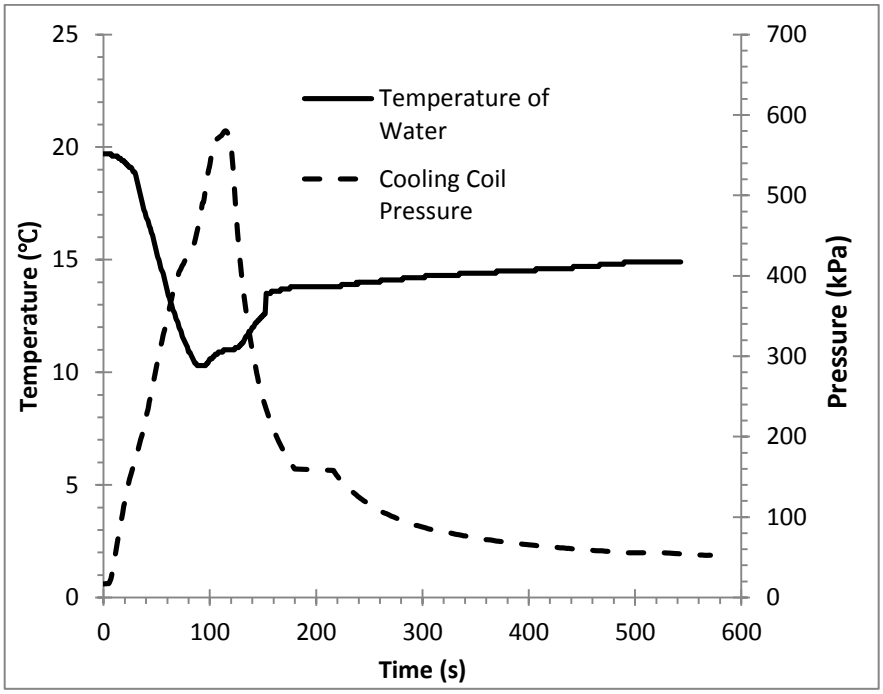

Figure 6.2: Ammonia expansion experiment run at 3 turns of the throttling valve and magnesium chloride (50%wt) and aluminum oxide (50%wt) in the adsorption bed.

The pressure in the cooling coil peaks at 566 kPa and rapidly drops back down afterwards. This shows that the adsorption into the salt mixture has a high adsorption rate. When comparing the pressures from experimental case 2 to experimental case 1 the pressure profile in the salt-mixture experiments have far better results. Because of the

higher rate of adsorption the heat transfer from the water to the coil is much higher. The ammonia is allowed to effectively throttle for longer because there is adequate adsorption to keep the back pressure low. Keeping the back pressure low also makes the self-cooling beverage can safer for its use.

Temperature of the throttled ammonia ranges between -55℃ and -10℃ because initially ammonia at around 800 kPa (depending on the ambient temperature of the lab) is throttled into a near vacuum, and then throttling is considered ineffective after the pressure in the coil reach above 400 kPa. In the analytical and numerical model of the conceptual design, an assumption of -30℃ is made for the temperature of throttle ammonia in the cooling vessel wall. -30℃ is the average temperature of the throttle ammonia inside the cooling coil during the cooling phase.

6.1.1.3 Experimental Case 3

Experimental case 3 is performed to study the cooling rate of the ammonia expansion method if there is no back pressure in the after the cooling coil. The pressure inside the coil remains relatively constant at ambient pressure. This allows for continuous throttling of ammonia from around 800 kPa to 100 kPa. In this experiment 300 ml of water is cooled from 17.1℃ to 6.1℃ in 531 seconds, which is just under 10 minutes. Rate of cooling in this experimental case is slower than the rate of cooling in experimental case 2, where there is ammonia adsorption. The adsorption of ammonia helps with the throttling process, thus providing faster cooling. This is a great advantage that ammonia adsorption has over direct releasing of ammonia into the fume hood.

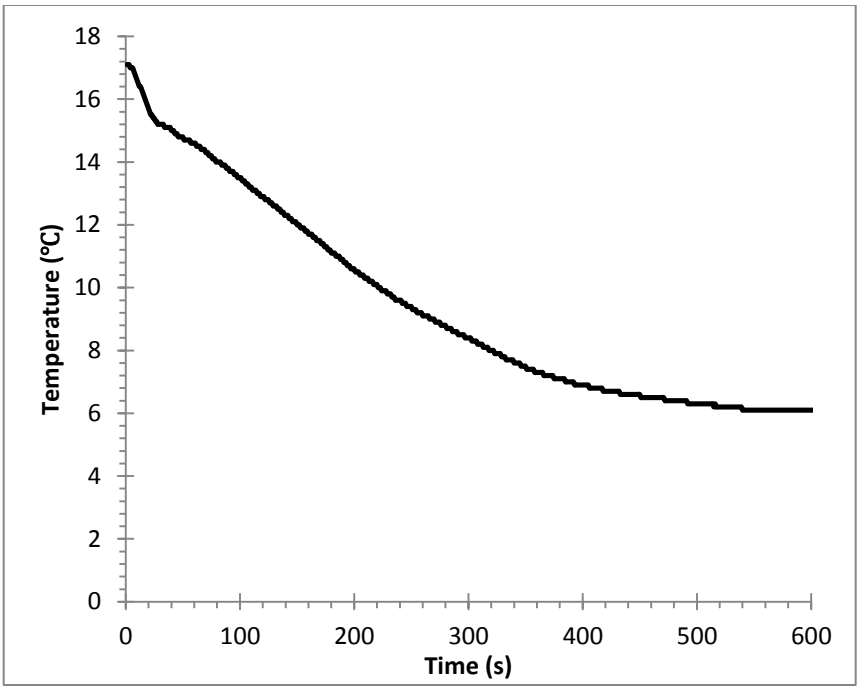

Figure 6.3: Ammonia expansion experiment run at 3 turns and vented directly into the fume hood after evaporation for zero back pressure.

6.1.2 Experiment 2

Experiment 2 tests the validity for using endothermic reaction as a cooling method for a self-cooling beverage can. The experimental test cases are presented in Table 6.2. In all of the endothermic reaction cases 100 g of ammonium thiocyanate and 50 g of barium hydroxide are used. Effect of initial fluid temperature played an important role in the potential ice formation around the reaction vessel during the cooling process. The results are presented as temperature over time graphs of the temperature of the beverage, and temperature inside of the reaction vessel.

At the end of each of these experiments it is observed that all the reactants has not undergone full reaction. The contents inside of the reaction vessel have reached equilibrium. The reaction could not continue any further because the temperature of the water is too low to provide additional heat that the reaction requires. During mass

production of this design, the chemicals within the reaction vessel can be recycled by separating the products and subjecting them to several chemical reactions to arrive back to the original reactants. However the cost of such processes has not be considered for this study.

Table 6.2: Endothermic reaction experimental cases with experimental parameters.

Experimental Case	**Fluid**	**Mass of NH_4SCN (g)**	**Mass of $Ba(OH)_2 \cdot 8H_2O$ (g)**	**Initial Temperature of Fluid**
1	Cola	100	50	20
2	Water	100	50	20
3	Water	100	50	26

6.1.2.1 Experimental Case 1

Experimental case 1 involves the cooling of 300 ml of cola with an endothermic reaction between ammonium thiocyanate and barium hydroxide octahydrate. Figure 6.4 shows the results for this experimental case 1. In 3 minutes the cola is able to cool from 20.7℃ to an average of 8.8℃. That is an average temperature drop of 11.9 degrees which is considered very satisfactory in terms of performance. The temperature continues to drop further after the 3 minute mark. The minimum temperature that is shown in the graph is 4.6 degrees at 444 seconds. This experiment proves that using the before mentioned endothermic reaction to cool 300 ml of beverage is an adequate cooling method.

The line in the graph for reaction temperature is fluctuating continuously between 91 and 210 seconds. The fluctuations are occurring because of mixing the reactants with a stirring rod. The mixing is performed periodically to increase the endothermic reaction

rate. The reaction average temperature is around -20℃ from what is observed in the experiment.

The temperature inside the reaction vessel drops down to an average of $-20℃$ and remains there from 91 seconds to 210 seconds. Most of the cooling of the beverage occurs during this time. In the analytical and numerical analysis of the conceptual design for an endothermic based self-cooling beverage can the temperature of the cooling vessel wall is set to -20℃.

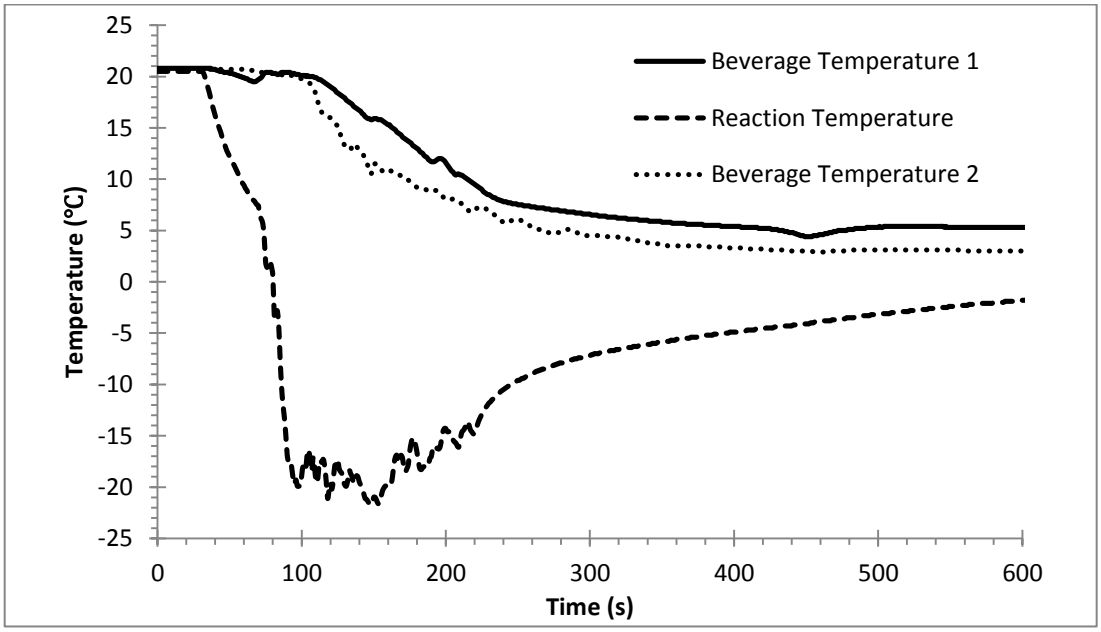

Figure 6.4: Endothermic reaction experiment with 300 ml of cola as beverage with initial temperature of $20.8℃$.

6.1.2.2 Experimental Case 2

In experimental case 2, water is the fluid being cooled in the experimental setup. The initial temperature of the water is around 20℃. The temperature of the water did not rapidly decrease until much later in the experiment as seen in Figure 6.5. Although the temperature inside the reaction vessel is well below 0℃, and from 234 to 290 seconds the average reaction temperature is close to around -20℃, the cooling rate of water does not

change much until after 300 seconds. Majority of the cooling for the water is achieved between 300 seconds and 380 seconds of the experiment. In this time frame, the temperature of the water drops from an average temperature of 16℃ to 8.4℃.

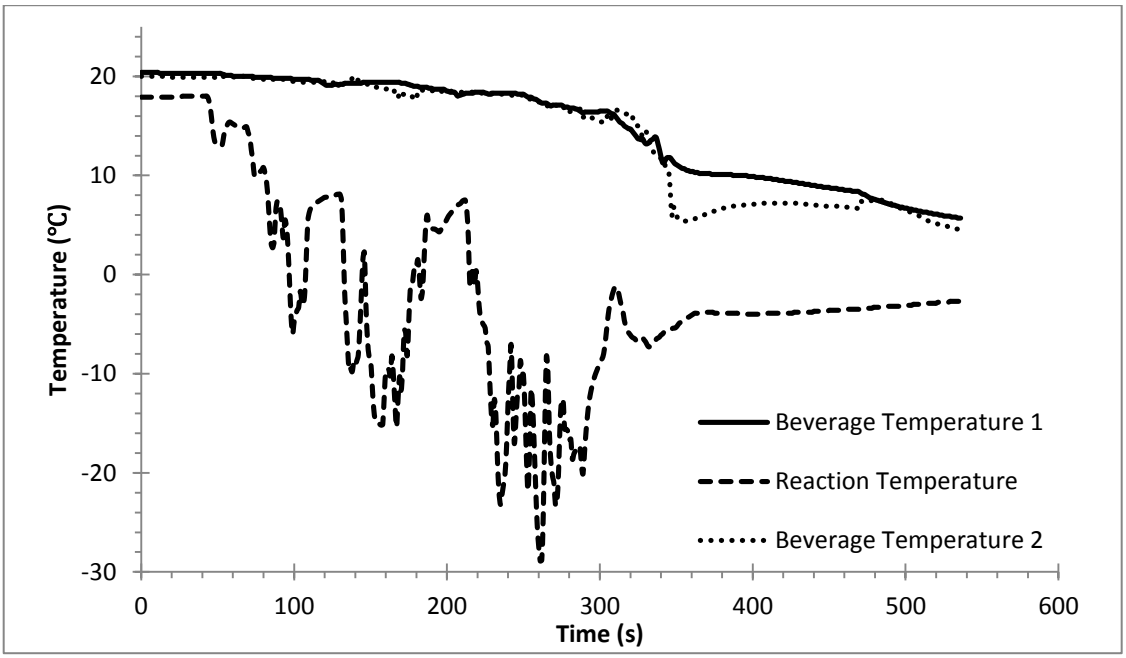

Figure 6.5: Endothermic reaction experiment with 300 ml of water as beverage with initial temperature of 20.4℃.

The reason for the delayed cooling is due to the formation of a layer of ice surrounding the reaction vessel. The ice formed during the initial parts of the experiment when the temperature dropped quickly to the negative temperatures. This is why even though the average reaction temperature is -20℃ between 234 to 290 seconds, the water did not rapidly cool because the ice provided a layer of insulation between the cooling medium and the beverage.

The iced that is formed around the reaction vessel is shown in Figure 6.6. The reason for the ice formation is because the water immediately in contact with the reaction vessel cooled rapidly and formed ice. Ice formation is affecting the heat transfer rate negatively because of the additional insulating boundary between the water and cooling

medium. The thermal energy of the beverage takes more time to reach the endothermic reaction. However, the ice may be considered as a positive phenomenon since it can still provide cooling to the beverage over a longer period of time. The ice acts a phase changing material used to provide cooling over longer time. As seen the graph, rapid cooling of the beverage still occurs, but with a delayed time compared with no ice formation as seen in experimental test case 1.

One solution to this issue is to increase the initial temperature of the water so that it has a lower chance to form ice around the reaction vessel. In experimental case 3 the initial temperature is increased.

Figure 6.6: Ice formation on the reaction vessel due to high rate of cooling from endothermic reaction.

6.1.2.3 Experimental Case 3

Experimental case 3 uses 300 ml of water at initial temperature of 26℃. In this case there is no ice formation around the reaction vessel. Increasing the initial temperature decreases the formation of ice significantly. In Figure 6.7 the graph shows that the temperature drops from 26.3℃ to an average temperature of 12.3℃ between 52 seconds to 200

seconds. That is an average temperature drop of 14 degrees in approximately 2.5 minutes. The reaction temperature during major cooling phase, between 57 to 136 seconds is again close to an average temperature of -20℃. The fluctuations in the temperature of the reaction are again due to mixing during the experiment.

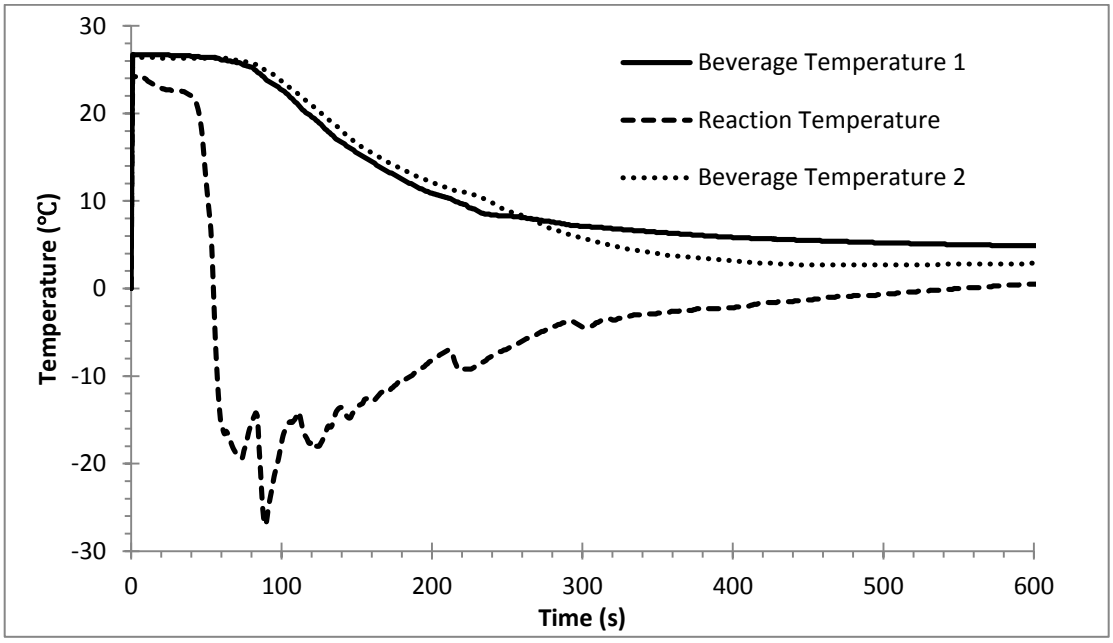

Figure 6.7: Endothermic reaction experiment with 300 ml water as beverage with initial temperature of 26.5℃.

6.2 Analytical Results of Conceptual Can Designs

Figure 6.8 and Figure 6.9 shows the temperature profile through the radial direction of the can with respect to boundary condition in the form of absolute temperature and dimensionless temperature parameter. Two cases have been considered in the analysis with two different initial temperature of the centre of the can. For the ammonia expansion case, the centre temperature is -30℃. For the endothermic reaction case the centre temperature is -20℃. The initial temperature of the water is considered as the ambient temperature, for this case is 25℃. Temperature is increasing in both cases with radial direction r. θ is decreasing in the radial direction because it's a function of instantaneous

temperature at any point on the radial direction. This is expected as the coolest part of the beverage is located at the centre where the cooling vessel is located. The warmest part of the beverage after the cooling phase would be the outer wall of the beverage can since it is in direct contact with the ambient air.

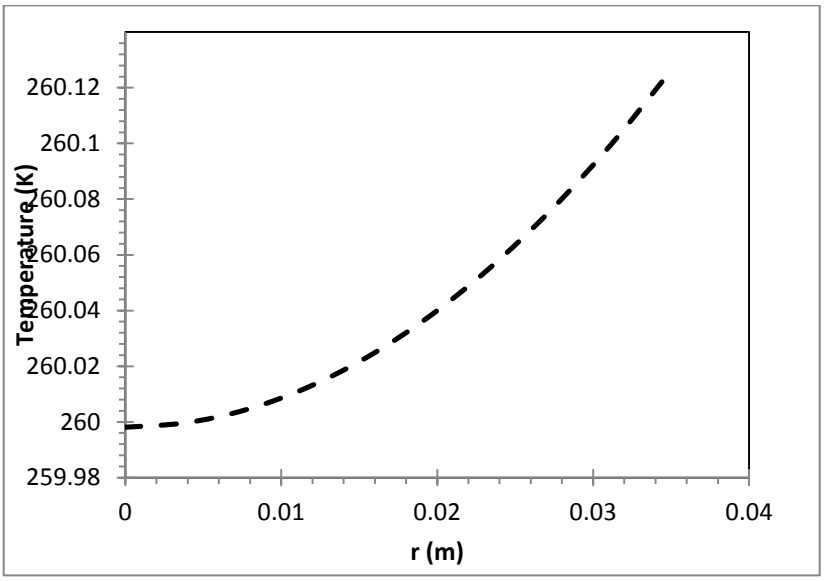

Figure 6.8: Temperature profile across the radial direction of the cylinder for the analytical analysis with inner temperature of -20℃.

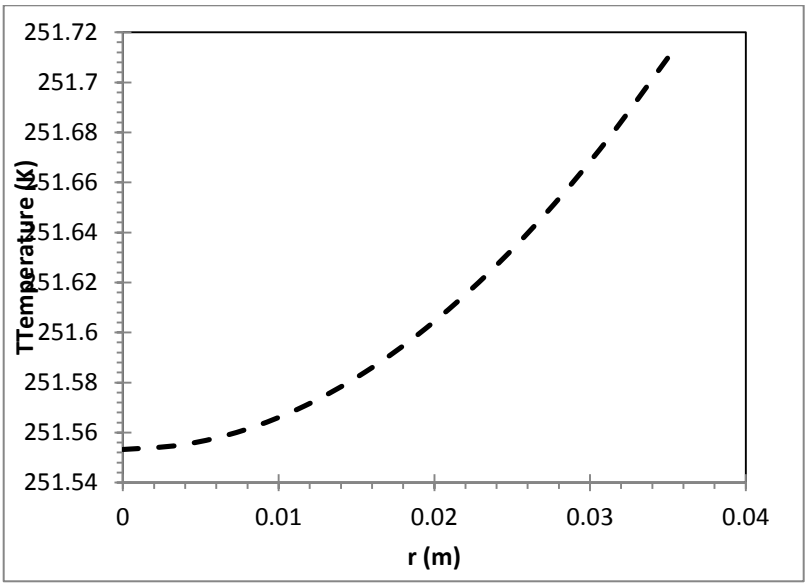

Figure 6.9: Temperature profile across the radial direction of the cylinder for the analytical analysis with inner temperature of -30℃.

6.3 Numerical Results for Conceptual Designs

The numerical model results are presented in this section. The results of the grid independence test justify the use of the normal density mesh generated in COMSOL. A comparison of cola and water is presented to show that using water as the beverage is adequate enough for obtaining results for this numerical study. Finally, a parametric study of aspect ratio and ambient temperature is presented to show how they affect the performance of the self-cooling beverage can for both ammonia expansion and endothermic reaction cooling methods.

6.3.1 Grid Independence Test Results

From Table 6.3 it can be observed that the finer the mesh has the longest computation time. However the element sizes are smaller, thus providing the most accurate solution.

Table 6.3: Computation time and maximum and minimum mesh sizes for the different mesh densities. All tests are done using the same aspect ratio, T_c and T_{amb}.

Mesh Density	Computation Time (s)	Maximum Element Size (cm)	Minimum Element Size (cm)
Finer	14546	0.555	0.00188
Normal	4641	1.010	0.00450
Coarse	2045	1.500	0.03000
Coarser	1446	1.950	0.09000
Extremely Coarse	739	4.950	0.75000

In Figure 6.10 the effects the different mesh densities are apparent. The finer the mesh size is, the finer the model's resolution is. As the meshes become coarser, there is significant loss in resolution of detail in the fluid flow of the liquid.

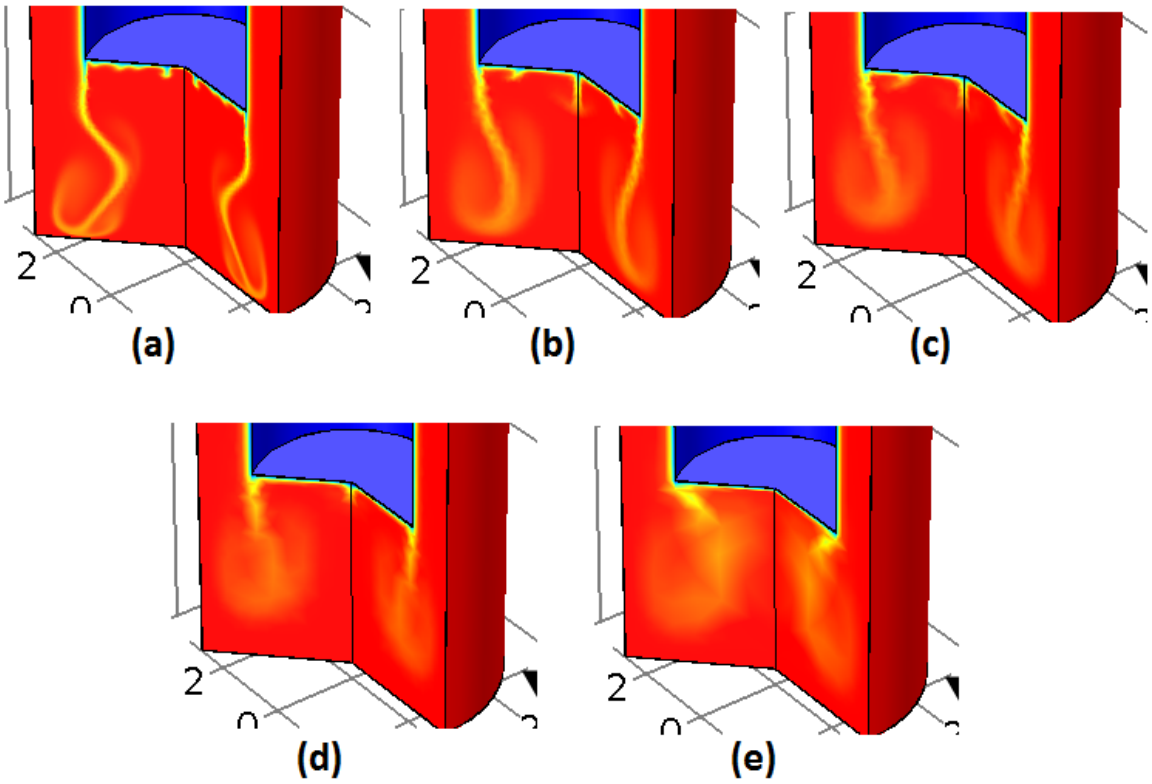

Figure 6.10: Temperature distributions after 6 seconds for different mesh densities. (a) finer, (b) normal, (c) coarse, (d) coarser, (e) extremely coarse.

In Figure 6.11, the average volume temperature of the 355 ml of water is graphed over time. Each line in the graph represents one of the mesh densities. From first glance, all of them seem to be very similar, but when observed closely the mesh density which matches the finer mesh density's solution closest is the coarser mesh. However, the normal mesh is chosen to perform the simulations for the model because the resolution of the flow better resembles the temperature profile images from the finer mesh in Figure 6.10. The results obtained from a normal mesh are also very close to the finer mesh results, and it takes less than half the time it takes to solve for finer mesh. This is why the normal mesh is chosen for compiling the numerical model results.

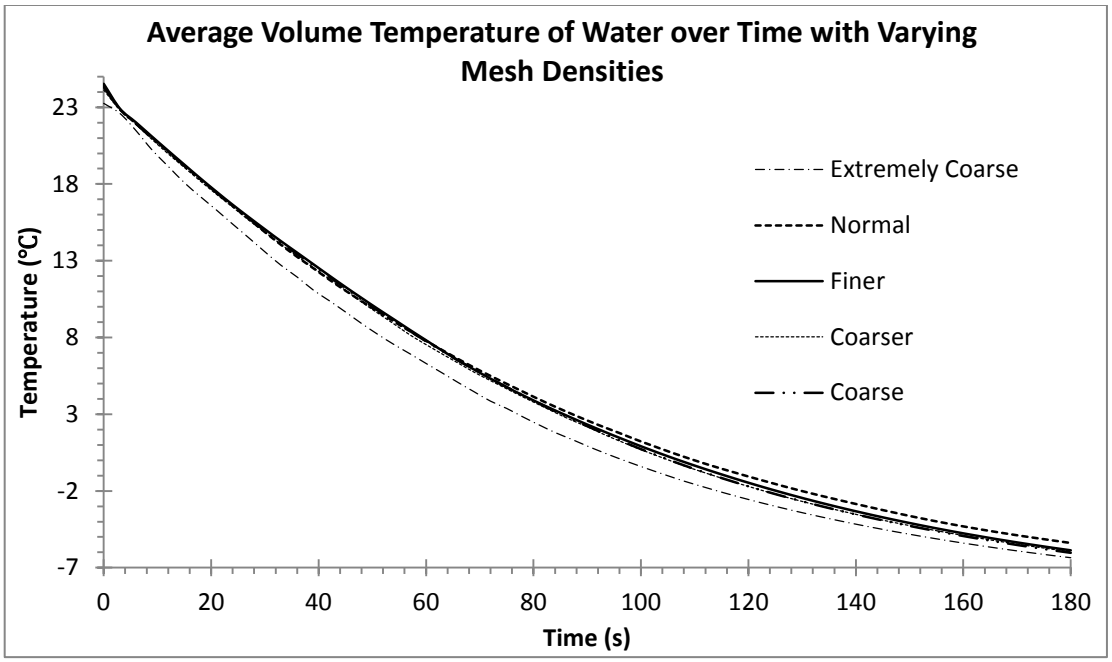

Figure 6.11: Results of average volume temperature of water over time with varying mesh densities.

6.3.2 Water and Cola Comparison

The numerical model uses water as the beverage fluid for all of the test cases. Using water is justified in this section by comparing the results of water and cola. The cola results are obtained by applying a factor to change the specific heat capacity, thermal conductivity, and density functions for water in COMSOL. The test condition for this set of results are obtained by using Aspect Ratio 4, cooling vessel wall temperature of -30℃ and ambient temperature of 25℃.

Figure 6.12 compares the average fluid velocity in the can for 180 seconds. From the graph it is clear that the water and cola have a very small difference in average velocity. Water has more minor fluctuations in velocity than cola does. The increase in fluctuations in velocity for water is attributed to the lower density in the water. Water is able to move more freely during the temperature induced convective currents, thus producing more temperature fluctuations. However, even with these minor fluctuations,

the average percentage difference of the results is 14.3%, which is within an acceptable range. Using water as a base line material for simulating the results of a self-cooling beverage can is viable.

Figure 6.13 shows the results for average temperature of water and cola over 180 seconds. The graph shows that the temperature of the cola and water are nearly the same. The lines for water and cola have the same curvature. This shows that the cooling rates of the two fluids are very close in magnitude. The calculated average percentage difference between water and cola is 12.03% for the average temperature.

Figure 6.14 shows a graph for the average total heat flux of water and cola. The graph has the same shape as the graph for average velocity in Figure 6.12. The heat flux is directly proportional to the velocity of the beverage; therefore the two graphs are very similar. The calculated percentage difference between water and cola for average total heat flux is 16.52%.

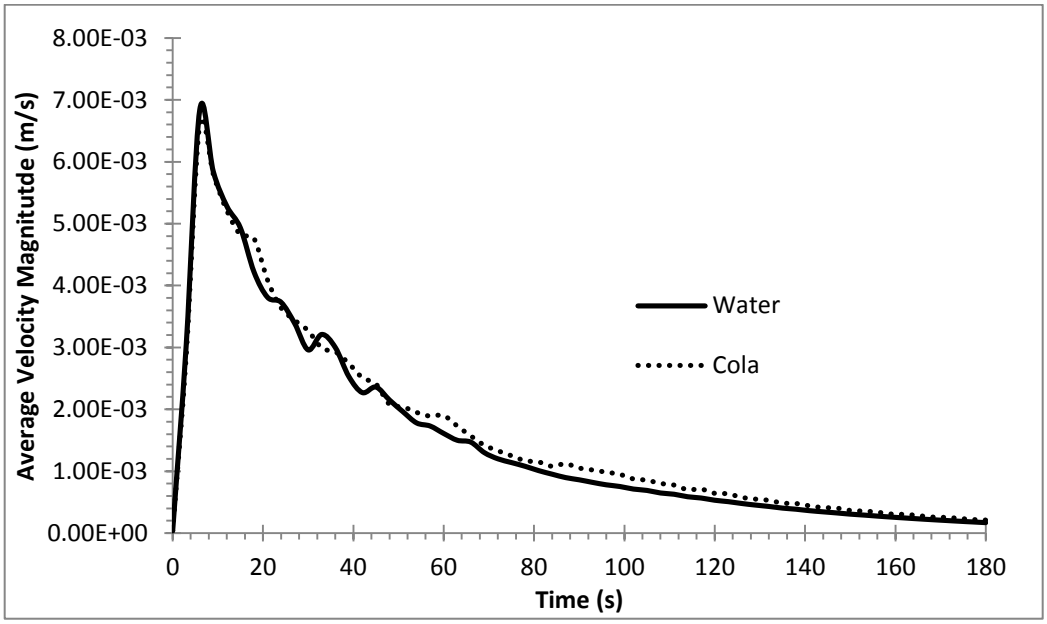

Figure 6.12: Average velocity of water and cola over 180 seconds for the same test case.

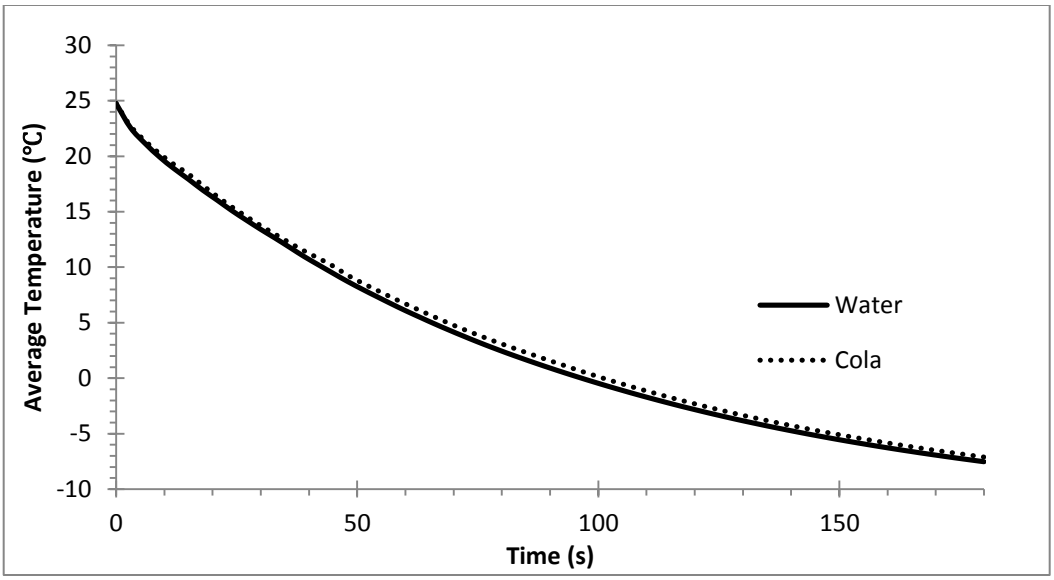

Figure 6.13: Average temperature of water and cola over 180 seconds for the same test case.

Figure 6.15 shows a graph of the heat capacity values for water and cola. In the model, the heat capacity of cola is obtained by multiplying a factor with COMSOL's heat capacity function for water. As such the graph shows two curves that are separated by a distance created by this factor. On average the percentage difference between the heat capacity of water and cola is 8.37%.

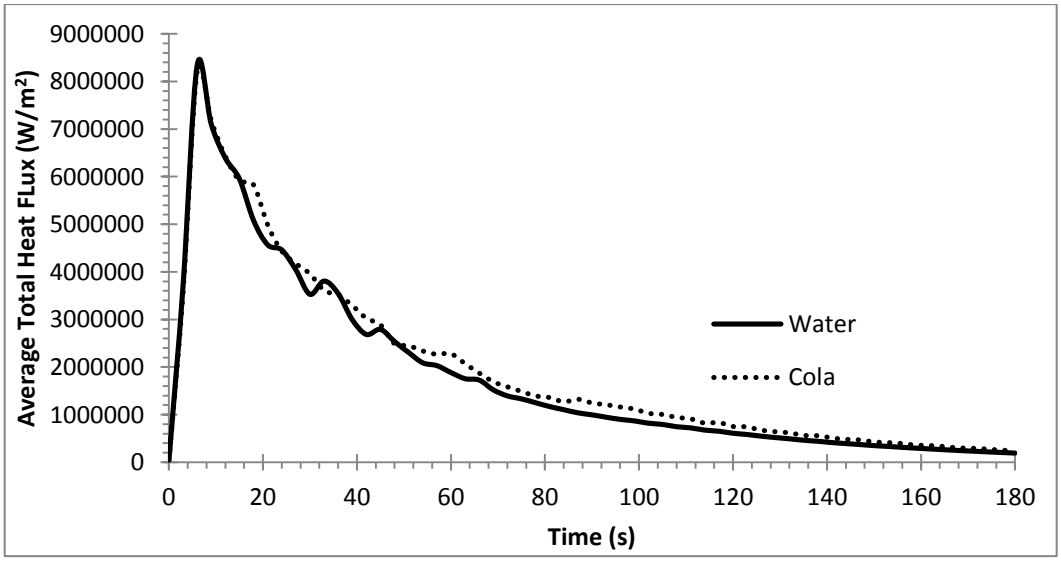

Figure 6.14: Average total heat flux of water and cola over 180 seconds for the same test case.

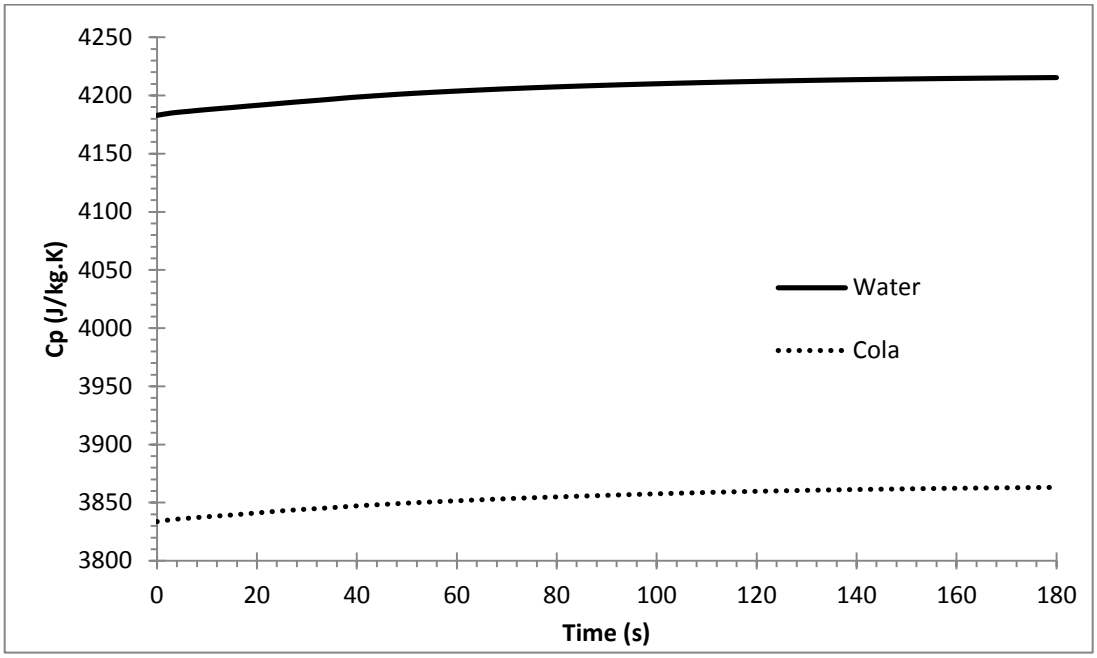

Figure 6.15: Heat capacity at constant pressure of water and cola over 180 seconds for the same test case.

Figure 6.16 shows a graph for the average outer can surface temperature for water and when using cola test cases. For the first minute the percentage difference between the results is less than 10%, but as time increases so does the difference between the results of cola and water. However, the difference is not a lot. Even though the lines diverge slightly, the average percentage difference of this result is 24.09%. The average percent difference is higher in this case because the temperature values crosses over into negative temperatures. At time 165 the magnitude of can surface temperatures for the water and cola are -0.02989℃ and 0.72722℃. At this point the percent difference is 2532.99%. If this asymptotic point is neglected from the average percent difference, it becomes 17.73%.

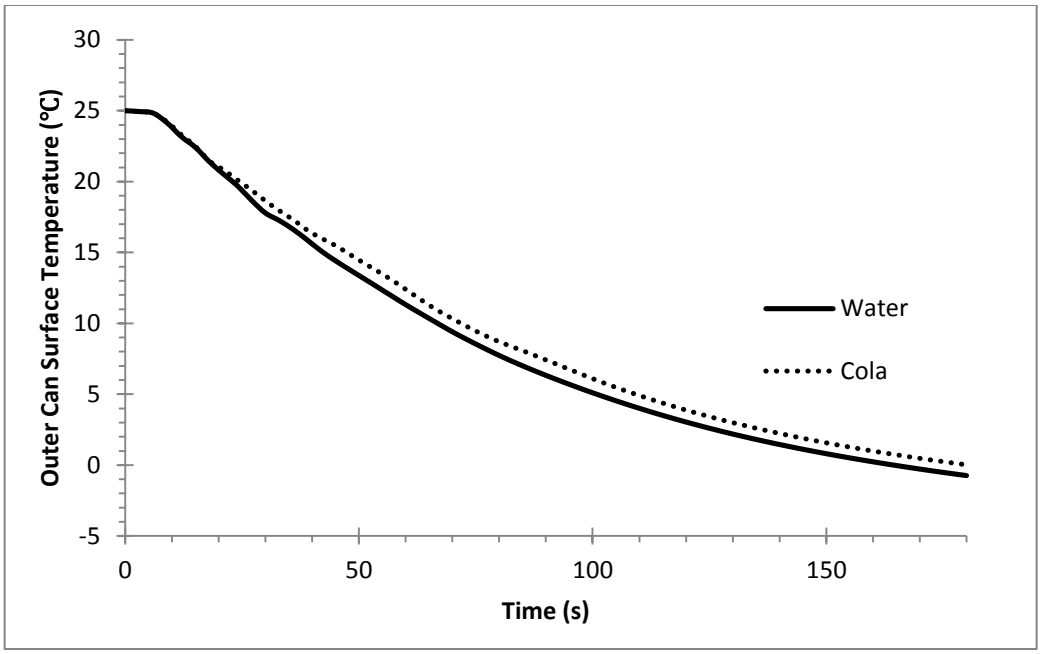

Figure 6.16: Outer can surface temperature of water and cola over 180 seconds for the same test case.

Water is used as the fluid for the beverage in modeling the self-cooling beverage can. The average percent difference between the results of water and cola are less than 20% on average. This is an acceptable difference for the purposes of this thesis. It is safe to assume that water can be used to represent beverages such as cola or other beverages which have similar thermo physical properties as cola.

6.3.3 Aspect Ratio

The aspect ratio is defined as the length of the cooling vessel over the radius of the cooling vessel. A parametric study of the aspect ratio is conducted. The results of the 5 aspect ratios are presented for ammonia expansion and endothermic reaction cases. As started earlier the cooling vessel wall temperatures are -30℃ and -20℃ for ammonia expansion and endothermic reaction methods respectively. The ambient temperature is kept constant at 25℃ for the results presented in this section.

Figure 6.17 shows the graph for average velocity magnitude of water for the 5 different aspect ratios for the ammonia expansion case. The results for the different aspect ratios are quite varying. This is due to the geometrical configurations of the aspect ratios. Aspect ratio 1 is one of the extreme cases, it has a cooling vessel radius equal to the beverage can radius. On average aspect ratio 1 has the highest velocity. This is because the geometry in aspect ratio 1 has the largest body of uninterrupted body of water. The top end of the water is in direct contact with the cooling vessel wall. In this configuration, convection currents in the water can form easily and more often, thus giving aspect ratio the highest average velocity. Aspect ratio 5 is also an extreme case. It has the longest cooling vessel length, but shortest cooling vessel radius. In this geometry it is harder to form faster free moving convection currents since the body of water is segregated by the cooling vessel. It is observed that as the aspect ratio of the cooling vessel increases, the average velocity of water decreases.

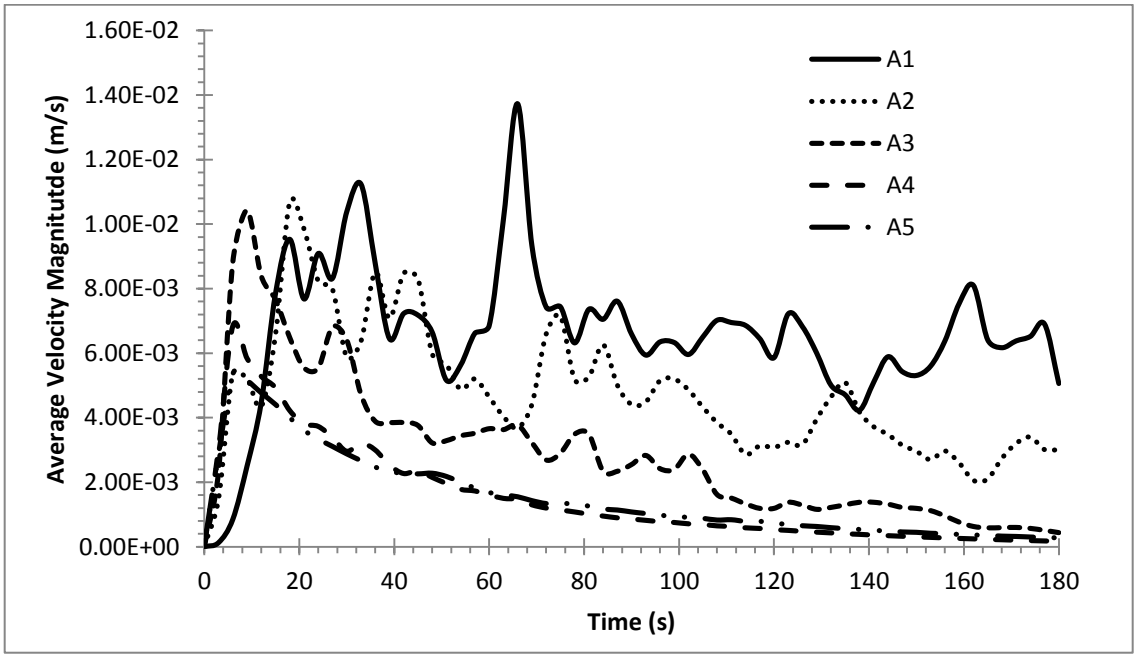

Figure 6.17: Average velocity of the 355 ml of water for different aspect ratios over 180s, with a cooling vessel temperature of -30℃.

The graph for average velocity magnitude of water for the 5 different aspect ratios for the endothermic reaction case is shown in Figure 6.18. The same relationship between geometry and average fluid velocity is observed as in the ammonia expansion case. However, since the temperature difference between the cooling vessel wall and the initial temperature of the water is smaller in this case due to a warmer cooling vessel wall, the magnitude of velocity is comparatively slower. Temperature difference between the beverage and cooling vessel wall is proportional to the average velocity of the water during the cooling phase.

The graph for average total heat flux for the 5 aspect ratios is shown in Figure 6.19 for the ammonia expansion case. This graph is similar to Figure 6.17 in terms of the shape of the lines. Total heat flux, as started before is directly proportional to velocity, therefore the graphs look the same. The heat flux is highest for aspect ratio 1 since it has the highest velocities. The lowest heat flux is in aspect ratio 5 which has the lowest magnitude of velocity.

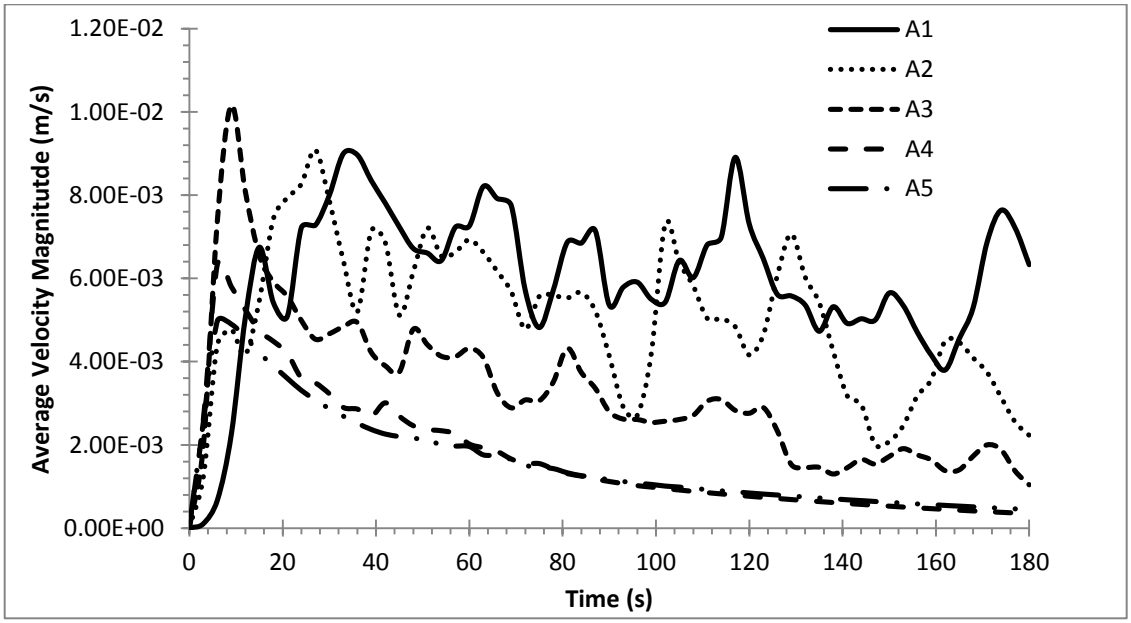

Figure 6.18: Average velocity of the 355 ml of water for different aspect ratios over 180s, with a cooling vessel temperature of -20℃.

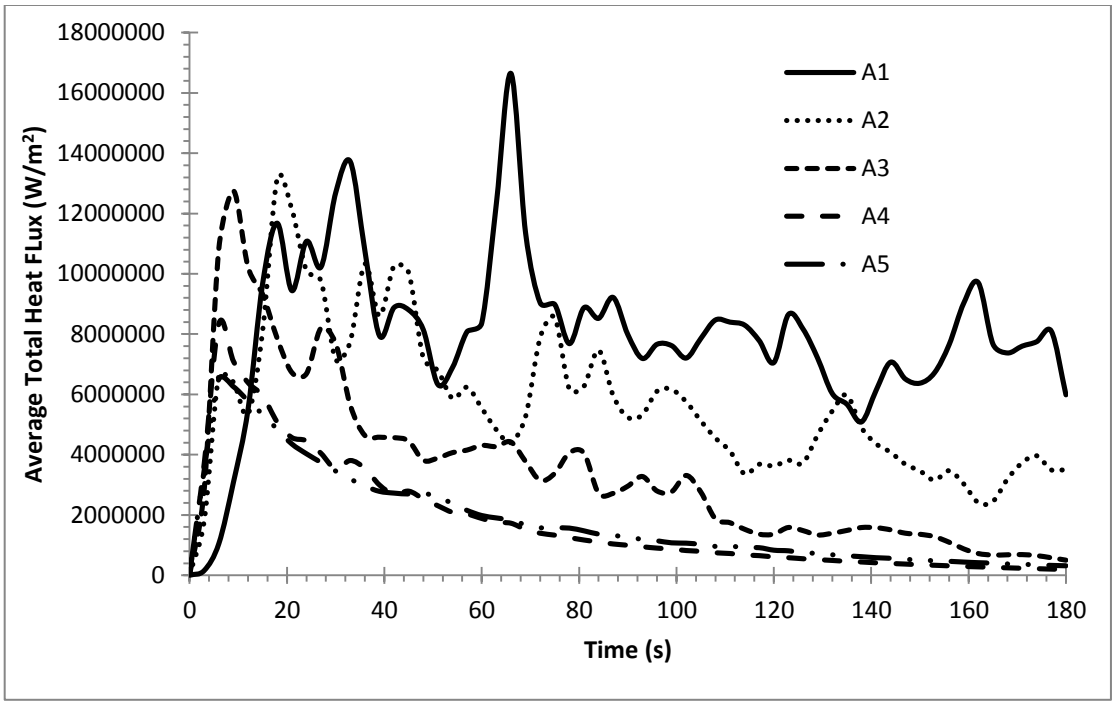

Figure 6.19: Average total heat flux of the system at different aspect ratios over 180s, with a cooling vessel temperature of -30℃.

The graph for average total heat flux for the 5 aspect ratios for the endothermic reaction case is shown in Figure 6.20. The graph highly resembles Figure 6.18 which is the graph for average velocity magnitude of the water with the same conditions. Total heat flux, as started before is directly proportional to velocity, therefore the graphs are appear very similar. The heat flux is highest for aspect ratio 1 since it has the highest velocities. The lowest heat flux is in aspect ratio 5 which has the lowest magnitude of velocity. It is expected that the two extreme cases would have the highest and lowest average heat fluxes. When considering the aspect ratios that are not extreme cases, aspect ratio 2 has the fast velocity and highest heat flux. Aspect ratio 4 has the slowest average velocity and the lowest heat flux.

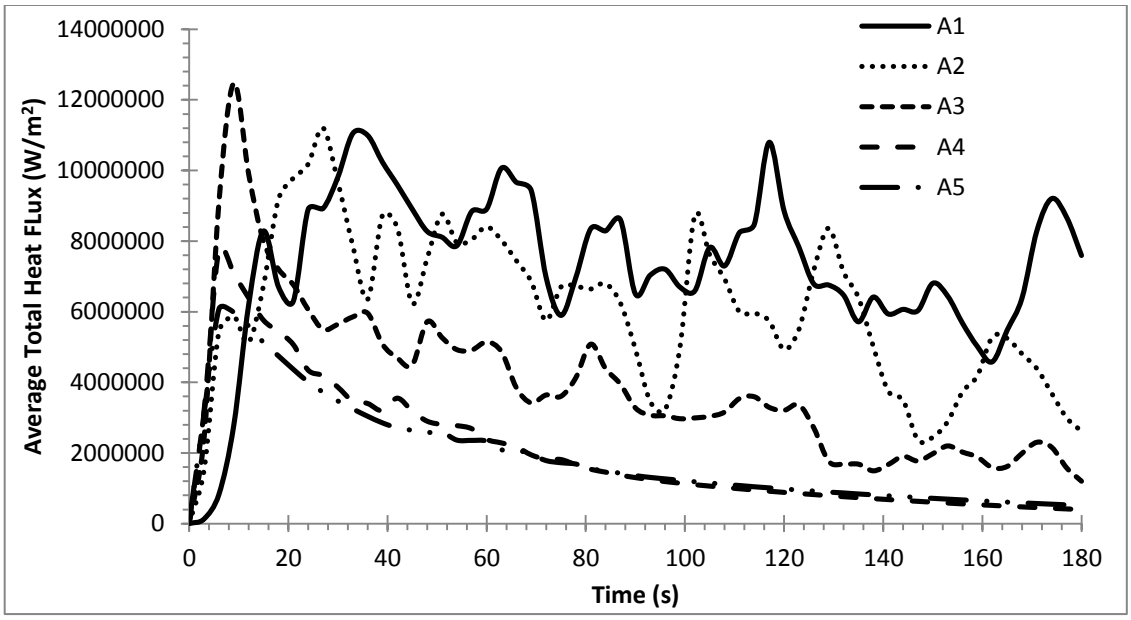

Figure 6.20: Average total heat flux of the system at different aspect ratios over 180s, with a cooling vessel temperature of -20℃.

The specific heat for water is increasing over time for both ammonia expansion and endothermic reaction cases as seen in Figure 6.21 and Figure 6.22. Specific heat changes with temperature. The specific heat of water increases when it nears the freezing point. Initially, the specific heat of water is 4.181 kJ/kg · K for an ambient temperature of 25℃. As water nears 0℃ it the specific heat increases to 4.210 kJ/kg · K. The difference in geometry of each aspect ratio changes the rate of heat transfer that the beverage experiences. This causes the temperature of the beverage to decrease at different rates. The heat capacity in each aspect ratio changes at a its own rate relative to the temperature of the beverage. In both cases the specific heat for water cooled by a can with aspect ratio 4 demonstrates the fastest change in specific heat capacity. This is a good indication that aspect ratio 4 has the highest heat transfer rate for a self-cooling beverage can.

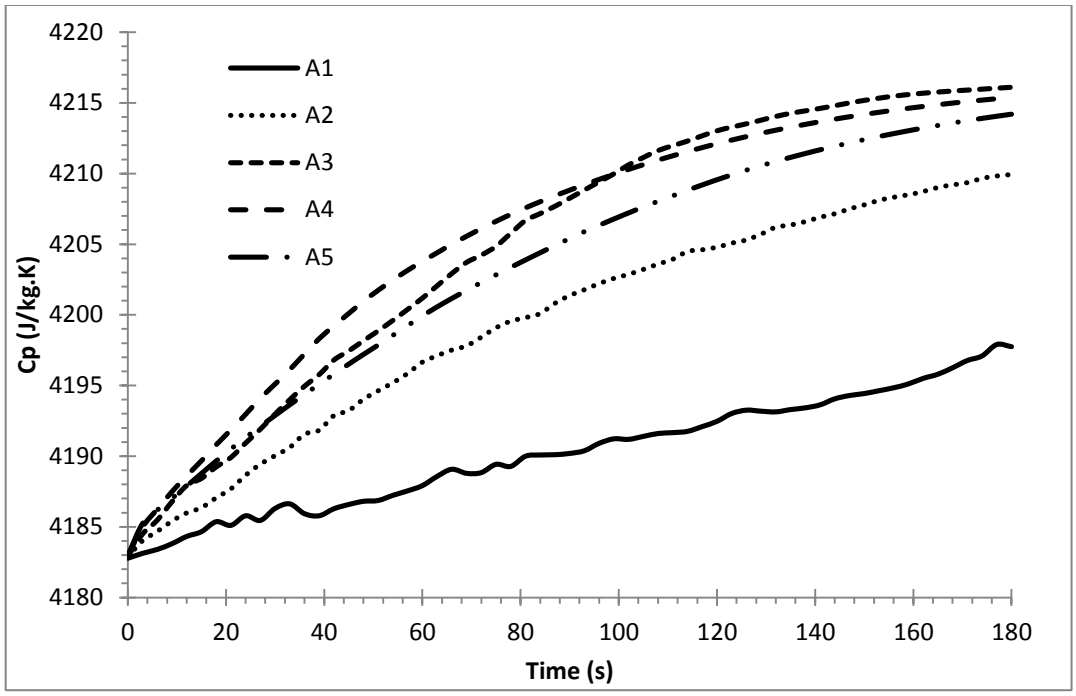

Figure 6.21: Heat capacities for water inside the can at constant pressure for different aspect ratios over 180s, with a cooling vessel temperature of -30℃.

The average temperature of the water over time is of most interest. This graph shows how fast the conceptual designs can cool in 3 minutes. In Figure 6.23 the average temperature of 355 ml of water over 180 seconds is shown for the ammonia expansion case. From 0 seconds to 150 seconds, aspect ratio 4 has the fastest cooling rate. However, after 150 seconds aspect ratio 5 surpasses aspect ratio 4. But since aspect ratio 5 is an extreme case, it would not be feasible to construct. Therefore, the best performing aspect ratio is actually aspect ratio 4. Aspect ratio 4 achieves the lowest average temperature of water out in 180 seconds when considering the 3 physically possible aspect ratios. This means that a skinner longer cooling vessel is more preferable for the heat transfer rate in a self-cooling beverage can design with a set volume constraint.

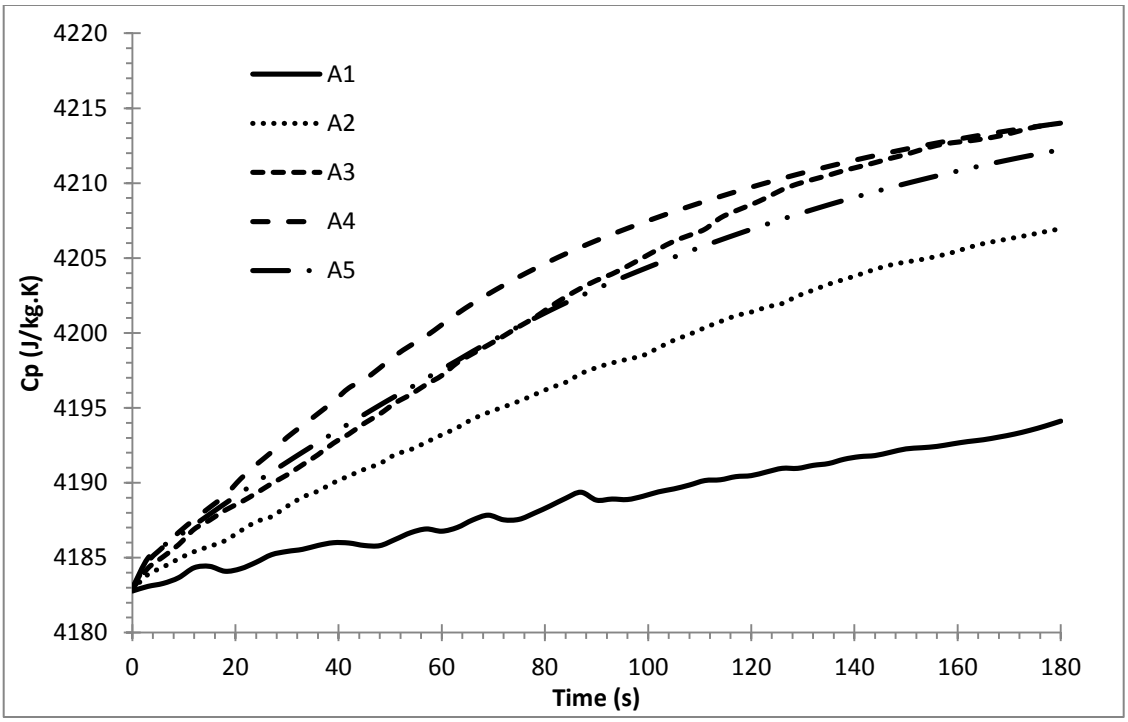

Figure 6.22: Heat capacities for water inside the can at constant pressure for different aspect ratios over 180s, with a cooling vessel temperature of -20℃.

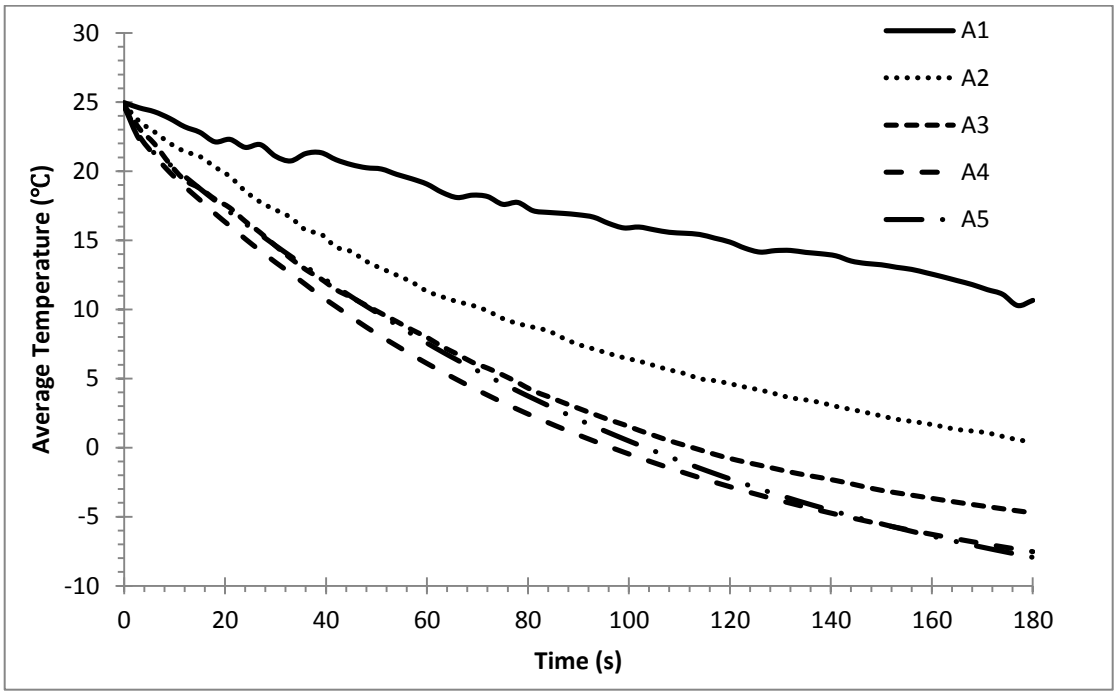

Figure 6.23: Average temperature of the 355 ml of water for different aspect ratios over 180s, with a cooling vessel temperature of -30℃.

In Figure 6.24 the average temperature of 355 ml of water over 180 seconds is shown for the endothermic reaction case for the five aspect ratios. The results in this graph also indicate that aspect ratio 4 is the best performing aspect ratio for cooling the beverage down in the shortest period of time. Since this design uses the endothermic reaction based cooling method, the temperature of the cooling vessel wall is not as cold as the ammonia expansion case. Therefore the temperatures are warmer when compared to the ammonia expansion graph at 180 seconds. There is a difference of 4.32℃ in the final average temperature when comparing the final average temperatures of water for aspect ratio 4.

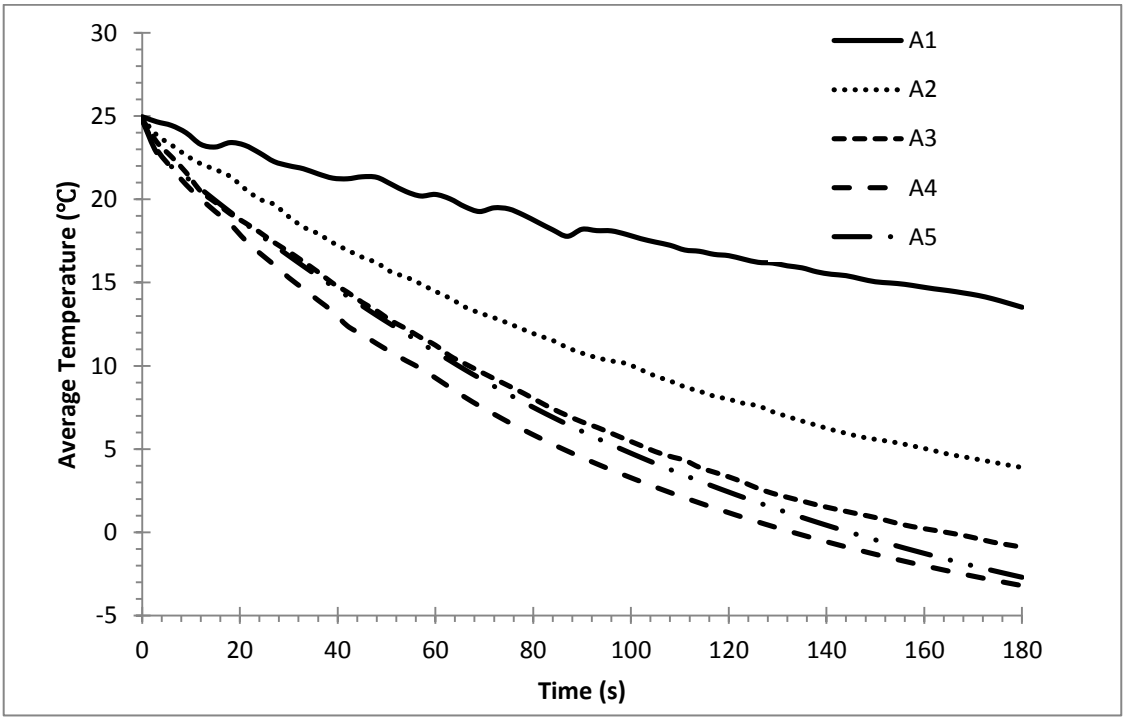

Figure 6.24: Average temperature of the 355 ml of water for different aspect ratios over 180s, with a cooling vessel temperature of -20℃.

Aspect ratio 4 has the lowest outer can surface temperature over time in both the ammonia expansion and endothermic reaction case as seen in Figure 6.25 and Figure 6.26. Interestingly enough, aspect ratio 2 comes really close to beating aspect ratio 4 for

lowest surface temperature. In the ammonia expansion case, aspect ratio 2 achieves a lower outer can surface temperature than aspect ratio 4 between 6 to 69 seconds. This can be explained by the heat transfer that is occurring during the cooling process. Aspect ratio 2 has a higher average velocity of fluid throughout. This helps to decrease the can's surface wall temperature quicker. However, the heat transfer rate in aspect ratio 4 causes the average temperature of the beverage quicker, which ultimately leads to a cooler outer surface temperature.

The same phenomenon occurs in the endothermic reaction case in Figure 6.26. Between 3 and 93 seconds, aspect ratio 2 has a lower can surface temperature than aspect ratio 4. Aspect ratio 4 is considered the best performing aspect ratio. Although the velocity of fluid in this aspect ratio is not as high as the aspect ratio 3 or 2, it is able to provide higher heat transfer rate due to the higher heat transfer rate. The heat transfer between the vessel wall and beverage has both convective and conductive components. In aspect ratio 4, the conductive heat transfer is higher. This explains why aspect ratio 4 is able to provide the best heat transfer performance with a lower average velocity.

6.3.4 Ambient Temperature

In this section, the ambient temperature is varied between 25℃, 30℃ and 35℃. The boundary conditions that are affected by this change are the free convective heating provided by the surrounding air, and the initial temperature of the can system. The ambient temperature parametric study is performed on aspect ratio 4 because it has the best heat transfer performance out of the other realistic aspect ratios. The study investigates ammonia expansion and endothermic reaction cases separately.

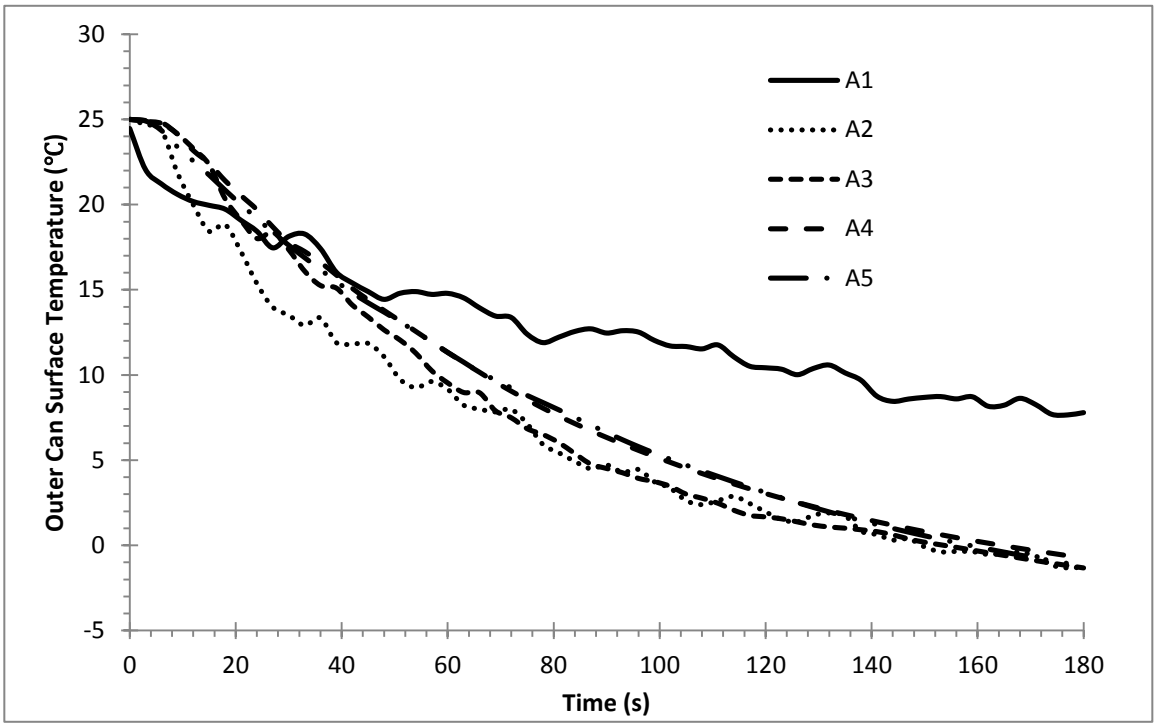

Figure 6.25: Average out can surface temperature for different aspect ratios over 180s, with a cooling vessel temperature of -30°C.

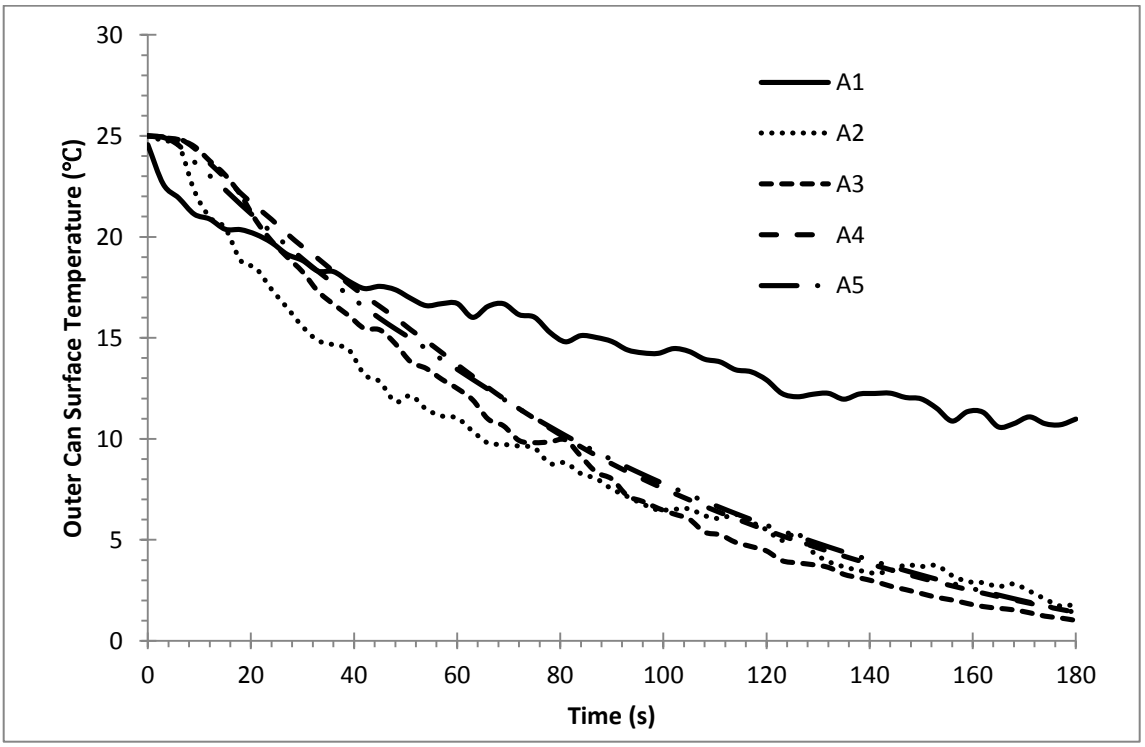

Figure 6.26: Average out can surface temperature for different aspect ratios over 180s, with a cooling vessel temperature of -20°C.

In Figure 6.27 it is observed that increasing the ambient temperature also increases the average velocity in the beverage. It is also observed that there are more frequent and greater velocity fluctuations seen in the water when the ambient temperature is at 35℃ than when compared to an ambient temperature of 30℃ and 25℃. This is because there is a greater temperature differences between the initial temperature of the beverage and the cooling vessel wall. When the temperature difference is higher the convective currents that are created can travel faster.

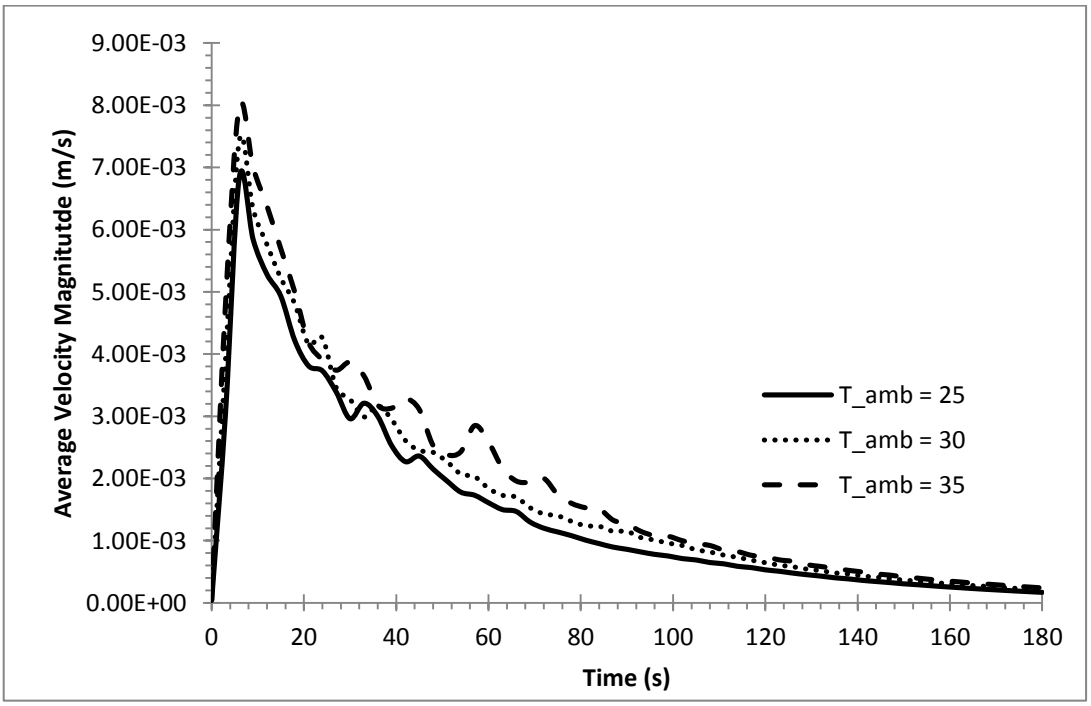

Figure 6.27: Average velocity of the 355 ml of water for different ambient temperatures over 180s, with a cooling vessel temperature of -30℃ for the same test case.

The same is observed in the endothermic reaction case in Figure 6.28. Since the cooling vessel temperature is -20℃ the temperature difference between with the ambient temperature is less compared to the ammonia reaction case. The velocity fluctuations are not as great and has one less fluctuation when comparing the average fluid velocity when the ambient air is at 35℃.

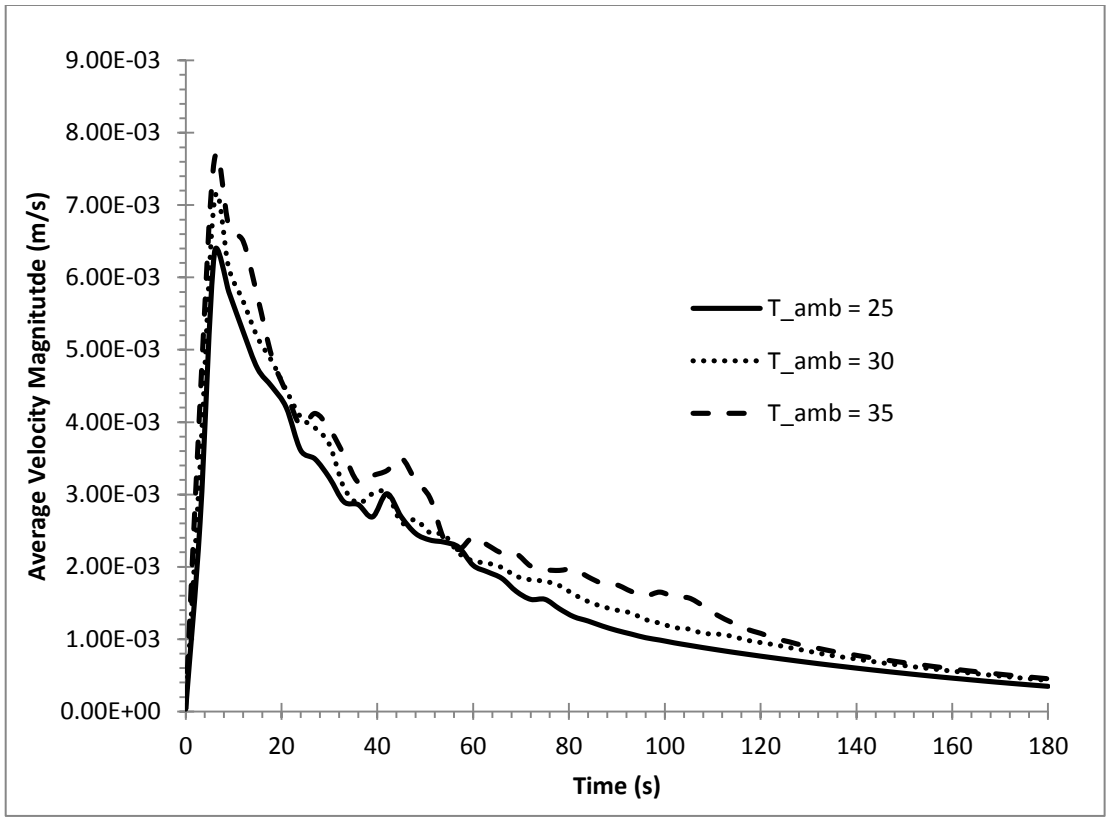

Figure 6.28: Average velocity of the 355 ml of water for different ambient temperatures over 180s, with a cooling vessel temperature of -20℃ for the same test case.

The effect of ambient temperature on heat flux is presented in Figure 6.29 and Figure 6.30. In both the ammonia expansion and endothermic reaction case, the average total heat flux increases for the water increases as the ambient temperature is increased. The fluctuations and magnitudes of heat flux for both ammonia expansion and endothermic reaction cases are related to their respective average velocities presented in Figure 6.27 and Figure 6.28.

Just as observed with the average velocity, the magnitude of heat flux for the ammonia expansion case is higher than the heat flux for the endothermic reaction case. This is again due to the temperature difference between cooling vessel temperature for each case compared to the same ambient temperature.

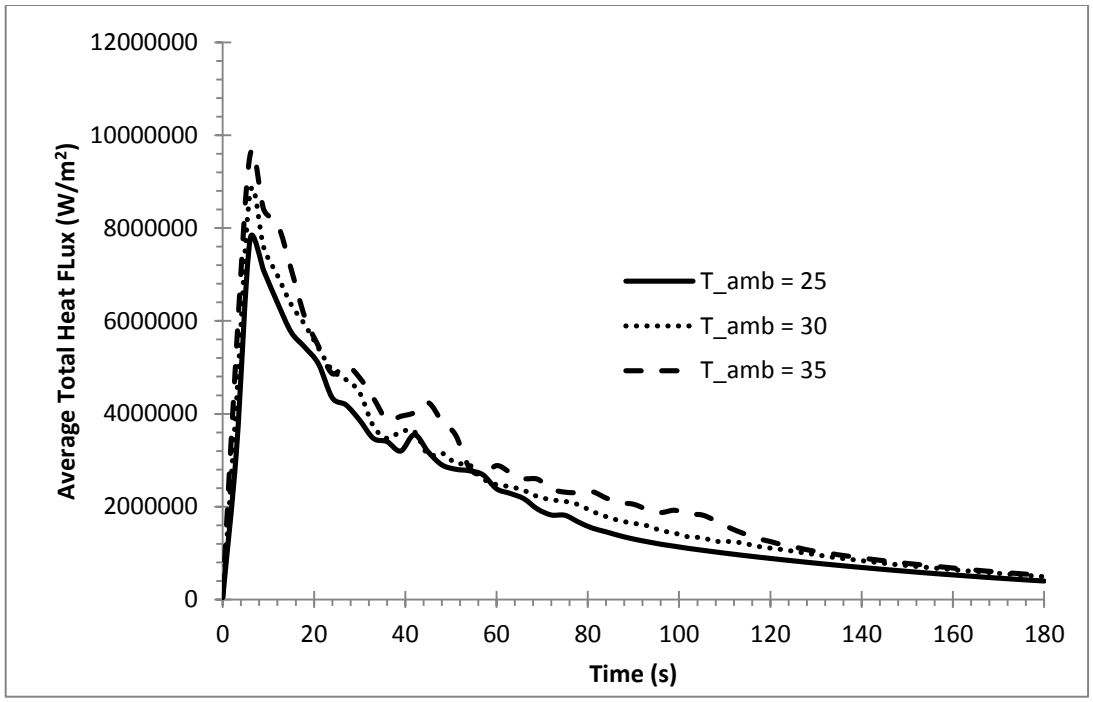

Figure 6.29: Average total heat flux of the can system for different ambient temperatures over 180s, with a cooling vessel temperature of -30℃ for the same test case.

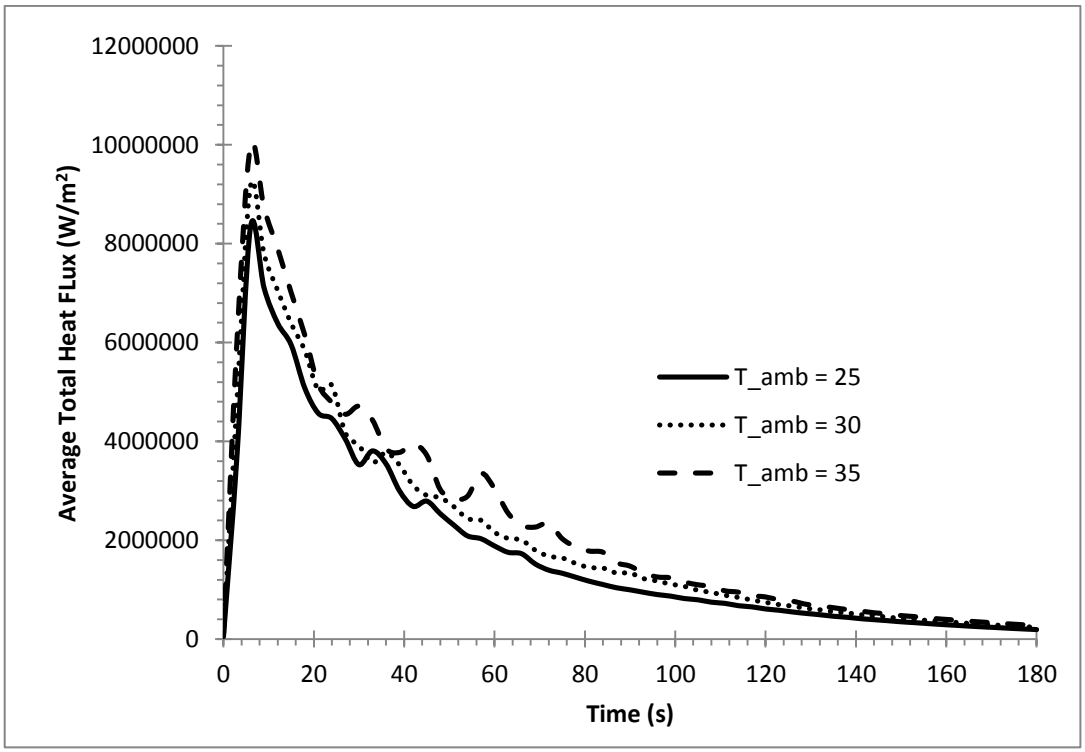

Figure 6.30: Average total heat flux of the can system for different ambient temperatures over 180s, with a cooling vessel temperature of -20 for the same test case.

Figure 6.31 and Figure 6.32 shows the specific heat capacity for both cases over 180 seconds. Initially there is a difference in the heat capacities due to the fact that each case starts at different ambient temperatures. However, eventually the specific heat of the water converges to 4.2 kJ/kg·K at 180 seconds.

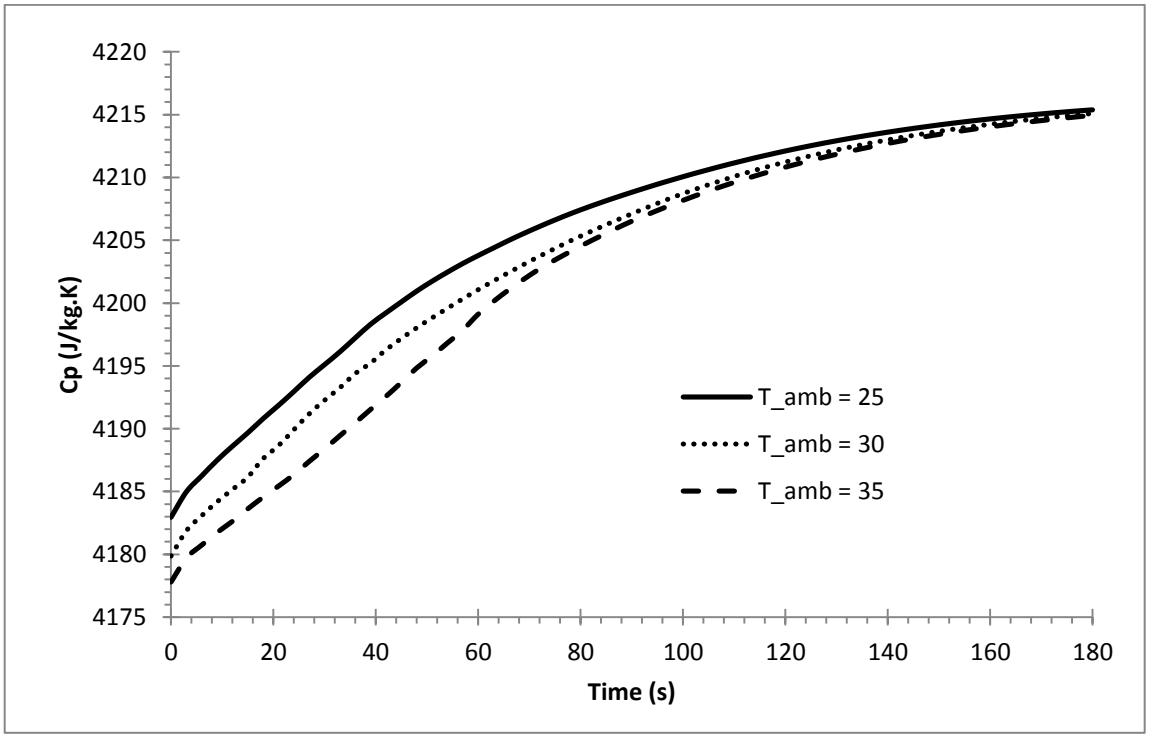

Figure 6.31: Heat capacities at constant pressure of the water inside the can for different ambient temperatures over 180s, with a cooling vessel temperature of -30℃ for the same test case.

There does not appear to be any significant change to the specific heat of water during the simulation due to a change in ambient temperature. The only observable change is that the lower the ambient temperature is, the higher the specific heat capacity initially. Vice-versa, a higher ambient temperature has initially a lower specific heat capacity. The specific heat capacities converge to the same value because the water temperature must be converging to the same temperature for their respective cases.

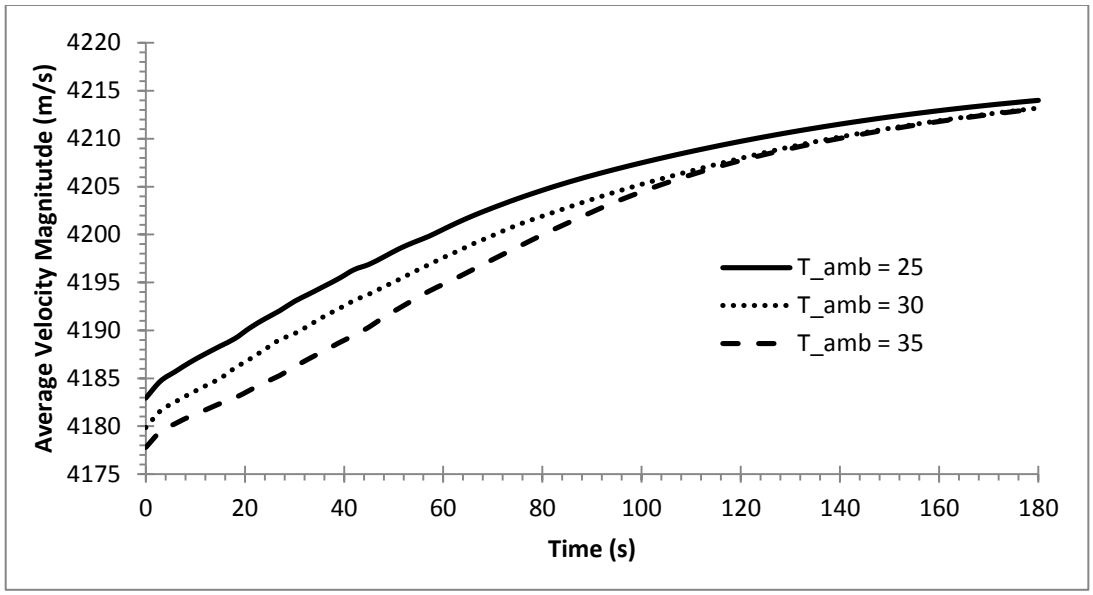

Figure 6.32: Heat capacities at constant pressure of the water inside the can for different ambient temperatures over 180s, with a cooling vessel temperature of -20℃ for the same

Ambient temperature does not seem to have an effect on final average temperature of the water in both the ammonia expansion and endothermic reaction cases as shown in Figure 6.33 and Figure 6.34. In each case the initial temperature differ by 5℃, but by the end of 180 seconds all 3 cases cool to around -6.5℃.

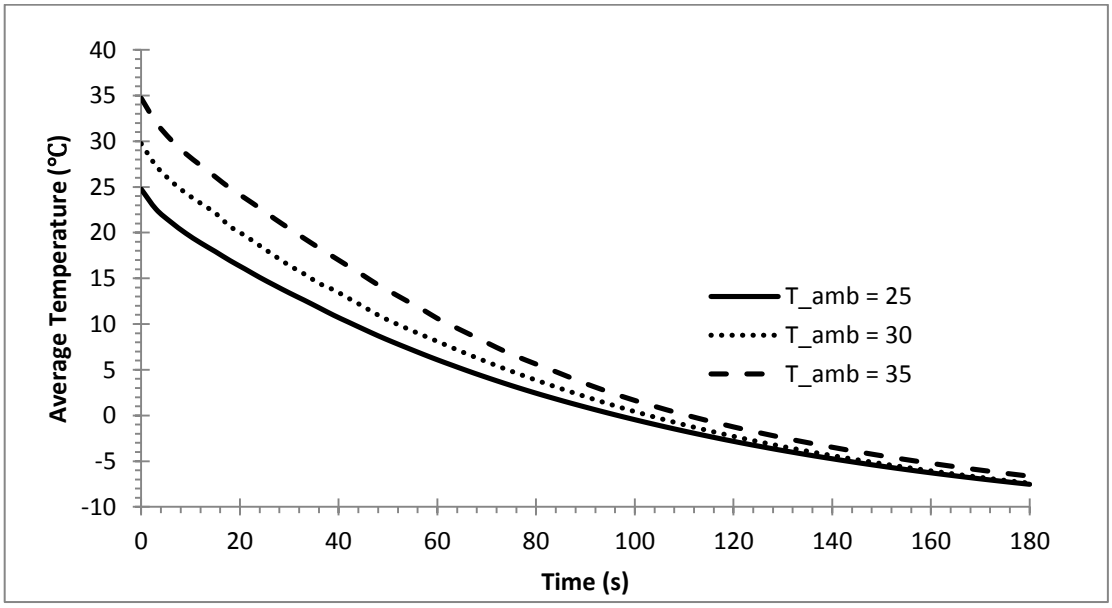

Figure 6.33: Average temperature of the 355 ml of water for different ambient temperatures over 180s, with a cooling vessel temperature of -30℃ for the same test case.

The convergence to of the water temperature in the ammonia expansion case is faster and reaches a lower temperature than the endothermic reaction case. This is expected since the temperature difference between the cooling vessel wall and ambient temperatures is greatest in the ammonia expansion case. Ammonia expansion provides the faster heat transfer when compared to endothermic reaction case. The average difference of final average temperature between to two cooling methods is about 5℃.

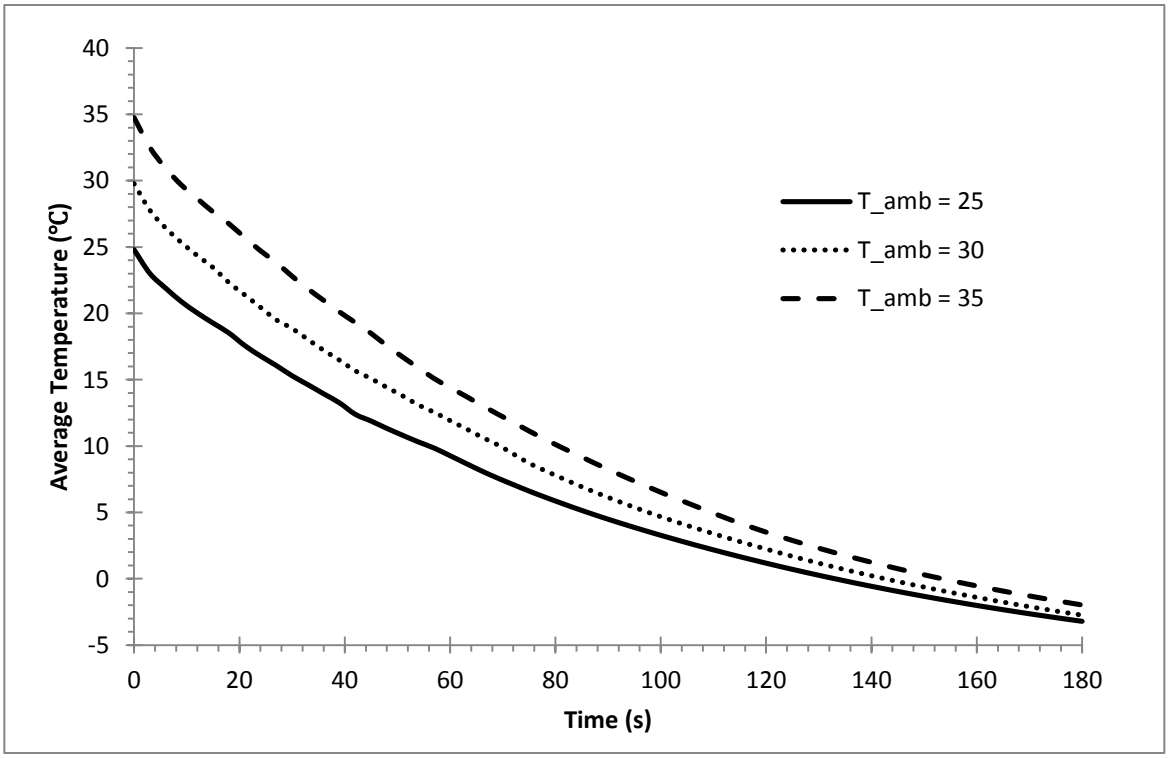

Figure 6.34: Average temperature of the 355 ml of water for different ambient temperatures over 180s, with a cooling vessel temperature of -20℃ for the same test case.

Finally, the changing the ambient temperature does not seem to affect the final surface temperature of the can. In both the ammonia expansion and endothermic reaction cases the results are similar. Again, there is a temperature convergence of the can surface temperature seen in both Figure 6.35 and Figure 6.36.

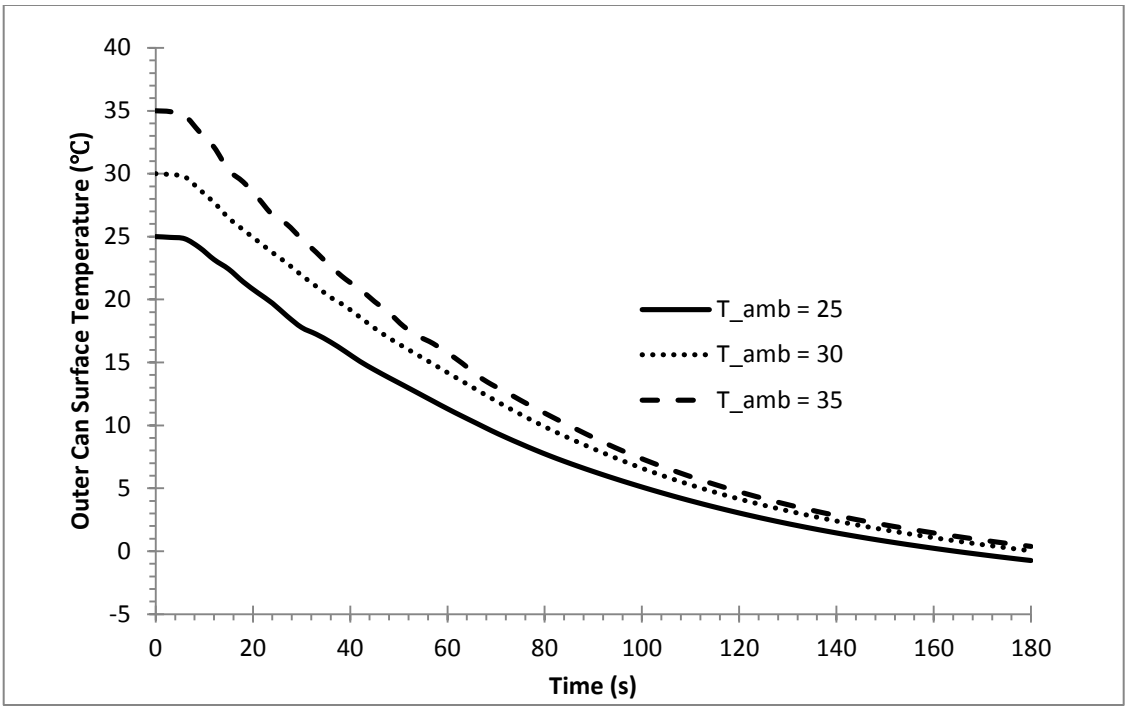

Figure 6.35: Average outer can surface temperature for different ambient temperatures over 180s, with a cooling vessel temperature of -30℃ for the same test case.

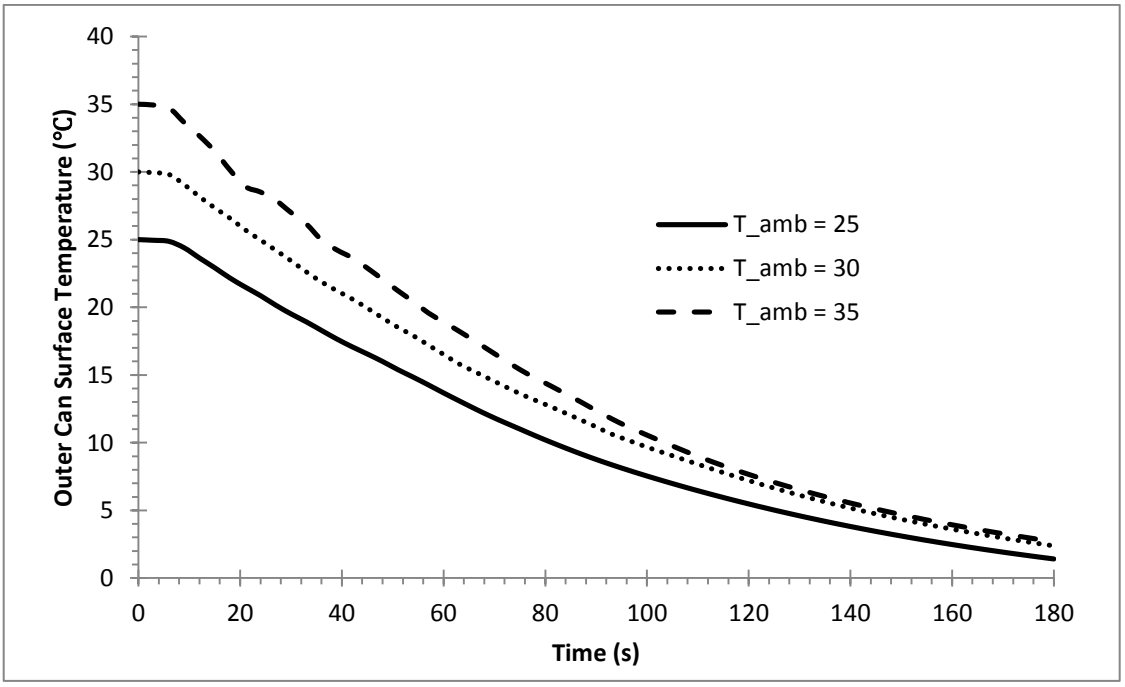

Figure 6.36: Average outer can surface temperature for different ambient temperatures over 180s, with a cooling vessel temperature of -20℃ for the same test case.

From these results, ambient temperature does not seem to have a great effect on the end result of the cooling process. The graphs show that eventually at the end of the 3 minutes the temperatures of the water eventually converge near the same temperature. The convergence occurs because after 180 seconds of cooling, the heat transfer rate plateaus and slows down. The different heat transfer rates between the test cases are such that eventually all three scenarios produce a similar end result. This is because the temperature difference between the cooling vessel wall and the average beverage temperature decreases over time. In the case for ambient temperature of 25℃ the difference decreases the soonest, whereas the in the 35℃ case it takes a bit more time. The cooling rate is lower in the 25℃ case, and higher in the 35℃ case. This difference in heat transfer rate is what allows for the convergence at 180 seconds.

6.4 Cooling Effectiveness Results

The cooling effectiveness results for the ammonia expansion method are presented in this section. The results from the numerical analysis are used for determining estimated changes in temperature of the beverage. The initial amount of saturated ammonia that is used to calculate the theoretical amount of cooling is 100 ml and 120 ml.

The cooling effectivenesseses for the 5 different aspect ratios in the numerical study are presented in Figure 6.37 and Figure 6.38 for 100 ml and 120 ml of initial saturated liquid ammonia respectively. The cooling effectiveness of the beverage can increases as the aspect ratio increases for both the energy and exergy cooling effectiveness. The highest cooling effectiveness is achieved with aspect ratio 5. However

aspect ratio 5 is an extreme case, so therefore the aspect ratio with the best cooling effectiveness is aspect ratio 4.

The cooling effectiveness that is achieved with aspect ratio 4 with 100 ml of ammonia is 0.7293 and 0.7154 for the energy and exergy cooling effectiveness respectively. For 120 ml of initial ammonia, the cooling effectiveness is 0.6078 and 0.5962 for energy and exergy effectiveness respectively. The cooling effectiveness decreases as more ammonia is introduced into the system to perform the same amount of cooling.

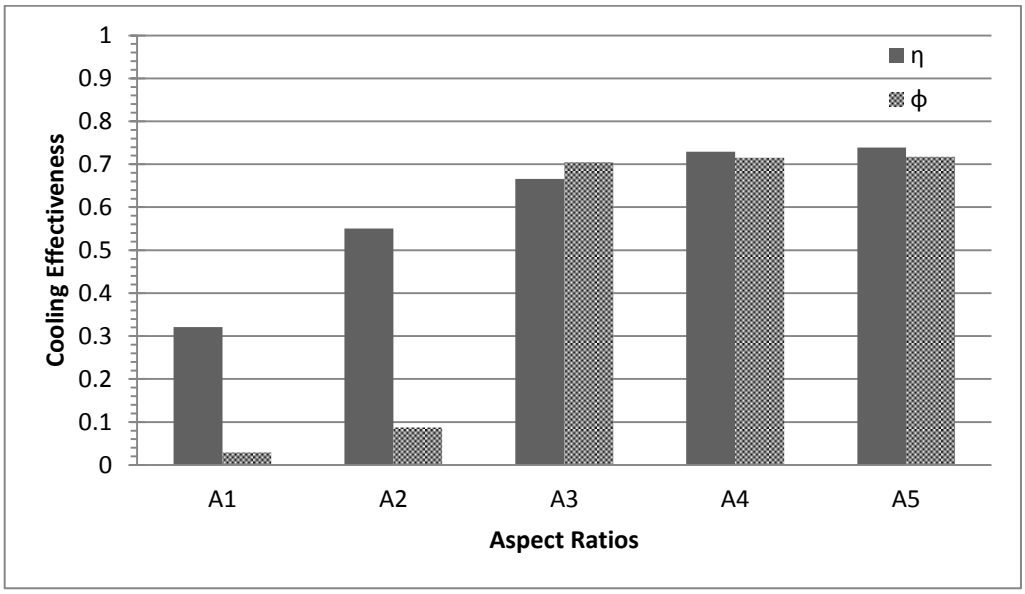

Figure 6.37: Cooling effectiveness with vary aspect ratios at ambient temperature of 25℃ and 100 ml of ammonia.

Since aspect ratio 4 is the best case scenario for the self-cooling beverage can. The ambient temperature study for cooling effectiveness is performed by using this aspect ratio. In Figure 6.40 and Figure 6.10 the cooling effectiveness of aspect ratio 4 is presented for varying ambient temperatures using 100 ml and 120 ml of ammonia respectively. The graphs show that as ambient temperature increases the cooling

effectiveness increases as well. This is due to the fact that the temperature differences in the beverages are greater when using the self-cooling beverage can in hotter climates. From the numerical model, it is observed that the final temperature of the beverage is relatively the same when varying the ambient temperature. Therefore it is expected that there is a greater temperature drop in the beverage as the ambient temperature increases. This explains why the cooling effectiveness increases as well when ambient temperature increases.

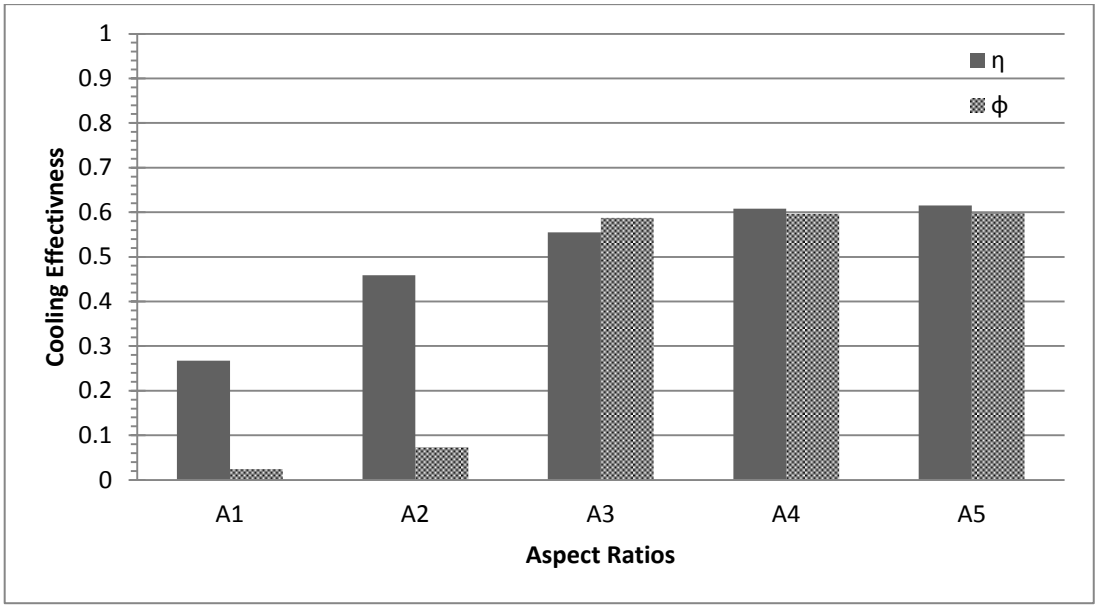

Figure 6.38: Cooling effectiveness with vary aspect ratios at ambient temperature of 25℃ and 120 ml of ammonia.

Using more ammonia decreases the cooling effectiveness in each study that is shown here. The design of the self-cooling beverage can that uses the ammonia expansion cooling method should be designed to provide effective cooling for climates of 35℃. In one of the test cases in Figure 6.39, 100 ml of ammonia shows that the cooling effectiveness would be close to 100%. The design of the can should opt for using 120 ml

because the real process is never ideal. Having more ammonia ensures that the beverage would achieve the desired temperature drop, and possibly cools even further.

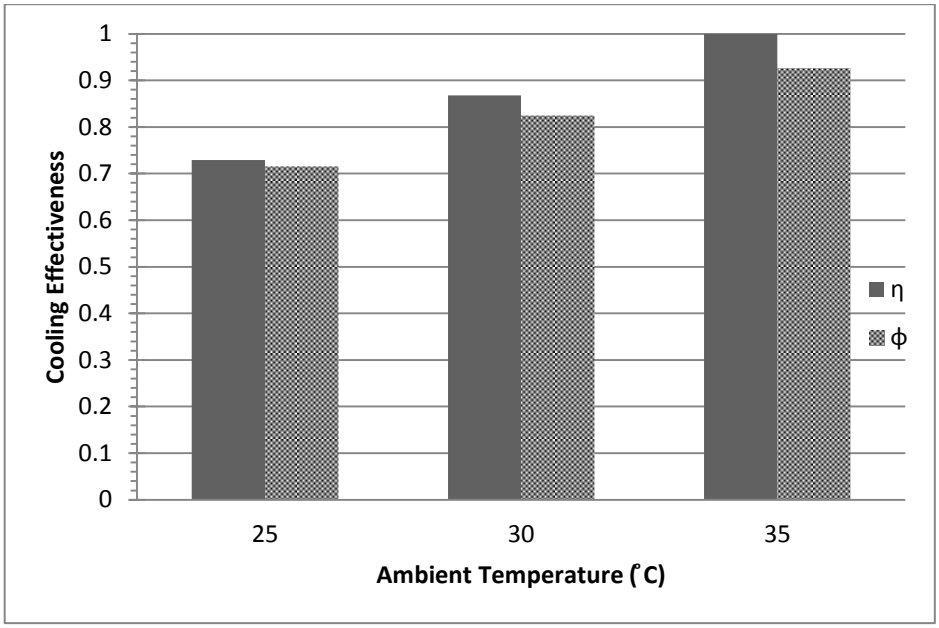

Figure 6.39: Cooling effectiveness with vary ambient temperatures using aspect ratio 4 and 100 ml of ammonia.

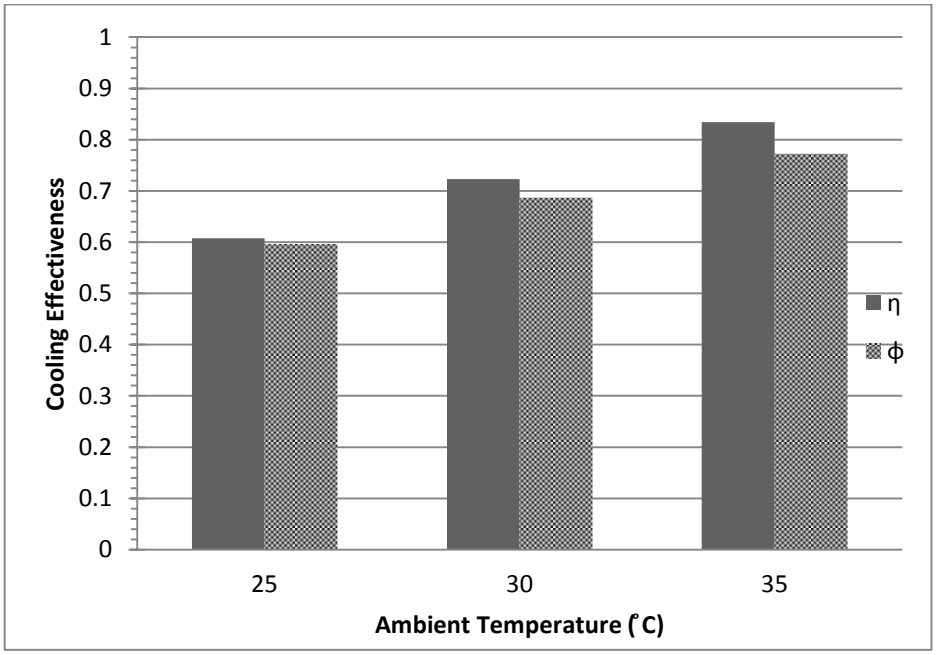

Figure 6.40: Cooling effectiveness with vary ambient temperatures using aspect ratio 4 and 120 ml of ammonia.

6.5 Optimization Results

In this section the results from the optimization study are presented. A Pareto front is graphed for objective functions 1 and 2 in Figure 6.41. The Pareto front for objectives 2 and 3 is graved in Figure 6.42. The Pareto front for objectives 1 and 3 is shown in Figure 6.43. Finally, a 3D Pareto front for all 3 objectives is presented in Figure 6.44. All Pareto front graphs are very well defined because of a sufficiently high population size used in the MOGA. All solutions presented on a Pareto front are non-dominating solutions. This means that every solution presented in the Pareto front is an optimal solution when considering all 3 objective functions. A solution cannot be moved to increase the fitness for one of the objective functions without compromising another.

The Pareto front for objective functions 1 and 2 resembles an increasing logarithmic relationship. It can be observed from looking at the Pareto front that the cooling time and volume of beverage is in competition with each other. When minimizing cooling time, the volume of the beverage is decreasing. This can be explained by analyzing the geometry that is used in both functions. As surface area increases to achieve a faster cooling rate; thus minimizing the cooling time, the volume of the cooling vessel must increase. The increase of size of the cooling vessel must decrease the volume of the beverage, hence the competition between objective functions 1 and 2. The designer would have to choose which design goal is most important to the company that is manufacturing the self-cooling beverage cans.

The Pareto front for objective functions 2 and 3 resembles an increasing exponential relationship as seen in Figure 6.42. The two objective functions are not competing, and both functions benefit from the maximization of the other. This can be

explained again with the geometry of the can design. As the beverage volume increases, the cooling vessel volume decreases. Decreasing the cooling vessel volume results in less ammonia refrigerant stored in the system, but this amount of ammonia is still able to provide the necessary cooling, therefore the cooling effectiveness increases. The optimal point for these two functions is their maximum point, but this greatly compromises cooling time.

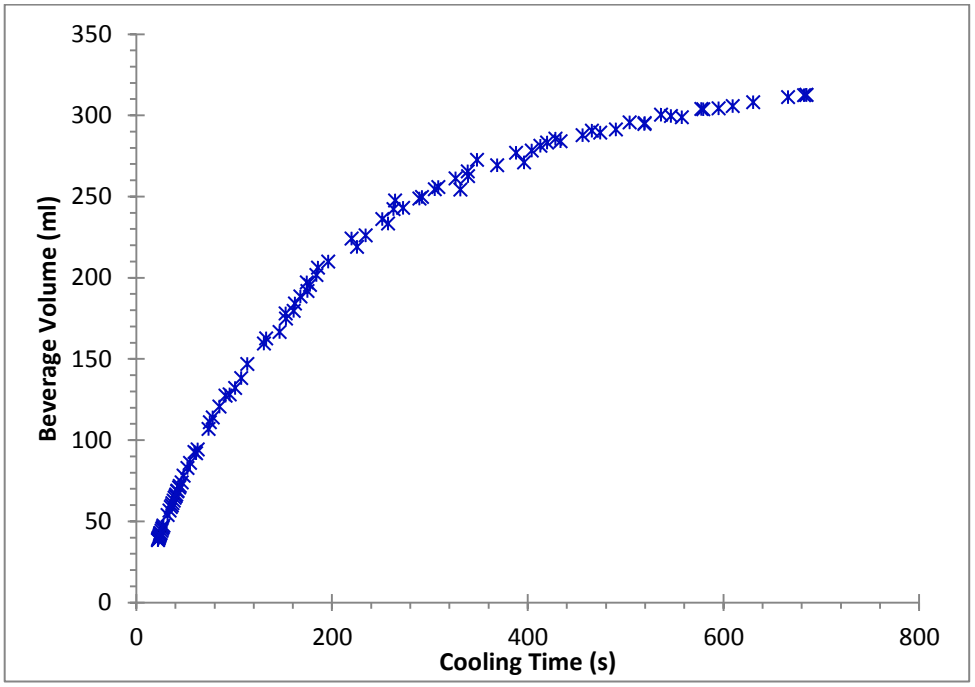

Figure 6.41: Pareto front for objective functions 1 and 2.

Figure 6.43 shows the Pareto front for objective functions 1 and 3. The Pareto front for objective functions 1 and 3 resembles an increasing linear relationship. However, these two functions are competing. Having a faster cooling time means having a lower cooling effectiveness. This is due to fact that as the volume of the vessel increases, the cooling rate increases, but then there is more cooling potential from the cooling vessel but less water too cool, hence to poor cooling effectiveness. A balance

between these two objectives need to found to ensure adequate cooling rate and effectiveness.

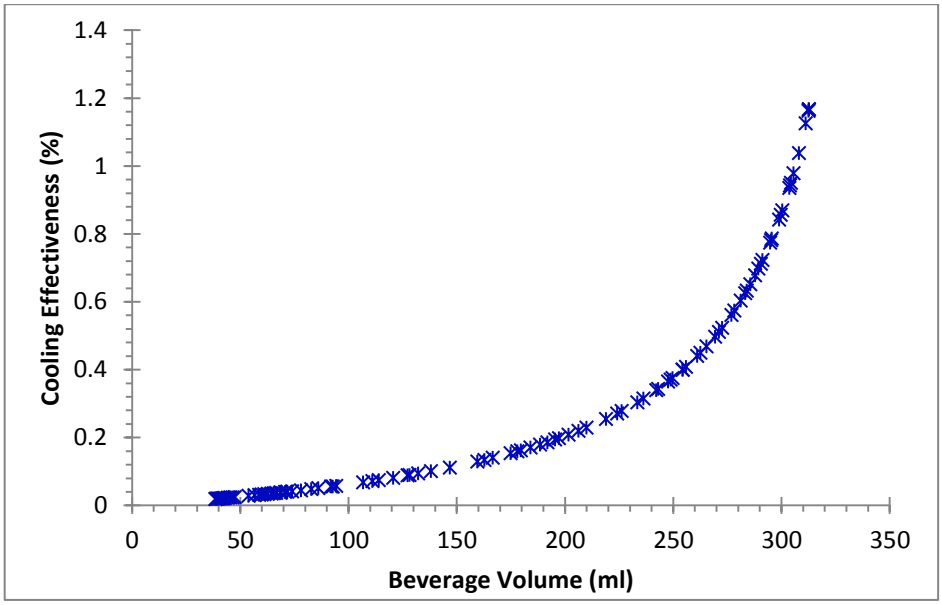

Figure 6.42: Pareto front for objective functions 2 and 3.

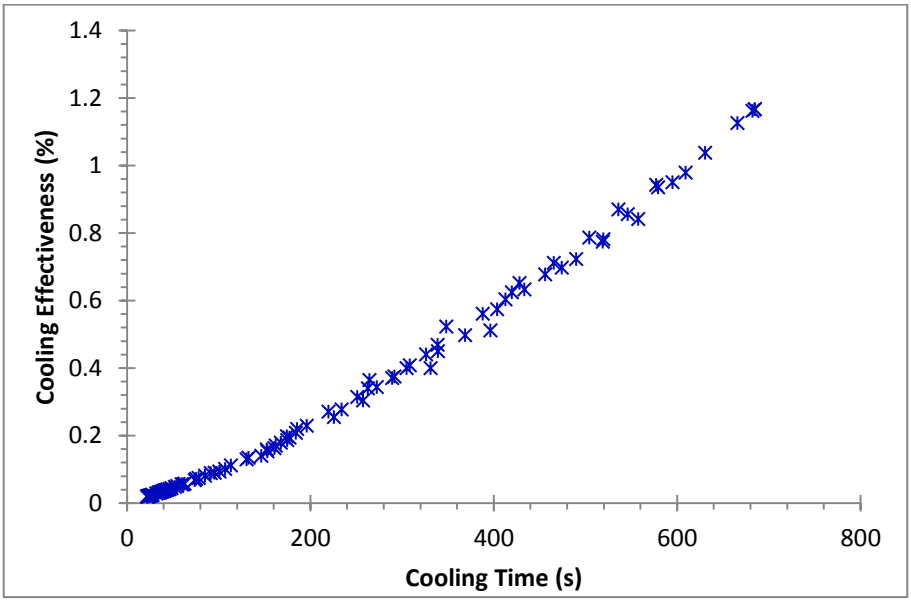

Figure 6.43: Pareto front for objective functions 1 and 3.

Finally the Pareto set of all three objective functions is graphed in a 3 dimensional Pareto front graph in Figure 6.44. The cluster of optimum points form a curved line in 3D

space that demonstrates all the relationships previously defined when describing all the 2D Pareto front graphs. Each point on the Pareto front are optimal points when consider the three objective functions. A balance between cooling time, beverage volume, and cooling effectiveness should be determined by the manufacturing company to meet market demand.

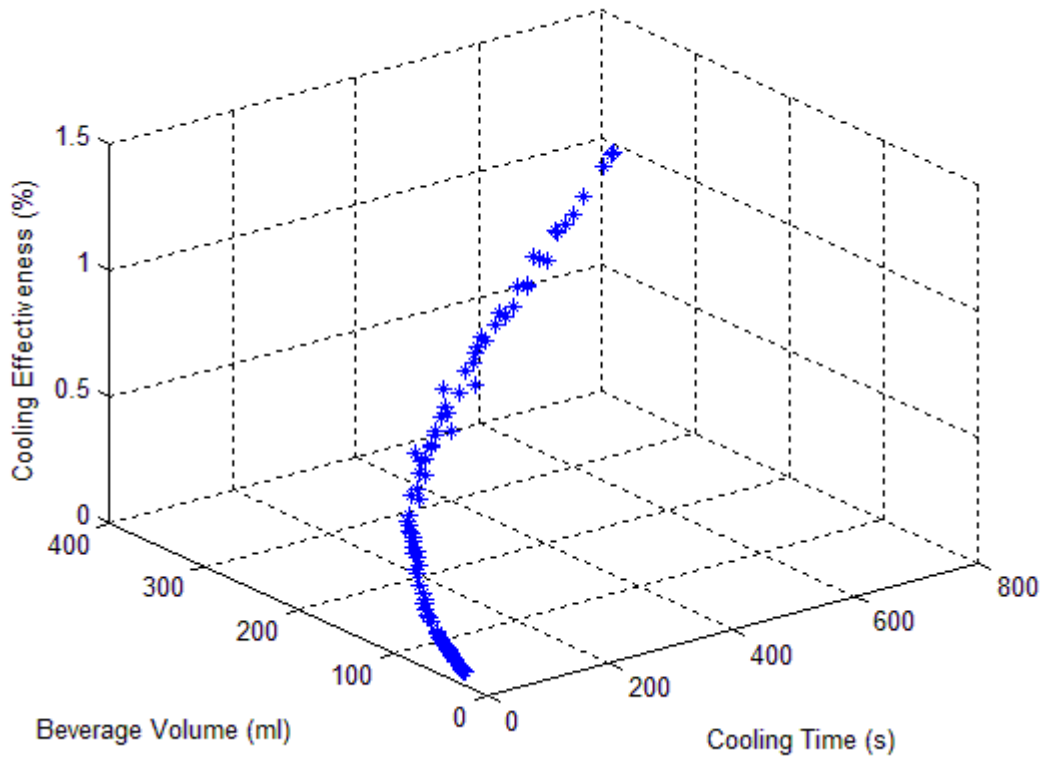

Figure 6.44: Pareto front for objective functions 1, 2 and 3.

The variable space for optimization study is shown in Figure 6.45. Each point in this graph corresponds to the geometry of the cooling vessel for a given optimal point that is presented in Figure 6.44. The points are spread out in area within the bounds of the constraints imposed on the study. The spread appears to be random and does not take on any known geometric shape. However, there appears to be a higher concentration of points near the top right region of the population.

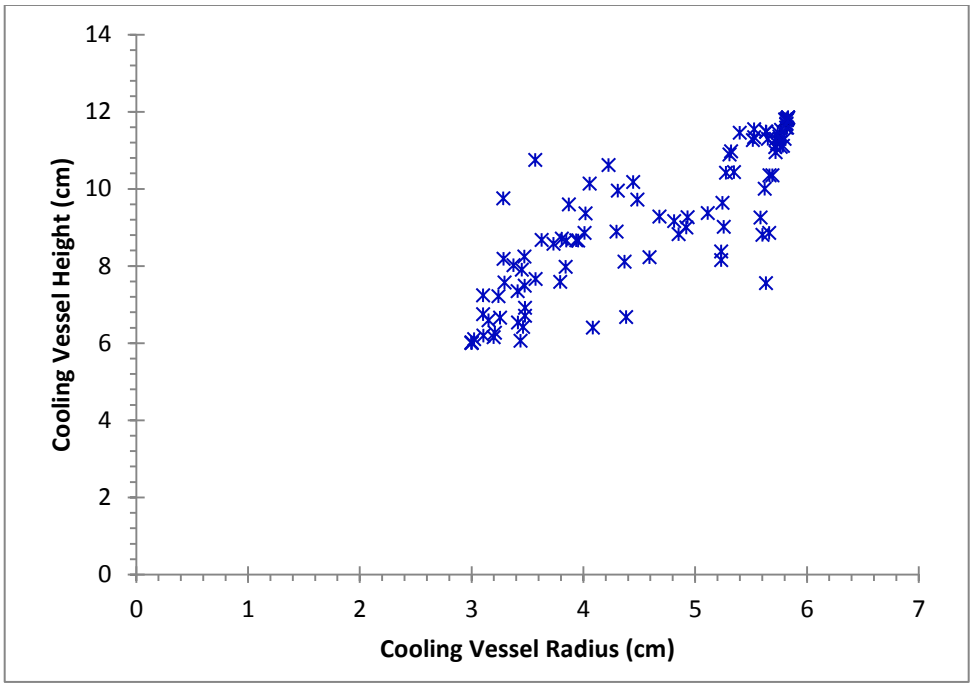

Figure 6.45: Optimization study variable space shows the optimal diameter and height for each optimal solution.

Table 6.4 holds a sample of 9 possible optimal solutions from the Pareto sets. This table shows values of cooling time in decreasing order from approximately 10 minutes, decreasing by approximately 1 minute until 2 minutes of cooling time. As described before, when the cooling time decreases, the cooling effectiveness and beverage volume decrease. In this table, the dimensions of diameter and height of the cooling vessel is presented for the corresponding optimal point. A manufacturer would use this graph to help determine the appropriate diameter and height of the cooling vessel to use for the final design.

The way a manufacturer would decide which optimal solution to use is by knowing their hard constraints for the design and having good knowledge of market demands. For an example, if a manufacturer knows that they must have no less than 200 ml of beverage and it must achieve a cooling time of 3 minutes or less. Then looking at

the table, the manufacturer would choose a cooling vessel radius and height of 4.48 cm and 9.72 cm respectively. From the discussions with the sponsoring company, it appears that the market is looking for a cost effective design which should not compromise the volume size of standard beverages. So for a standard beverage that has a volume of 355 ml, the size of the can would have to be increased to accommodate the addition of an internal cooling system.

Table 6.4: Table of some non-dominated solutions of interest.

Cooling Time (s)	**Beverage Volume** (ml)	**Cooling Effectiveness** (%)	**Diameter** (cm)	**Height** (cm)
609.46	305.57	0.98	3.20	6.15
546.18	299.58	0.86	3.25	6.66
474.09	289.34	0.70	3.48	6.92
419.80	283.23	0.62	3.38	8.02
368.77	269.26	0.50	3.79	7.59
304.81	254.34	0.40	3.85	8.65
251.30	236.15	0.31	4.02	9.36
184.08	201.65	0.21	4.48	9.72
130.29	159.47	0.13	5.25	9.02

Chapter 7: Conclusions and Recommendations

In this thesis, the cooling methods for a self-cooling beverage can are investigated experimentally. The experiments confirm two feasible methods of cooling that may be used. Two conceptual self-cooling beverage cans are proposed as possible solutions for development and production. The designs are studied analytically and numerically to show how well they can perform in different climatic areas based on changing the ambient temperature, and the aspect ratio of the cooling vessel is studied. In this chapter the major findings of the research are summarized and presented here. Along with the major findings of the research recommendations are made for future work, based on the challenges faced during the research work.

7.1 Conclusions

This study presents new proposed designs for a self-cooling beverage can using ammonia expansion with desiccant capturing or endothermic reaction cooling. Experimental case studies are carried out to determine the validity of the methods and certain key parameters for use in the analysis of the proposed self-cooling beverage can designs. In addition optimization of the geometry of a can is conducted using a multi-objective genetic algorithm in MATLAB. The optimization objectives are for cooling time, volume of the beverage, and cooling effectiveness. The main findings of the study are summarized as follows:

- Ammonia expansion with desiccant capture is a valid method for cooling of 300 ml of beverage in less than 3 minutes. The cooling rate is improved by using a

desiccant salt mixture of 50%wt of $MgCl_2$ and 50%wt of AlO_2. The cooling rate is significantly slower when using 100%wt $MgCl_2$.

- Endothermic reaction method of cooling is a valid method for cooling 300 ml of beverage. Ice formation around the reaction vessel is present when cooling water that has an initial temperature around 20℃ or lower. However, if the initial temperature is higher then there is less likely chance of forming ice. Ice formation is less likely in beverages such as cola since the freezing point is lower, approximately -10℃.
- Numerical modeling of the can designs, which have similar geometries and only differed by the cooling wall temperature based on the method of cooling, shows that aspect ratio 4 for the self-cooling beverage of 500 ml performs the best. Ambient temperature does not greatly affect the final temperature of beverage at the end of the 3 minute cooling phase.
- The cooling effectiveness study shows that the best performance is achieved when using aspect ratio 4 in an ambient temperature of 35℃. The cooling effectiveness for this specific case is 0.834 for energy and 0.772 for exergy respectively.
- Optimization of a generic 355 ml can is conducted to determine the optimal geometry using multi-objective genetic algorithm gives a numerous optimal solutions for the design the self-cooling beverage can. However, it is up to the manufacturer to decide which optimal points on the Pareto front would best suit their specifications and the market demand.

7.2 Recommendations

In this section, certain recommendations are made for possible future work in the field of self-cooling beverage cans. The following is a list of all these recommendations:

- A comprehensive chemical engineering study on the rates of ammonia adsorption with different weight combinations of magnesium chloride and aluminum oxide should be carried out to determine an optimal adoption rate to provide continuous and effective cooling.
- There is a lack of heat transfer properties for the numerous varieties of different beverages currently available on the market. The analysis of the self-cooling beverage can would benefit greatly from studying specific products. An in depth comprehensive study of key heat transfer properties such as thermal conductivity, heat capacities, specific gravity, dynamic viscosity, etc. should be carried out on name brand soft drinks, energy drinks, beer, and sports drinks.
- In addition to the study of the heat transfer properties, a numerical model should be developed to take into account the effects of carbon dioxide in beverages.
- Finally, further prototype designs should be built and tested. The prototypes should be as close to the final product as possible to prepare for marketing and commercialization.

References

[1] BozoCoop. (2014). *Cooler*. Available: https://www. bozo.coop/sites /default/files /cooler.jpg

[2] T. Ge, Y. Dai, R. Wang, and Y. Li, "Feasible study of a self-cooled solid desiccant cooling system based on desiccant coated heat exchanger," *Applied Thermal Engineering*, vol. 58, pp. 281-290, 2013.

[3] E. H. Parks, "Self-cooling Device for Beverage Container," United States Patent US3597937, 1971.

[4] H. K. Shen, "Cooling device for a can containing a beverage," ed: Google Patents, 1987.

[5] R. S. Allison, "Beverage can cooling system," ed: Google Patents, 1995.

[6] K. G. Oakley, "Self-cooling fluid container with integral refrigerant chamber," ed: Google Patents, 1996.

[7] M. A. Childs, "Self-cooling beverage container," ed: Google Patents, 1998.

[8] F. J. Baroso-Lujan and E. M. Galvan-Duque, "Self-cooling beverage container with evacuated refrigerant receiving chamber," ed: Google Patents, 1994.

[9] E. M. Halimi and W. C. Gans, "Self-carbonating self-cooling beverage container," ed: Google Patents, 2001.

[10] P. C. Claydon, "Self-cooling can," ed: Google Patents, 2004.

[11] D. D. Leavitt and J. R. Bergida, "Self Chilling Beverage Container With Cooling Agent Insert," ed: Google Patents, 2012.

[12] P. Collins, "Self-Cooling Beverage Can," ed: Google Patents, 2013.

[13] J. N. Rasmussen, S. Vesborg, and M. G. Andersen, "self cooling container and a cooling device," ed: Google Patents, 2011.

[14] WestCoastChill. (2014, June). *West Coast Chill How it Works*. Available: http://westcoastchill.com/how-it-works-2/

[15] D. Cull and M. Sillince, "Heat exchange unit for self-cooling containers," ed: Google Patents, 2013.

[16] Icetec. (2014). *Self-Cooling Can*. Available: http://www.gobizkorea.com/ blog/ProductView.do?blogId=icetec&id=898075

[17] W. G. Suh, "Self-cooling beverage container," ed: Google Patents, 2003.

[18] T. T. a. C. Holdings, "I C CAN," ed, 2014.

[19] I. Dincer and M. Kanoglu, *Refrigeration systems and applications*: John Wiley & Sons, 2011.

[20] F. C. Trusell, *Efficiency of Chemical Desiccants*: Iowa State University, 1961.

[21] V. E. Sharonov and Y. I. Aristov, "Ammonia adsorption by MgCl2, CaCl2 and BaCl2 confined to porous alumina: the fixed bed adsorber," *Reaction Kinetics and Catalysis Letters*, vol. 85, pp. 183-188, 2005/05/01 2005.

[22] Y. A. Cengel and Y. Cengel, "Heat Transfer A Practical Approach with EES CD," *McGraw Hill Professional*, 2003.

[23] A. Hadjadj, S. Maamir, and B. Zeghmati, "A new study of laminar natural convection in two concentric vertical cylinders," *Heat and mass transfer*, vol. 35, pp. 113-121, 1999.

[24] D. Knuth, "MOP Evolutionary Algorithm Approaches," ed, 2012.